AN ABSTRACT OF THE DISSERTATION OF

Hui Nian for the Doctor of Philosophy in Biochemistry and Biophysics presented on February 26, 2010.

Title: Dietary Organosulfur and Organoselenium Compounds as HDAC Inhibitors

Abstract approved:

Roderick H. Dashwood

Histone deacetylase (HDAC) inhibitors have the potential to de-repress epigenetically silenced genes in cancer cells, leading to cell cycle arrest and apoptosis. Dietary HDAC inhibitors derived from natural phytochemicals are promising anticancer agents. In this thesis, metabolites from natural organosulfur and organoselenium compounds, i.e. allyl mercaptan (AM), β-methylselenopyruvate (MSP) and α-keto-γ-methylselenobutyrate (KMSB), were discovered to serve as HDAC inhibitors and exhibit anticancer activities in human colon cancer cells.

AM is a metabolite of garlic-derived organosulfur compounds, whereas MSP and KMSB are the newly discovered α-keto acid metabolites of Se-methylselenocysteine (MSC) and selenomethionine (SM) respectively. In this thesis research, all three compounds were shown to inhibit HDAC activity in a competitive manner at micromolar levels. Molecular modeling suggested they can fit into the active site of HDAC enzymes and chelate catalytic Zn^{2+} via

sulfhydryl group (AM) or keto acid group (MSP and KMSB). Studies on the structural analogs indicated that the selenium atom was also important for MSP/KMSB's HDAC inhibitory effects.

In human colon cancer cells, AM, MSP and KMSB decreased HDAC activities, and induced rapid histone hyperacetylation in a dose-dependent manner. All three compounds induced rapid and sustained expression of the cell cycle inhibitor p21 at both mRNA and protein levels. There was enhanced *P21* promoter activity, and hyperacetylated histone H3 was associated with the gene promoter. The induction of p21 required a Sp1/Sp3 binding sites but was independent of p53 status. P21 induction may mediate cell cycle arrest in AM/MSP/KMSB-treated colon cancer cells. MSP and KMSB also induced apoptosis in colon cancer cells, as evidenced by morphological changes, Annexin V staining and increased cleaved caspase-3, -6, -7, -9 and poly(ADP-ribose)polymerase. MSP dramatically induced the expression of pro-apoptotic Bcl-2 family gene Bmf, and knocking down Bmf expression by siRNA significantly decreased caspase activation in MSP-treated colon cancer cells. As a result of cell cycle arrest and/or apoptosis induction, these compounds significantly inhibited colon cancer cell growth.

Formation of MSP was directly detected in MSC-treated colon cancer cells. MSC, the parent compound also induced histone hyperacetylation, p21 and Bmf expression in the cells. Knocking down Bmf expression reduced MSC's apoptotic effects. In colon cancer cells, SM cannot be converted to KMSB, and histone acetylation remained unchanged in SM-treated colon cancer cells. Histone hyperacetylation was also observed in the tissues of the mice gavaged with AM and its parent organosulfur compounds. These results indicate that AM/MSP/KMSB could be active metaobolites of organosulfur or organoselenium compounds contributing to their chemopreventive effects.

Dietary Organosulfur and Organoselenium Compounds as HDAC Inhibitors

by

Hui Nian

A DISSERTATION

submitted to

Oregon State University

in partial fulfillment of

the requirements for the

degree of

Doctor of Philosophy

Presented February 26 2010

Commencement June 2010

Doctor of Philosophy dissertation of Hui Nian

Presented on February 26 2010.

APPROVED:

Major Professor, representing Biochemistry and Biophysics

Chair of the Department of Biochemistry and Biophysics

Dean of the Graduate School

I understand that my dissertation will become part of the permanent collection of Oregon State University libraries. My signature below authorizes release of my dissertation to any reader upon request.

Hui Nian, Author

CONTRIBUTION OF AUTHORS

The author's responsibilities were as follows: Dr. Roderick H. Dashwood and Dr. Barbara Delage contributed to the study concept, research design and manuscript revisions; Dr. John T. Pinto synthesized MSC, SM, MSP and KMSB; Dr. William H. Bisson conducted molecular docking for MSP and KMSB; Alan Taylor conducted MSP/MSC HPLC measurements; Wan-Mohaiza Dashwood amplified the luciferase reporter plasmids.

TABLE OF CONTENTS

TABLE OF CONTENTS (Continued)

TABLE OF CONTENTS (Continued)

LIST OF FIGURES

LIST OF FIGURES (Continued)

LIST OF TABLES

Dietary Organosulfur and Organoselenium Compounds as HDAC inhibitors

Chapter 1 Introduction

1.1 Histone deacetylase inhibitors and their anticancer activities in colon cancer

In eukaryotes, the packaging of genomic DNA into the chromatin architecture provides a dynamic mechanism that allows the regulation of gene expression. The fundamental subunit of chromatin, the nucleosome, is composed of an octamer of four core histones, i.e. an H3/H4 tetramer and two H2A/H2B dimers, surrounded by 146 bp of DNA. The N-terminal tails of histones protruding from the nucleosome are subject to diverse posttranslational modifications, including acetylation, phophorylation, methylation, sumoylation, ubiquitination, and ADP-ribosylation (1). The pattern of these modifications can modulate the chromatin structure and hence regulate gene expression. The acetylation of core histones is the best understood type of modification. Acetylation can neutralize the positive charge of histones, loosening their interactions with the negatively charged DNA backbone and leading to a more "open" active chromatin structure that favors the binding of transcription factors for active gene expression (2). In general, increased levels of histone acetylation (hyperacetylation) are associated with increased transcriptional activity, whereas decreased levels of acetylation (hypoacetylation) are associated with repression of gene expression. The level of histone acetylation is maintained by a dynamic balance between the activities of histone acetyltransferases (HATs) and histone deacetylases (HDACs).

1.1.1 Histone deacetylases and their substrates

Histone deacetylases (HDACs) are enzymes that catalyze removal of an acetyl group from the ε-amino group of lysine residues. Eighteen mammalian HDACs have been identified to date (3). These can be categorized into four classes based on their homology to yeast HDACs. Mechanistically, class I, II and IV HDACs are distinct from Class III HDACs in co-factor requirement. The former require an active site zinc to mediate deacetylation catalysis while the latter are dependent on NAD^+. Class I HDACs, namely HDAC1, 2, 3 and 8, are homologous

to yeast Rpd3, and are ubiquitously expressed in many human tissues, and generally localized to the nucleus. Class II HDACs (HDAC4, 5, 6, 7, 9 and 10) are highly similar to the yeast HDAC Had-1, and are expressed in a tissue-specific manner. Class II HDACs shuttle between the nucleus and cytoplasm, suggesting potential extranuclear functions by regulation of the acetylation status of nonhistone substrates. Class II HDACs can be further separated into class IIa (HDAC4, 5, 7, 9) and IIb (HDACs 6 and 10) based upon the existence of tandem deacetylase domains in HDAC 6 and 10. Class I and II HDACs have similar the deacetylase domains but differ in their N-terminal sequence. HDAC11, which is less similar to both class I and II HDACs, is assigned to its own class, class IV. The third class of HDACs is the sirtuins (SIRT1-7), which are homologous to the yeast Sir2 family of proteins. These enzymes require NAD^+ for deacetylase activity, in contrast to the zinc-catalyzed mechanism used by Class I and II HDACs.

The most thoroughly studied of the substrates of HDACs are histones. HDACs catalyze the removal of an acetyl group from lysine residue of the core nucleosomal histones, thereby reconstituting the positive charge on the lysine. There are 30 lysine residues in histone H3, H4, H2A and H2B that are subject to deacetylation by HDACs. Acetylation status of these lysines particularly in the histone H3 and H4 tails dramatically affect the condensation state and higher order chromatin structure, owing to their capacity to modulate the exposure of charge patches on the surface of the nucleosomes.

In addition to histones, HDACs are also responsible for removing acetyl groups from diverse types of non-histone proteins(4). These include transcription factors (FOXO1, NFκB), signal transduction mediators (Stat3, Smad7), microtubule components (α-tubulin), and molecular chaperone (Hsp90). This list is rapidly increasing. The acetylation of lysine residues on these nonhistone proteins can compete with other posttranslational modifications, such as ubiquitination and sumoylation, or can influence phosphorylation status. Consequently, the stability, localization, protein dimerization, and protein–protein interactions of these acetylated nonhistone proteins can be altered.

1.1.2 Histone deacetylase inhibitors (HDACi)

The use of HDAC inhibitors pre-dated the discovery of the HDACs themselves. Several structurally distinct classes of HDAC inhibitors have been purified from natural sources or synthetically developed, and some of them have advanced into Phase I and/or phase II clinical trials in solid tumors and hematological malignancies(5). With a few exceptions, HDAC inhibitors (HDACi) can be divided into four chemical classes: short-chain fatty acids, hydroxamic acids, benzamide derivatives, and cyclic peptides (**Figure 1.1**) (4). Trichostatin A (TSA), which belongs to hydroximic group is a fermentation product of *Streptomyces*, and the most potent HDACi discovered so far. TSA, as well as its structural analog, suberoyl anilide hydroxamic acid (SAHA) is effective at nanomolar concentrations *in vitro*, and SAHA has entered clinical trials. Depsipeptide (romidepsin, FK-228), belonging to the cyclic peptides group, is a natural product extracted from *Chromobacterium violaceum*, and it has been under multiple Phase I and II trials for cancer therapy. The short-chain fatty acid group includes butyrate, phenylbutyrate, valproic acid and their derivatives. This group has been limited in clinical application due to its high millimolar concentrations when assessed in cells. Benzamide HDAC inhibitors such as MS-275 and CI-994 are now in Phase I and II clinical trials (6).

It is thought that HDACi function by blocking access to the active site of HDACs (7). The HDAC catalytic domain consists of a narrow, tube-like pocket, and a Zn^{2+} cation is positioned near the bottom of this enzyme pocket facilitating the deacetylation catalysis. The structures of many HDAC inhibitors can be divided into three motifs, each of which interacts with a discrete region of the enzyme pocket. For TSA, these include a Zn^{2+}–chelating function (hydroxamic acid), a conjugated, aliphatic chain as linker, and a polar cap group (the dimethlaminophenyl moiety) (**Figure 1.1**). This mode of ligand-HDAC interaction might also apply to benzamides and depsipeptide after metabolic activation. Short-chain fatty acid HDACi was supposed to mediate HDAC inhibition through nonspecific hydrophobic interactions with surface residues located at the enzyme pocket entrance and or inside the hydrophobic tube-like pocket. All HDACi inhibit HDAC in a reversible fashion, except for trapoxin and depudesin, which inhibit the enzyme irreversibly via covalent binding to the epoxyketone group. Most HDAC inhibitors work equally well against class I, II and IV HDACs, with few having preferential inhibition towards specific class or individual HDACs.

1.1.3 HDACs and HDACi in colon cancer

1.1.3.1 HDAC expression in colon cancer

Several studies reported increased expression of the class I HDACs (HDAC1, HDAC2 and HDAC3) in colon tumors relative to adjacent normal mucosa (8-10), in both the protein and mRNA levels. It has been proposed that HDAC overexpression may facilitate progression of colon tumors by epigenomic repression of tumor suppressor genes, or by hypoacetylation and modification of the function of non-histone substrates. However, the mechanisms by which class I HDACs are upregulated in colon cancer are unknown. And it is also unclear the expression status of the HDACs of other classes in colon tumors versus normal mucosa. The majority of *in vitro* studies using colon cancer cell lines have demonstrated a role for class I HDACs in promoting colon cell proliferation and survival (8, 9). Knockdown of the class I HDACs, 1, 2, and 3 reduces growth of several colon cancer cell lines including HCT116, HT29 and SW480(8, 9, 11). Mechanistically, the proliferative effects of HDACs in colon cancer cells have been linked to transcriptional repression of the cdk-inhibitor, p21. Knockdown of HDACs 1, 2, and 3 induce p21 expression in colon cancer cell lines, while their overexpression represses basal as well as HDACi-mediated p21 induction (12).

1.1.3.2 Anti-tumor effects of HDACi in colon cancer

The anticancer effects of HDACi have been demonstrated in colon cancer cell lines as well as in animal models of colon cancer. Structurally different HDAC inhibitors including valproic acid (VPA), butyrate, TSA, SAHA and benzamide MS-275 have been shown to induce growth inhibition and apoptosis in colon cancer cell lines (13-15). Butyrate and TSA have also been shown to efficiently reduce growth of colon cancer xenografts (16). Direct infusion of butyrate into the colon of rats using a surgical intubation model reduced aberrant crypt formation following azoxymethane (AOM) treatment (17). VPA has been shown to reduce adenoma formation in APC^{Min} mice (9).

1.1.3.3 Mechanisms of HDACi's anti-tumor effects in colon cancer

The majority of the evidence generated to-date has been in support of HDACi mediating their phenotypic effects through transcription dependent effects.

Growth arrest. Treatment of colon cancer cells with HDACi induces G0/G1 or G2/M growth arrest within 12-16 hours depending on the cell line and HDACi concentrations (18-21). HDACi induced growth arrest in colon cancer cells consistently involves induction of p21, which is induced rapidly in a Sp1/Sp3-dependent manner, and independently of p53 (12, 22-24). Butyrate-mediated growth arrest was attenuated on p21 deficient HCT116 cells, indicating of critical role of p21 induction in growth arrest (12). HDACi also induce expression of several other growth inhibitory proteins including p15, p16 and GADD45α and β, and down-regulate expression of some pro-proliferative genes including c-myc, cyclinB1 and cyclinD1 in colon cancer cells (19, 25-30). However, the role of these genes' change in HDACi-induced growth arrest has not been directly tested.

Apoptosis. Most studies show that HDACi induces apoptosis in colon cancer cells via the intrinsic pathway. This involves a cascade of events including a decrease in mitochondrial potential, cytochrome c release and caspase-9 and 3 activation (31). Inhibitors of caspase 3 and 9, but not 8, inhibit butyrate-induced apoptosis in Caco-2 cells (32), indicating the importance of the intrinsic apoptotic pathway. It has been reported that HDACi induce expression of the pro-apoptotic Bak protein, and down-regulate expression of the anti-apoptotic protein Bcl_{XL} (32, 33). HDACi also modulate expression of genes involved in the extrinsic apoptotic pathway, including upregulation of the pro-apoptotic DR5 gene and downregulation of the anti-apoptotic caspase inhibitor, FLIP, in colon cancer cells. Consistent with these effects, HDACi sensitize colon cancer cells to TRAIL and FAS-induced apoptosis (34-36). HDACi induced apoptosis in colon cancer cells has also been linked to increased ROS production (37), but whether ROS is critical for HDACi-induced apoptosis has not be demonstrated in colon cancer cells.

Differentiation. It has been reported that HDACi enhanced differentiation in colon cancer cells. This was evidenced morphologically by the formation of dome-like structures and improved tight-junction function, and biochemically by the increased expression of the differentiation markers intestinal alkaline phosphatase, sodium hydrogen exchanger NHE3, the adherens junction protein E-cadherin and the cytoskeletal proteins villin (13, 38-43).

1.2 Garlic organosulfur compounds in cancer prevention

Garlic (*Allium sativum L.*) has been used for medicinal purposes by many cultures for centuries. The known health benefits of garlic and their constituents include lowering of serum cholesterol level, inhibition of platelet aggregation and increased fibrinolysis, stimulation of immune function through activation of macrophages and induction of T-cell proliferation, reduction of blood glucose level, radioprotection, improvement of memory and learning deficit, protection against microbial, viral and fungal infections, and anticancer effects (44).

1.2.1 Chemistry of garlic organosulfur compounds

Fresh garlic contains water, carbohydrates, proteins, fiber, fat, 17 amino acids, other trace elements and 33 sulfur compounds. Garlic particularly abounds in organosulfur compounds, which are thought to be responsible for its flavor and aroma, as well as its potential health benefits (45).

In intact whole garlic cloves, there are two major organosulfur compounds: the cysteine sulfoxides and the γ-glutamylcysteines. They are present in roughly equal amounts by weight. Together, they contain some 95% of the total sulfur in garlic. Allylcysteine sulfoxide (Alliin) is by far the most abundant of the cysteine sulfoxides (5-14 mg/g), and γ-glutamyl-*S*-*trans*-1-propenylcysteine (3-9mg/g) is the most abundant of the γ-glutamylcysteines. Others include *S*-methylcysteine sulfoxide (methiin), isoalliin, cucloalliin, γ-glutamyl-*S*-allylcysteine and γ-glutamyl-*S*-methylcysteine, although at much smaller amounts (46).

When raw garlic cloves are crushed, chopped, or chewed, the vacuolar enzyme alliinase is released, which very quickly, within several seconds, transforms alliin into sulfenic acid (R-SOH). Sulfenic acid is exceptionally reactive and spontaneously undergoes condensation with another sulfenic acid molecule yielding the diallyl thiosulfinate (allicin). The allicin, absent in the intact garlic but formed within 10-60 seconds of crushing garlic, is the main component of a freshly prepared garlic homogenate. Allicin is poorly soluble in water and is responsible for the pungent flavor of garlic. Allicin is a very unstable compound, and breaks down to form a variety of fat-soluble polysulfides, mostly diallyl sulfide (DAS), diallyl disulfide (DADS) and

diallyl trisulfide (DATS). These compounds have very low water solubility and are the primary compounds in steam-distilled garlic oil. They are very stable and change very little over the time span of years. In oil macerates, allicin forms ajoene (E,Z-4,5,9-trithiadodeca-1,6,11-triene 9-oxide) and vinyl dithiins. In ethanol extraction of crushed garlic, allicin yields DATS, DADS, and ajoene. The proportions of these compounds vary with concentration of alcohol and aging of the extract. Additionally, the reactions of allicin with –SH groups can yield water-soluble compounds *S*-allylcysteine (SAC) or *S*-allylmercaptocysteine (SAMC) (47, 48) (**Figure 2.2**).

The γ-glutamylcysteines found in whole garlic are not affected when the cloves are crushed. During the long-term incubation of crushed garlic in aqueous solutions, γ-glutamylcysteines are converted to form SAC, *S*-*trans*-1-propenylcysteine and SAMC, which are components of aqueous extracts of garlic (49).

1.2.2 Bioavailability and metabolism of garlic organosulfur compounds

The absorption and metabolism of organosulfur compounds is still not fully understood. Animal studies using radiolabeled compounds indicate that allicin or its breakdown products are absorbed intestinally (50, 51). However, allicin and allicin-derived compounds, including diallylsufides, ajoene and vinyldithiins, have never been detected in human blood, urine or stool, even after the consumption of up to 25g of fresh garlic or 60mg of pure allicin, suggesting that allicin and its transformation products are rapidly metabolized (52). *In vitro*, allicin, DATS, DADS, SAMC and ajoene have all been demonstrated to form allyl mercaptan when exposed to human blood, and presumably *in vivo* as well (53). It appears that some allyl mercaptan is further metabolized to allyl methyl sulfide. Allyl mercaptan, allyl methyl sulfide and DADS have been found in the breath of people consuming garlic (54, 55).

γ-glutamylcysteines are thought to be absorbed intact and hydrolyzed to SAC and *S*-1-propenylcysteine, since metabolites of these compounds have been measured in human urine after garlic consumption (56, 57). SAC was found also in human blood after ingesting of aged garlic extract, the main component of which is SAC (58, 59).

1.2.3 Anticancer activities of garlic organosulfur compounds

Epidemiological studies. Epidemiological studies conducted in different countries have shown the significant correlation between increased garlic consumption and decreased risk of gastric, colorectal, prostate and breast cancers (60-64).

In vivo studies. In vivo studies have provided convincing evidence that garlic or individual organosulfur compounds, mostly oil-soluble, are highly effective in suppressing cancers induced by chemical carcinogens in animal models (**Table 1.1**). Garlic organosulfur compounds have been shown to inhibit cancer cell growth *in vivo* in the xenograft models. Sundaram and Milner reported an inhibitory effect of DADS on growth of human colon tumor cells (HCT-15) implanted in nude mice (65). Singh et al. have shown that DADS suppressed growth of H-ras oncogene-transformed tumor xenografts in nude mice (66). DATS significantly inhibited growth of PC-3 prostate cancer xenografts in male nude mice (67).

In vitro studies. In vitro studies also showed antiproliferative properties of garlic organosulfur compounds in various cancer cell lines, as listed in **Table 1.2**.

1.2.4 Mechanisms of cancer prevention by garlic organosulfur compounds

Several mechanisms have been proposed to explain the cancer-preventive effects of garlic and related organosulfur compounds. These include interference with carcinogen metabolism, antioxidant effects, and induction of cell cycle arrest and apoptosis.

Inhibition of phase I biotransformation enzymes. Some chemical carcinogens do not become active carcinogens until they have been metabolized by phase I biotransformation enzymes, such as those belonging to the cytochrome P450 (CYP) family. Inhibition of specific CYP enzymes involved in carcinogen activation inhibits the development of cancer in some animal models. Both DAS and DADS efficiently inhibit one of the isoenzymes of cytochrome P450 CYP2E1, which is responsible for the activation of nitrosoamines, hydrazines and benzene (68). CYP2E1 inhibition decreases carcinogenic properties of these compounds. Davenport and Wargovich reported that DAS, DADS and AMS significantly decreased hepatic CYP2E1, but did not change CYP2E1 mRNA level, indicating of post-translational modification of enzyme by these compounds (69). It has been shown that DAS can be metabolized by

CYP2E1 by oxidation at the sulfur atom to form DASO and DASO2, which can bind to the enzyme and cause its inactivation (70).

Induction of phase II biotransformation enzymes. Reactions catalyzed by phase II biotransformation enzymes generally promote the elimination of drugs, toxins and carcinogens from the body. Therefore, increasing the activity of phase II enzymes, i.e. glutathione S-transferase, epoxide hydrolase, quione reductase and glucuronate transferase, may help prevent cancer by increasing the clearance rate of toxic compounds. Glutatione S-transferases (GST) are important detoxifying enzymes that remove harmful electrophiles, including carcinogens, by conjugating them with glutathione. Several studies have shown the elevation of GST activity by DAS and DADS administered orally and intraperitoneally (71, 72). Fukao et al. found that ip administration of DATS to rats caused a marked increase in the activities of GST and quinone reductase (QR) (73). Chen et al. reported that gene expression of NAD(P)H: quinone oxidoreductase 1(NQO1) and heme oxygenase 1 (HO1) was increased by treatments with DADS and DATS (74).

Antioxidant effects. Cancer is connected with oxidative modifications of biological molecules by reactive oxygen species including free radicals. Garlic stimulated the activity of glutathione peroxidase (GPx) and inhibited the ratio of reduced/oxidized glutathione produced by TPA in epidermal cells (75). GPx activity was also increased in animal tissues by DAS administration against B[a]P-induced genotoxicity in mouse forestomach. DAS and DADS also increased the activity of glutathione reductase, and garlic oil increased the activity of superoxide dismutase (SOD) (76). AGE, SAC, and SAMC exhibited radical scavenging activity in both chemiluminescence and 1,1-diphenyl-2-picrylhydrazyl (DPPH) assays against *t*-butyl hydroperoxide-induced ROS in liver microsomal fraction (77).

Induction of cell cycle arrest. Many studies have shown that garlic organosulfur compounds caused antiproliferative effects in various cancer cells through blocking cells within the G1/S or G2/M (mostly) arrest. DADS was reported to arrest human colon tumor cells (HCT-15) in G2/M phase accompanied by inhibited Cdk1 kinase activity and increased cyclin B1 protein expression (78). Wu and coworkers found that human liver tumor cells J5 were significantly arrest in G2/M phase following DADS and DATS treatments presumably by increasing cyclin

B1 and decreasing Cdk7 kinase expression (79). Cell cycle arrest in the G2/M phase upon treatment with DADS or DATS was also reported in other cancer cell lines, and the underlying molecular events include activation of p38 MAP kinase pathways, reduction in the level of Cdc25C phosphatase, hyperphosphorylation and reactive oxygen species-mediated destruction of Cdc25C (80-82). Xiao et al. also found that SAMC affect cell cycle progression in colon cancer cells SW480 and caused G2/M arrest (83).

Induction of apoptosis. Garlic organosulfur compounds, including allicin, ajoene, DAS, DADS, DATS, and SAMC, have been found to induce apoptosis when added to various cell lines grown in culture (84, 85). Oral administration of aqueous garlic extract and SAC has been reported to enhance apoptosis in an animal model of oral cancer (86, 87). Molecular mechanisms involved in the induction of apoptosis and caspase activation by garlic organosulfur compounds are complex and only partially known. Studies have shown that garlic organosulfur compounds stimulated mitochondrial apoptotic pathway. DADS-induced apoptosis in breast cancer cells was correlated with upregulation of Bax and down-regulation of Bcl-x_L (88). A change in intracellular Bcl2/Bax ratio was also observed in DAS-, DADS- and garlic extract-treated lung cancer cells (89). Kwon reported that DADS increased production of intracellular hydrogen peroxide in human leukemia HL-60 cells and DADS-induced apoptosis was prevented by preincubation with catalase and by the presence of exogenous antioxidants, such as N-acetylcysteine, suggesting reactive oxygen species mediated DADS-induced apoptosis (90). The same results were also reported in DADS-treated human bladder cancer cells T24 where DADS induced apoptosis through activation of mitochondrial pathway: decreased Bcl-2 level, cytochrome c release into the cytosol, caspase-3 activation, PARP degradation as well as an increase in intracellular hydrogen peroxide production (91). Reactive oxygen species(ROS) production was also reported in neuroblastoma cells SH-SY5Y following DADS treatment, which was assumed to activate the JNK/c-Jun transduction pathway (92). In HepG2 cells, DADS increased phosphorylated p38 MAPK and phosphorylated p42/44 MAPK presumably as a consequence of oxidative stress (93). Xiao et al. reported that DATS-induced apoptosis in human prostate cancer PC-3 cells was associated with phosphorylation of Bcl-2 , activation of caspase-9 and -3, and activation of ERK1/2 and JNK1. Overexpression of catalase inhibited DATS-induced JNK activation and apoptotic death

(94). These studies showed that oxidative stress may play an important role in the apoptosis induction by garlic organosulfur compounds. Some other studies have suggested that apoptosis induction by garlic organosulfur compounds can be connected with an increase in free intracellular calcium (Ca^{2+}) level. Disruption of cellular Ca^{2+} homeostasis can lead to apoptosis. It has been shown that DADS induced a dose-dependent increase in intracellular Ca^{2+} levels in colon tumor cells HCT-15 and lung cancer cells A549 as early as 4 minutes after treatment (95). Parl et al. found that the treatment of HCT-15 cells with BAPTA, an intracellular Ca^{2+} chelator, abolished DADS-induced Ca^{2+} elevation and hydrogen peroxide production, which further prevented caspase-3 activation and DNA fragmentation (96).

1.3 Natural seleno-compounds in cancer prevention

Selenium is an important trace element involved in different physiological functions of human body. There are several seleno-compounds in tissues of plants and animals. Basic research and clinical studies have supported the protective role of selenium against various types of cancers.

1.3.1 Chemistry and metabolism of natural seleno-compounds

1.3.1.1 Seleno-compounds in plants

The most common inorganic forms of selenium that exist in nature are selenite (Se^{4+}) and selenate (Se^{6+}), which plants absorb from the soil. Selenate is the inorganic form of selenium commonly present in plants. Plants are also capable of synthesizing selenoamino acids from selenite and selenate. Selenite and selenate are reduced to selenide (Se^{2-}) by a number of steps that involved reduced glutathione. Selenide reacts with O-acetylserine to form selenocysteine in a manner directly analogous to S metabolism. The S-amino acid cysteine is the starting point for a series of reactions that lead to the synthesis of methionine, and it has been postulated that selenocysteine is also metabolized by this same pathway. Se enters the food chain through incorporation into plant proteins, mostly as selenocysteine and selenomethione (SM) at normal Se level. However, with elevated Se levels, Se-methylselenocysteine (MSC) can be the predominant seleno-compound. There are several other non-protein seleno-compounds identified in plants including γ-glutamyl-

selenocystathionine, γ-glutamyl-Se-methylselenocysteine, Se-methylselenomethionine, selenocystathionine and selenopeptide. However, their concentrations are usually very low. Synthesis of the non-protein seleno-amino acids by plants probably occurs along pathways normally associated with S metabolism. Conversion of selenocysteine to MSC has been shown to involve the transfer of a methyl group from S-adenosylmethionine analogous to the synthesis of S-methylcysteine. (97, 98) (**Figure 1.2**)

The selenium content of plants is dependent upon the region of growth, and vegetables such as rutabagas, cabbage, peas, beans, carrots, tomatoes, beets, potatoes and cucumbers contained a maximum of 6 μg selenium per gram even when grown on seleniferous soil. Some other plants such as onions and asparagus can accumulate extremely large amounts of selenium, ranging from 1000 to 10,000 μg selenium per gram and these plants are called indicator plants or selenium accumulators. As much as 80% of the total selenium in these accumulator plants is present as MSC (99).

The chemical forms of selenium in enriched plants or supplements are as follows: most of the selenium in enriched wheat grain, maize, rice and soybeans is present as SM; in selenium-enriched yeast, which is a common source of selenium available commercially, 16-62% selenium is present in the form of SM depending on the sources of yeast; The major form of selenium in Se-enriched garlic, onions, broccoli florets, broccoli sprouts and wild leeks is MSC (99).

1.3.1.2 Seleno-compounds in animals and humans

When selenium is absorbed in the inorganic form of selenite or selenate, the higher-valence Se is reduced to the selenide state using reducing equivalents from reduced glutathione and reduced NADPH. Selenide is further transformed into selenocysteine via cotranslational biosynthesis (100). When rats are injected with selenite, the majority of the Se is present in tissues as selenocysteine (101). Selenocysteine can be degraded to selenide by the enzyme β-lyase, or can be incorporated into proteins to form selenoproteins. There are twenty-five selenoproteins that have been identified in eukaryotes, in all of which, selenium is present as selenocysteine. These selenoproteins include glutathione peroxidases, thioredoxin reductases, and deiodinases.

There is no known pathway in animals for synthesis of selenomethionine (SM) from selenocysteine or inorganic selenium. Upon absorption, selenomethionine can be incorporated randomly in animal proteins in place of methionine. By contrast, the incorporation of selenocysteine into proteins is not random and selenocysteine has its own triplet code. SM can also undergo transsulfuration to produce selenocysteine, or like methionine, be catabolized via transamination-decarboxylation pathway (102). Unlike SM, Se-methylselenocysteine (MSC) cannot be incorporated non-specifically into proteins. The absorbed MSC has been reported to be cleaved by a lyase to form methylselenol in the tissue (103). The excretion of Se occurs by the methylation or sugar derivation of selenides. Methylselenol and dimethylselenide are excreted across the lungs, and trimethylselenonium and selenosugar are excreted in urine (100).

1.3.2 Anticancer activities of natural seleno-compounds

There have been numerous epidemiological studies, the majority of which strongly suggest protective role of selenium against prostate, lung, colorectal, stomach and other cancers (104-111). The epidemiological findings have provided encouragement in the possible use of seleno-compounds as potential cancer chemopreventive agents.

Trials with human subjects. There have been nine trials conducted on the effects of Se supplementation on the incidence of cancer or biomarkers in human subjects. Except the recent Selenium and Vitamin E Cancer Prevention Trial (SELECT), the other eight have shown positive effects of Se, as reviewed in (102) .

In vivo studies have been conducted and provided strong evidence that seleno-compounds can inhibit tumorigenesis of various cancers induced by chemical carcinogens in mice or rats, as listed in **Table 1.3**. There were also several studies on the relationship between tumor cell growth/metastasis to seleno-compounds *in vivo* using the xenograft models. Selenite was shown to inhibit prostate LAPC-4 and colon SW480 tumor growth in nude mice (112, 113). Yan et al. reported that selenite and SM inhibited metastasis of melanoma cells in mice (114, 115). Xu et al. reported that Se-enriched green tea extract significantly suppressed HepG2 human hepatoma cell growth in Kunming mice (116).

In vitro studies also generated data supporting the chemopreventive effects of seleno-compounds in various cancer cell lines (**Table 1.4**).

1.3.3 Mechanisms of cancer prevention by natural seleno-compounds

Role of selenoenzymes. Selenium is an essential part of enzyme glutathione peroxidase. The glutathione peroxidase is an antioxidant enzyme involved in removal of hydroperoxides and lipid hydroperoxides which is critical in the enzymatic chemopreventive action of selenium (117). Another selenoprotein thioredoxin reductase is also involved regeneration of anti-oxidant systems, maintenance of intracellular redox state, and reduction of nucleotides in cell synthesis. It has been also found to be critical for cellular viability and proliferation (118). Behne *et al.* have shown chemopreventive nature of another 15kDa selenoprotein against development of carcinoma in human prostate cells (119).

Effects on carcinogen metabolism. In rats, treatment with selenite decreased dimethylbenz(a)anthracene–DNA adduct formation, thus reducing its carcinogenetic effects (120). Selenite was also shown to reduce the hepatic microsomal production of mutagenic metabolites of benzo(a)pyrene (121).

Cell cycle arrest and induction of apoptosis. In cultured cell models, seleno-compounds have been shown to inhibit cancer cell growth by decreasing cell proliferation through cell cycle arrest and/or increasing apoptosis (**Table 1.4**). It has been assumed that hydrogen selenide and methylselenol are major pools of seleno-compounds' metabolites that induce distinct types of biochemical and cellular responses (122, 123). Hydrogen selenide, the primary active metabolite of selenite, can cause apoptosis and S/G2-M cell cycle arrest by first inducing redox-mediated DNA single-strand breaks (124). Another active metabolite of seleno-compounds, methylselenol, appears to inhibit specific protein kinases, cyclin-dependent kinases, and target a growth control mechanism during G1 in a manner similar to that of PI3K inhibitors (125).

Effects on tumor cell invasion. It was reported that brief pre-exposure of HeLa cells to selenite resulted in a dose-dependent decrease in the rate of their subsequent attachment to a solid matrix, and these effects involved reduced adhesion to the collagen matrix. Studies

have suggested that selenite can suppress the expression of matrix metalloproteinases (MMPs) and urokinase-type plasminogen activator while up-regulating the expression of a tissue inhibitor of metalloproteinase 1, an effect directly related to the inhibition of tumor cell invasion (126). Methylseleninic acid, the precursor of methylselenol, was also shown to inhibit pro-MMP-2 activation and tumor cell migration and invasion capacity (127). Methylseleninic acid was also reported to inhibited the expression and secretion of vascular endothelial growth factor in several cancer cell lines and in vascular endothelial cells, indicating its potential antiangiogenic effects on the cheoprevention of cancer (128).

1.4 Significance of dissertation work

Dietary organosulfur and organoselenium compounds have shown chemopreventive effects in colon cancer *in vitro* and *in vivo*, but the underlying mechanisms are not fully understood. This dissertation work proposed a new paradigm for the anticancer activities of these compounds, i.e. via generation of HDAC-inhibiting metabolites, and would help design new therapeutic strategy for the treatment of colon cancer from the perspective of epigenetic regulation.

Short-chain fatty acids

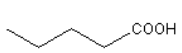

Butyrate

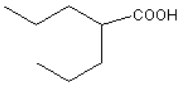

Valproate

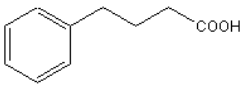

Phenylbutyrate

Hydroxamic acids

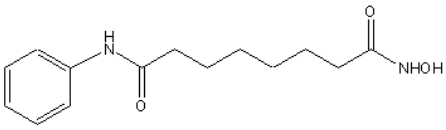

Suberoylanilide hydroxamic acid (SAHA)

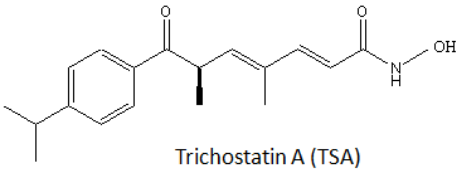

Trichostatin A (TSA)

Benzamides

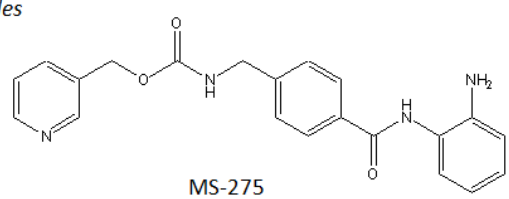

MS-275

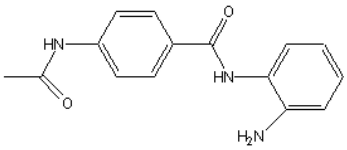

CI-994

Cyclic peptides

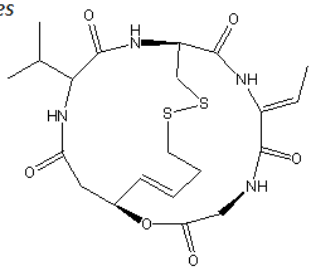

Depsipeptide (FK-228)

Figure 1.1 Classification of HDAC inhibitors.

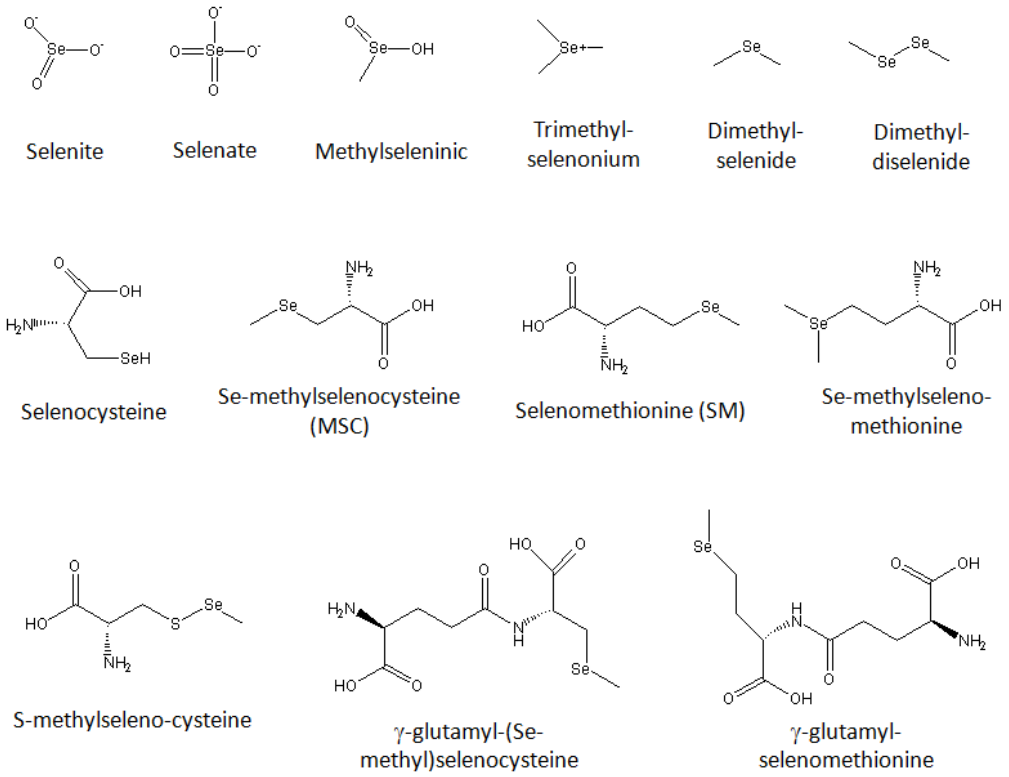

Figure 1.2 Structures of seleno-compounds

Table 1.1 *In vivo* studies on anticarcinogenetic effects of garlic organosulfur compounds

Garlic organosulfur compounds	Cancer type	Aminal model	References
Ajoene	Skin	Mouse	(129)
DAS	Skin	Mouse	(130)
	Mammary gland	Rat	(84)
	Lung	Rat	(84)
	Liver	Rat	(131)
	Colon	Rat	(132)
	Esophagus	Rat	(133)
	Forestomach	Rat	(134)
DADS	Colon	Rat	(135)
	Skin	Mouse	(136)
	Mammary gland	Rat	(137)
	Esophagus	Rat	(133)
	Renal	Rat	(138)
DATS	Prostate	Mouse	(139)
SAMC	Prostate	Mouse	(140)
SAC	Colon	Rat	(141)
	Liver	Rat	(142)
Garlic powder	Mammary gland	Rat	(143)
Garlic extract	Cervical	Mouse	(144)
	Colorectum	Rat	(145)
	Skin	Mouse	(146)

(Updated from (45))

Table 1.2 *In vitro* studies on the anticancer effects of garlic organosulfur compounds

Garlic organosulfur compounds	Cancer cell lines	Mechanisms	References
Ajoene	human leukemia	ROS generation, activation of NFkB	(147)
	HL-60 human leukemia	G2/M arrest, total amount of proteasome increased	(148)
DATS	MCF-7 breast cancer	Induced apoptosis, upregulated FAS, cyclinD1, Bax and p53, inhibit anchorage-dependent growth of cells	(149)
	T24 bladder cancer	induced Bcl-2 and caspase-3-dependent apoptosis via downregulation of Akt phosphorylation	(150)
	H358 and H460 lung cancer	G2/M arrest, Bax- and Bak-mediated apoptosis	(151)
	DU145 and PC3 prostate cancer	c-Jun and Erk-induced phosphorylation of Bcl-2, apoptosis, cell cycle arrest, Akt inactivation, ROS generation	(82, 152)
	BGC823 gastric cancer	apoptosis	(153)
	J5 human liver tumor	G2/M arrest, total amount of proteasome increased	(79)
	HepG2 human hepatoma	decreased expression of phase-1 enzymes induced by B(a)P	(154)
	HCT-15 and DLD-1 colon tumor	apoptosis, G2/M arrest, inhibition of tubulin polymerization	(155)
	KB-C2	modulation of MDR	(156)
	HEK293T human keratinocytes	Cox-2 inhibition	(157)
DADS	HepG2 human hepatoma	decreased expression of phase-1 enzymes induced by B(a)P	(154)
	MCF-7 breast cancer	inhibit anchorage-dependent growth of cells	(149)
	HL-60 human leukemia	inhibition of NAT activity and DNA-AAF adducts formation	(158)
	HT29 colon adenocarcinoma	G2/M arrest, decreased polyamine biosynthesis, increased intracellular Ca ions, DNA fragmentation	(159)
	non small cell lung cancer	apoptosis, p53 and Bax upregulation, Bcl-2 down-regulation	(160)

Table 1.2 *continued*

Garlic organosulfur compounds	Cancer cell lines	Mechanisms	References
DADS	HCT116 human colon cancer	G2/M arrest, apoptosis	(161)
	H1299 lung ccarcinoma	G2/M arrest, increased MAPK phosphorylation	(162)
	A549 lung cancer	increased intracellular ROS, cell cycle arrest, apoptosis	(163)
	SH-SY5Y neuroblastoma	ROS induction, G2/M arrest, apoptosis through mitochondrial pathway, downregulation of JNK pathway	(164)
	Caco-2 and HT29 human colon adenocarcinoma	cell proliferation inhibition, inhibition of histone deacetylase activity, increased p21 expression	(92)
	HEK293T human keratinocytes	Cox-2 inhibition	(157)
DAS	Colo 320 DM human colon carcinoma	increased ROS production, cell cycle arrest, apoptosis	(165)
	HL-60 human leukemia	inhibition of NAT activity and DNA-AAF adducts formation	(158)
	non small cell lung cancer	apoptosis, p53 and Bax upregulation, Bcl-2 down-regulation	(160)
	KB-C2	modulation of MDR	(156)
	K562 human leukemia	modulation of MDR	(166)
SAMC	HEL and OCIM-1 erythroleukemia	cell cycle arrest, apoptosis	(167)
	MCF-7 breast cancer, CRL-1740 prostate cancer	antiproliferation	(168)
	SW480 human colon cancer	G2/M arrest, apoptosis	(83)
SAC	MDA-MB-231 breast tumor	tumor cell adhesion and invasion	(169)
Garlic extract	human leukemia	proliferation inhibition	(170)

(Updated from (45))

Table 1.3 *In vivo* studies on the anticarcinogenetic effects of natural seleno-compounds

Seleno-compounds	Cancer type	Animal model	References
selenite	Liver	Rat	(171, 172)
	Mammary	Rat	(120)
	Intestinal	Mouse	(173)
	Hepatic and renal	Rat	(174)
	Colon	Rat	(175)
Se-methylselenocysteine	Mammary	Rat	(176)
	Prostate	Rat	(177)
	Prostate	Mouse	(178)
selenomethionine	Liver	Rat	(179)
	Mammary	Rat	(180)
Se-propylselenocysteine	Mammary	Rat	(176)
Se-allylselenocysteine	Mammary	Rat	(176)
Se-enriched Brazil nuts	Mammary	Rat	(181)
Se-enriched broccoli	Colon	Rat	(182-184)
	Mammary	Rat	(183)
Se-enriched garlic	Mammary	Rat	(185, 186)
se-enriched Japanese radish sprout	Breast	Rat	(187)
Se-enriched Kaiware radish sprouts	Colon	Rat	(188)
Se-enriched malt	Hepatocarcinoma	Rat	(189)
Se-enriched egg	Skin	Rat	(190)

Table 1.4 *In vitro* studies on the anticancer effects of natural seleno-compounds

Seleno-compound	Cancer cell line	Mechanisms	References
selenite	L1210 mouse leukemia	induction of DNA strand breaks and apoptosis	(191)
	MCF-7 and MDA-MB 231 human breast cancer	proliferation inhibition	(192)
	HT1080 human fibrosarcoma	invasion inhibition, reduced expression of MMP-2, MMP-9 and urokinase-type plasminogen activator, increased expression of metalloproteinase-1	(126)
	HT29 human colon carcinoma	induction of differentiation and apoptosis	(193)
	LnCap human prostate cancer	induction of apoptosis by generation of superoxide	(194)
	Hela Hep-2 cervical carcinoma	activation of p38 and p53 pathways, induction of caspase-independent apoptosis	(195)
	human brain tumor	inhibition of invasion and induction of apoptosis	(196)
	HCT116 colon cancer	G2 arrest, increased expression of Cyclin B1, Cdc2, p34 and p21	(197)
	DU-145 prostate caner	increased the activity of PTEN	(198)
	colon cancer	induction of redox-dependent Bac activation and apoptosis	(199)
Se-methyl-selenocysteine	TM6 mouse mammary epithelial tumor	reduced PKC activity,decreased cdk2 activity, elevated gadd gene expression; activated caspase-3 and PARP cleavage; inhibited PI3-K activity; dephosphorylated Akt and p38; reduced expressin of osteopontin	(200-203)
	MDA-MB-231 breast cancer	inhibited proliferation, induced apoptosis and cell cycle arrest	(204)
	LnCap prostate cancer	altered the expression of several types of collagen	(205)
	Caki renal cancer	sensitized TRAIL-mediated apoptosis via down-regulation of Bcl-2 expression	
	SKOV-3 ovarian cancer	induced apoptosis, activated caspase-3 and Bax cleavage, decreased expression of IAP family proteins,	(206)

Table 1.4 ***Continued***

Seleno-compound	Cancer cell line	Mechanisms	References
Se-methyl-selenocysteine	Colon cancer	antiproliferation	(207)
seleno-methionine	HCA-7 colon cancer	suppressed COX-2 expression	(208)
	SNU-1 gastric adenocarcinoma	stimulated ERK phophorylation and induced apoptosis	(209)
	SW48 colon cancer	sustained ERK and P90rsk activation, phosphorylation of histone H3, growth inhibition	(210)
	MCF-7/S breast carcinoma, DU-145 prostate cancer, UACC-375 melanoma	growth inhibition, cell cycle arrest, apoptosis	(211)
	murine melanoma	suppressed the invasive potential	(114)
	HCT116 colon cancer	inhibition of cyclin B and cdc2 kinase activity, growth inhibition	(212)
Se-allylseleno-cysteine	TM2H and TM12 mouse mammary tumor	growth inhibition, apoptosis, increased expression of p53, p21 and p27	(213, 214)
Se-enriched broccoli sprout	LnCap human prostate cancer	proliferation inhibition, apoptosis	(215)
Se-enriched garlic	MOD mouse mammary tumor	growth inhibition, cell cycle arrest, apoptosis	(216)

Modulation of histone deacetylase activity by dietary isothiocyanates and allyl sulfides: studies with sulforaphane and garlic organosulfur compounds

Hui Nian, Barbara Delage, Emily Ho, and Roderick H. Dashwood

Environmental and Molecular Mutagenesis
John Wiley & Sons, Inc. 605 Third Avenue, New York, New York 10158-0012
50:213-221 (2009)

2.1 Abstract

Histone deacetylase (HDAC) inhibitors reactivate epigenetically-silenced genes in cancer cells, triggering cell cycle arrest and apoptosis. Recent evidence suggests that dietary constituents can act as HDAC inhibitors, such as the isothiocyanates found in cruciferous vegetables and the allyl compounds present in garlic. Broccoli sprouts are a rich source of sulforaphane (SFN), an isothiocyanate that is metabolized via the mercapturic acid pathway and inhibits HDAC activity in human colon, prostate, and breast cancer cells. In mouse preclinical models, SFN inhibited HDAC activity and induced histone hyperacetylation coincident with tumor suppression. Inhibition of HDAC activity also was observed in circulating peripheral blood mononuclear cells obtained from people who consumed a single serving of broccoli sprouts. Garlic organosulfur compounds can be metabolized to allyl mercaptan (AM), a competitive HDAC inhibitor that induced rapid and sustained histone hyperacetylation in human colon cancer cells. Inhibition of HDAC activity by AM was associated with increased histone acetylation and Sp3 transcription factor binding to the promoter region of the *P21WAF1* gene, resulting in elevated p21 protein expression and cell cycle arrest. Collectively, the results from these studies, and others reviewed herein, provide new insights into the relationships between reversible histone modifications, diet, and cancer chemoprevention.

2.2 Introduction

There is much interest in the study of isothiocyanates and allyl sulfides, and the foods from which they are derived (217-222). For instance, entering the terms “isothiocyanates” and “allyl sulfides” into PubMed resulted in 10282 and 600 citations, respectively. This journal lists several papers on the topic, describing the antimutagenic effects of garlic extract in the Salmonella assay and in Chinese hamster ovary cells (223); the anti-clastogenic properties of garlic extract in mice given mitomycin C, cyclophosphamide, or sodium arsenite [(224); the protection by *Brassica campestris* mustard leaf towards chromosomal damage and oxidative stress induced by γ-radiation, cyclophosphamide, and urethane in mice (225); the inhibitory effects of diallyl sulfide in Chinese hamster V79 cells treated with dimethylnitrosamine (226);

and the anti-genotoxic activity of sulforaphane (SFN) in cultured human lymphocytes treated with ethyl methanesulfonate, vincristrine, H_2O_2, and mitomycin C(227).

SFN is an isothiocyanate, derived from glucoraphanin in broccoli and broccoli sprouts, that was first identified as a potent inducer of phase 2 detoxification enzymes (228) (229). Enzyme induction occurs via the Kelch-like ECH-associated protein 1–nuclear factor E2-related factor-2 (Keap1-Nrf2) pathway, although other mechanisms have been implicated in the chemoprotective effects of SFN (see (218, 221, 230, 231) for recent reviews). A phase I clinical study of broccoli sprout extracts examined the safety, tolerance, and metabolism of constituent glucosinolates and isothiocyanates in human volunteers (232).

Similarly, organosulfur compounds from *Allium* vegetables have garnered significant interest due to their reported health benefits, including anti-cancer properties (217, 233-238). A recent study, for example, found odds ratios among persons with high *versus* low intakes of garlic and onions that were associated with a significantly reduced risk of colorectal adenoma (239).

Our interest in dietary isothiocyanates and allyl sulfides evolved out of the growing body of evidence connecting their cancer chemopreventive effects with epigenetic mechanisms, and in particular the modulation of histone acetylation status and histone deacetylase (HDAC) activity. These findings are reviewed in the following sections.

2.3 HDAC inhibitors and cancer therapy

The term “epigenetics” refers to heritable changes in gene function that occur without a change in DNA sequence(240). Epigenetic changes have been implicated in the deregulation of gene expression during cancer development (241-243). There is much excitement in this area because, in contrast to genetic alterations, epigenetic changes are potentially modifiable. Epigenetic abnormalities can affect both the DNA methylation status and the pattern of histone “marks” in cancer cells, resulting in inappropriate gene silencing (221, 243). For example, loss of monoacetylation and trimethylation of histone H4 lysine 20 is a common hallmark of human tumor cells (244), and the risk of prostate cancer recurrence is predicted by altered patterns of histone acetylation and methylation (245). Human gastric

adenomas and carcinomas have reduced levels of acetylated histone H4[(246), and in human colon cancer cells expression of the cell cycle regulator $p21^{WAF1}$ (p21) is influenced by the acetylation status of histone H3 (247).

Histone acetylation typically results in an 'open' chromatin configuration that facilitates transcription factor access to DNA and gene transcription, but the reverse scenario can silence tumor suppressor genes in cancer cells (248). The acetylation and deacetylation of histones is catalyzed, respectively, by histone acetyltransferases (HATs) and histone deacetylases (HDACs). Over-expression and/or increased activity of HDACs occurs in many malignancies, and the repression of transcription can result in dysregulated cell cycle kinetics, apoptosis, and differentiation (249-251). HDAC inhibitors are a current 'hot topic', and in the past year alone over 300 publications mentioning HDAC inhibitors were cited in PubMed.

In cancer cells, HDAC inhibitors have the ability to de-repress epigenetically-silenced genes, resulting in the re-expression of cell cycle regulators that trigger growth arrest, apoptosis, or differentiation (252). This is not a genome-wide "shotgun" approach to gene activation, since only a select cadre of genes appears to be affected. For example, about 2-5% of silenced genes were reactivated within the initial hours of HDAC inhibitor treatment (253, 254), and p21 was an early target for upregulation (255-257).

Much of the work in this area has focused on competitive HDAC inhibitors with a hydroxamic acid functional group, such as trichostatin A (TSA) and suberoylanilide hydroxamic acid (SAHA) (255, 258-260). SAHA is marketed as Vorinostat (Zolinza®), and has shown promise in the treatment of patients with advanced cutaneous T-cell lymphoma (261). However, resistance to HDAC inhibitor drugs is of clinical concern in many patients, as well as toxicity, due to factors such as pharmacokinetics and the tumor micro-environment (262). As a consequence, there are ongoing efforts to develop newer class- and isoform-selective HDAC inhibitors (263, 264).

2.4 Dietary HDAC inhibitors – a chemoprevention paradigm

Based on some of the issues and concerns about HDAC inhibitor drugs currently used in the clinical setting, we turned our attention to dietary agents with structural features that might be compatible with HDAC inhibition. A simple working hypothesis was that the clinical response to HDAC inhibitor drugs, including pharmacokinetic variations, might be influenced by other HDAC inhibitors in the patient's diet.

As a starting point, we focused on food constituents with chemical structures that contained a spacer 'arm' that might fit the HDAC active site, and a functional group that could interact with the buried catalytic zinc atom(249, 250, 265). We were guided by prior work indicating that a carboxylate group can substitute for the hydroxamic acid moiety in binding to zinc within the HDAC pocket. Over three decades ago, the short-chain fatty acid butyrate was observed to cause histone modifications in HeLa and Friend erythroleukemia cells (266). Butyrate is generated during the fermentation of dietary fiber in the large intestine, and serves as the primary metabolic fuel for the colonocytes (267, 268). Recent studies identified butyrate as a competitive HDAC inhibitor, with an apparent inhibition constant (K_i) on the order of 46 μM (269).

Interestingly, carboxylate-based HDAC inhibitors are gaining interest in the treatment of a wide range of maladies besides cancer. The antiepileptic agent valproic acid (Depakene®, Convulex®) and the hyperammonemia drug phenylbutyrate (Buphenyl®) are clinically-used compounds with HDAC inhibitory activity (270, 271). Other applications may be found in treating bipolar disorder, Parkinson's disease, rheumatoid arthritis, amyotrophic lateral sclerosis, and Huntington's disease(270, 272-276), and this list is likely to grow in the future.

2.5 Isothiocyanates as HDAC inhibitors

In addition to butyrate, what other dietary constituents might contain a 'spacer-carboxylate' arrangement in their chemical structure? We hypothesized that SFN might act as an HDAC inhibitor, based on the published literature describing p21 induction and cell cycle arrest/apoptosis in various human cancer cell lines (277-281). Like other isothiocyanates, SFN is metabolized via the mercapturic acid pathway, and computer modeling predicted that

SFN-cysteine (SFN-Cys) was a good fit for the HDAC active site (**Figure 2.1**). HDAC inhibition was not observed in a cell-free assay with parent SFN, or when HeLa cells were treated prior to SFN exposure with a chemical that blocked the mercapturic acid pathway. However, when HeLa cells were incubated with 3-15 μM SFN, the surrounding media contained metabolite(s) that inhibited HDAC activity in the cell-free assay (282). Subsequent studies confirmed the HDAC inhibitory effects of SFN in human colon and prostate cancer cells (282, 283), as well as in human breast cancer cell lines (284). HDAC inhibition in prostate BPH-1, LnCaP, and PC3 cells was associated with increased global histone acetylation, along with localized histone hyperacetylation on the promoter regions of *P21WAF1* and *BAX*.

In vivo, dietary SFN retarded the growth of PC3 prostate cancer xenografts and spontaneous intestinal polyps in mouse preclinical models (285, 286), with evidence for HDAC inhibition and increased histone acetylation in tissues such as the gastrointestinal tract, prostate, and peripheral blood mononuclear cells (PBMCs). PBMCs have been used in human clinical trials with HDAC inhibitor drugs, serving as a surrogate for the changes that might be anticipated in other tissues with respect to HDAC activity and histone status (252, 261, 287). Thus, we performed a pilot study with SFN-rich broccoli sprouts in human volunteers (286). In brief, healthy volunteers in the age range 18–55 yrs, with no history of non-nutritional supplement use, refrained from cruciferous vegetable intake for 48 hours, and each person then consumed 68 g of broccoli sprouts with a bagel and cream cheese. Blood was drawn at 0, 3, 6, 24, and 48 hours, and PBMCs were assayed using a commercial HDAC activity kit. HDAC activity was inhibited as early as 3 hour after broccoli sprout intake, it returned to normal by 24 hours, and there was a concomitant induction of histone acetylation (286, 288). This was the first study to show that a naturally consumed food, broccoli sprouts, had such a marked effect on HDAC activity and histone acetylation in humans.

Importantly, the pilot study in human volunteers addressed, in part, the question of whether concentrations that inhibit HDAC activity *in vitro* might ever be achievable *in vivo*; by operational definition, the consumption of broccoli sprouts in human volunteers provided sufficiently high concentrations in PBMCs to affect HDAC activity and histone acetylation status. Because this might be due to SFN and/or other phytochemicals in broccoli sprouts,

we are repeating the studies to determine the specific concentrations of SFN and its metabolites achieved in human plasma and urine, following single and multiple ingestions of broccoli sprouts. Once the range of SFN concentrations in human PBMCs is established after broccoli sprout consumption, these data will be used to advance *in vitro* mechanistic studies. The latter will include "loss of function" experiments to define the relative importance of HDAC inhibition versus other potential mechanisms of chemoprevention. It is noteworthy that under conditions in the *Apc*^{min} mouse in which the development of spontaneous intestinal polyps was inhibited, tissue concentrations of SFN were in the range 3-30 μM (289), which is comparable to doses that inhibited HDAC activity in human colon cancer cells (282).

2.6 Allyl compounds as HDAC inhibitors

We also became interested in the inhibition of HDAC activity by dietary organosulfur compounds, such as those found in garlic (**Figure 2.2**). Induction of histone acetylation was reported previously in cancer cells treated with the garlic compounds diallyl disulfide (DADS) and *S*-allyl mercaptocysteine (SAMC) (290, 291), suggesting that these compounds may alter HDAC enzymes. In primary rat hepatocytes, DADS is metabolized to allyl mercaptan (AM) within 30 min (292), which is noteworthy given that AM was more effective than its precursors (DADS, SAMC) at inhibiting HDAC activity in cell-free conditions (164).

We screened several garlic organosulfur compounds and identified AM as the most potent HDAC inhibitor in assays with HeLa nuclear extracts, lysates from human colon cancer cells, or purified human HDAC8 (293). Using MacroModel® software v8.5 (Schrödinger Inc.) to execute iterative docking simulations with human HDAC8 (Protein Databank entry 1T67), AM was found to be a good fit for the enzyme active site (**Figure 2.3**). In an optimized truncated model, a strong interaction was predicted (-120 kcal/mol) between the buried zinc atom in the enzyme pocket and the sulfur atom of AM. Structure-activity studies confirmed the loss of HDAC inhibition after replacement of the –SH group in AM with an –OH moiety. Enzyme kinetics assays with a purified human HDAC provided evidence for a competitive mechanism (K_i = 24 μM AM).

Inhibition of HDAC activity by AM in human colon cancer cells was accompanied by a rapid, sustained accumulation of acetylated histones. Chromatin immunoprecipitation assays revealed an increase in acetylated histone H3 on the *P21WAF1* gene promoter within 4 hours of AM exposure, along with increased binding of the transcription factor Sp3. Twenty-four hours after AM treatment there was enhanced binding of p53 in the distal enhancer region of the *P21WAF1* gene promoter. The expression of p21(Waf1) protein was increased at time-points between 3 and 72 hours after AM treatment, and coincided with G1 growth arrest.

The working hypothesis is that metabolic conversion of organosulfur compounds to HDAC inhibitors *in situ* may contribute to the overall cancer chemoprotective properties of garlic and other *Allium* foods (68, 233). Support for this concept *in vivo* comes from studies demonstrating increased histone acetylation in colonocytes from rats treated with DADS (294), and in the liver of mice 6 h after oral exposure to AM, DADS, or garlic oil (**Figure 3S.**). It remains to be determined whether garlic organosulfur compounds can affect HDAC (or HAT) activities and histone acetylation in human volunteers, and without any associated toxicity (295). This is an important consideration, because dietary "chemopreventive" HDAC inhibitors typically are effective in the micromolar to millimolar range(240, 288, 296), whereas HDAC inhibitors used therapeutically are thought to be effective at nM concentrations, but not without some toxicity and drug resistance (262)

2.7 Future respective

The specific focus here has been on the HDAC inhibitory properties of dietary isothiocyanates and allyl compounds, but other compounds with the 'spacer-carboxylate' arrangement exist in the human diet and are worthy of further study (288, 296, 297). An evolving theme from this work is that metabolism plays a pivotal role in generating intermediates with HDAC inhibitory activity. We speculate that metabolic conversion of SFN to SFN-Cys might generate the 'ultimate' HDAC inhibitor, but this could hold true for several other dietary anticarcinogenic isothiocyanates, including those found in glucosinolate-containing plants such as mustard, radish, horseradish, wasabi, and daikon (220). Interestingly, the cysteine moiety in SFN-Cys occupied most of the HDAC active site in modeling simulations (**Figure**

2.1), but cysteine itself lacked appreciable HDAC inhibitory activity in vitro (296). This suggests that the Cys-conjugated intermediate is preferred, and that the isothiocyanate 'cap' group influences docking to the HDAC enzyme, perhaps helping to orient the inhibitor to the pocket region. Similar findings have been reported for hydroxamate-based HDAC inhibitors, where the 'cap' group influences enzyme specificity among various class I and class II HDACs (250, 298-300).

In the case of garlic and other *Allium* vegetables, water- and oil-soluble organosulfur compounds might be 'funneled' via metabolism to generate small molecule HDAC inhibitors, such as AM (**Figure 2.2**). AM exhibited competitive kinetics with purified human HDAC8, but this metabolite almost certainly reacts with other thiol-containing proteins, such as those in the microtubule network (301). An important avenue for future work will be to examine the relative importance of HDACs compared with other cellular targets of allyl compounds, under normal physiological conditions and food intake levels, bearing in mind that garlic supplements are popular in the U.S..

Finally, there is evidence that with oxidative stress, HDAC inhibition might result in genes becoming activated that further exacerbate the underlying pathological condition, such as in chronic obstructive pulmonary disease (302). Additional caveats were discussed elsewhere, such as the potential double-edge sword of targeting multiple HDAC enzymes (296). These considerations add to the growing fascination surrounding the study of diet, epigenetics, and cancer chemoprevention, and the possibility that HDAC inhibitors in food might help reverse aberrant patterns of histone changes in cancer cells. Broccoli with garlic sauce, anyone?

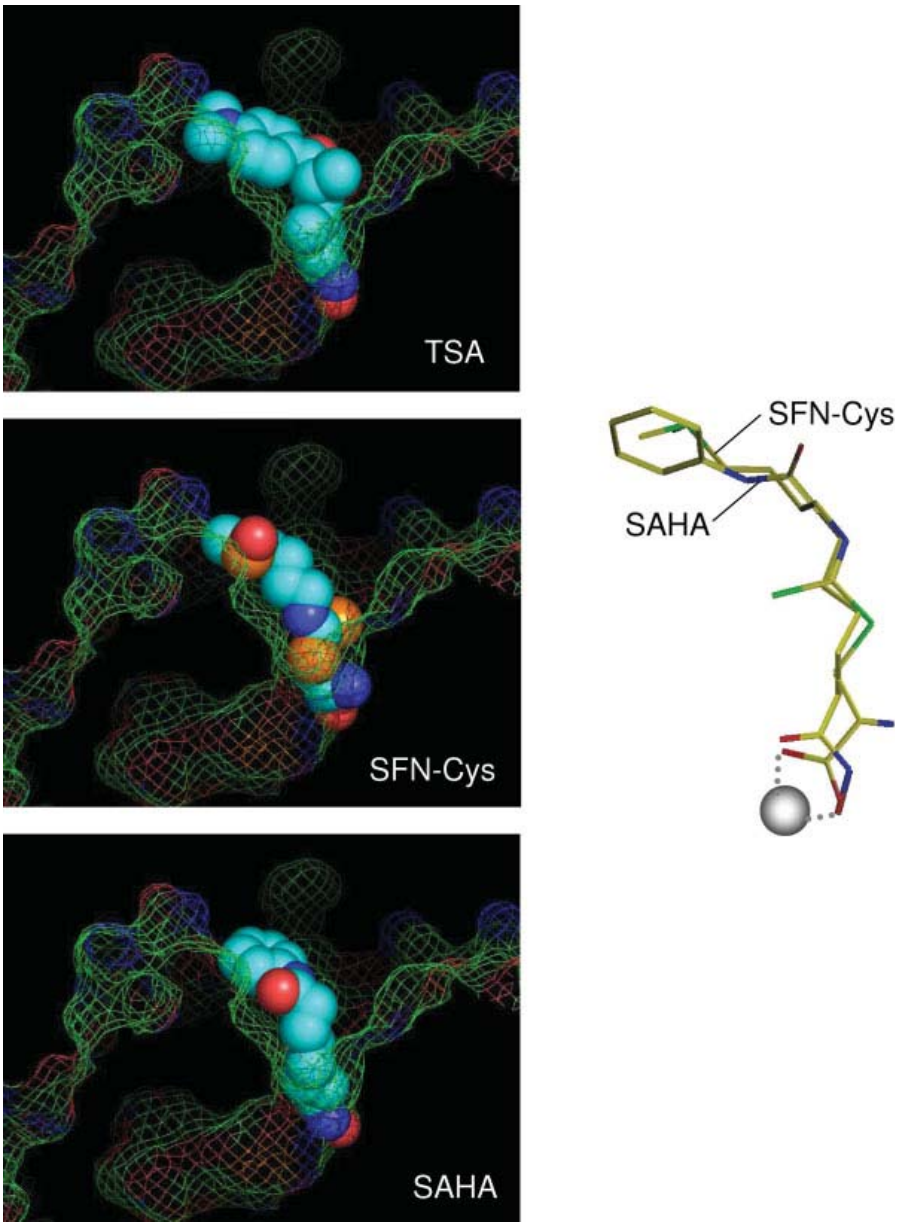

Figure 2.1 Inhibitors in the HDAC pocket. Binding of TSA (top) and SAHA (bottom) were from structural studies (303). Accelrys Insight II software was used to model interactions of putative inhibitors, with the following parameters: bidentate binding of the ligand to the zinc atom; H-bond partners for buried polar atoms; avoiding steric conflicts between ligand and enzyme based on a fixed protein; maintaining favorable torsion angles; following the favored positions of TSA and SAHA. SFN-Cys fit the HDAC pocket (center) and had comparable geometry to SAHA in the active site (right), with the α-carboxyl group of the cysteine moiety forming a bidentate ligand with the buried zinc atom (gray sphere). For full details, see (282).

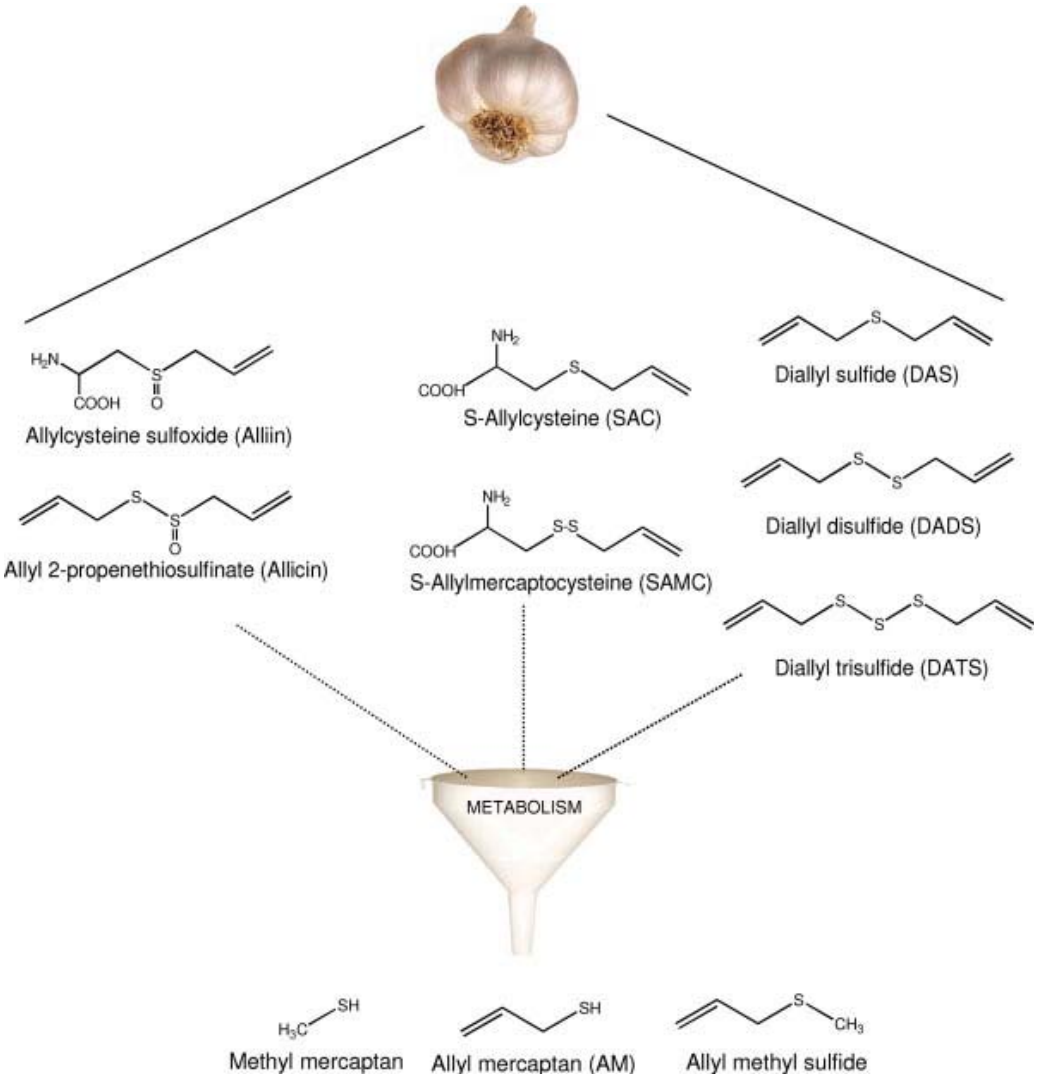

Figure 2.2 Organosulfur compounds in garlic. Garlic compounds such as Alliin, Allicin, *S*-allylcysteine (SAC), *S*-allyl mercaptocysteine (SAMC), diallyl sulfide (DAS), diallyl disulfide (DADS), and diallyl trisulfide (DATS) are metabolized to allyl mercaptan (AM), allyl methyl sulfide, and methyl mercaptan. AM was identified as a competitive HDAC inhibitor (K_i = 24 μM with human HDAC8) and induced histone acetylation in colon cancer cells (293).

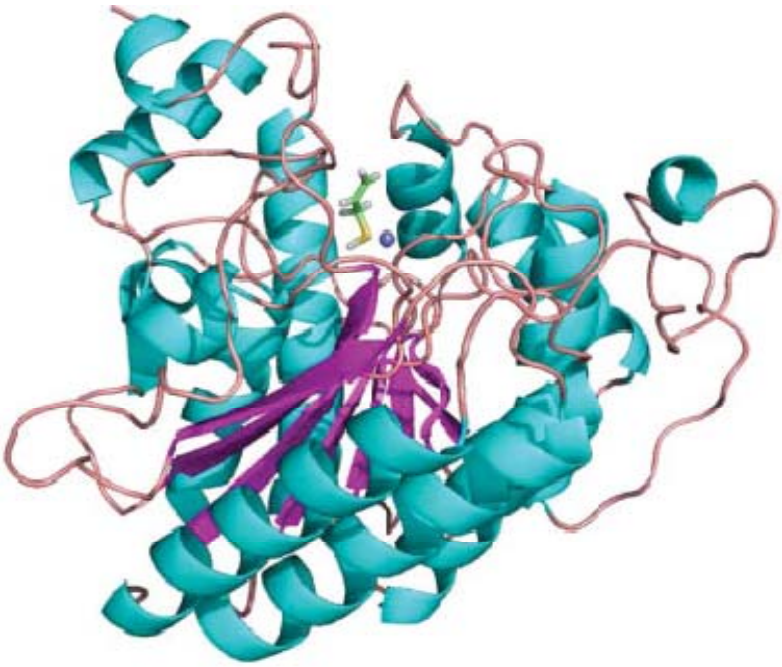

Figure 2.3 Allyl mercaptan docked in the HDAC pocket. The interaction of AM with human HDAC8 was simulated using MacroModel v8.5 and Jaguar v5.5 software (Schrödinger), as reported elsewhere (293). AM fit into the enzyme pocket with the sulfhydryl group (yellow) presumably ligated to the catalytic zinc atom (blue sphere).

Allyl mercaptan, a garlic-derived organosulfur compound, inhibits histone deacetylase and enhances Sp3 binding on the *P21WAF1* promoter

Hui Nian, Barbara Delage, John T. Pinto and Roderick H. Dashwood

Carcinogenesis

2001 Evans Road, Cary, NC 27513

Vol.29 no.9 pp1816-1824, 2008

3.1 Abstract

Histone deacetylase (HDAC) inhibitors have the potential to de-repress epigenetically-silenced genes in cancer cells, leading to cell cycle arrest and apoptosis. In the present study, we screened several garlic-derived small organosulfur compounds for their ability to inhibit HDAC activity *in vitro*. Among the organosulfur compounds examined, allyl mercaptan (AM) was the most potent HDAC inhibitor. Molecular modeling, structure-activity, and enzyme kinetics studies with purified human HDAC8 provided evidence for a competitive mechanism (Ki = 24 µM AM). In AM-treated human colon cancer cells, HDAC inhibition was accompanied by a rapid and sustained accumulation of acetylated histones in total cellular chromatin. Chromatin immunoprecipitation assays confirmed the presence of hyperacetylated histone H3 on the *P21WAF1* gene promoter within 4 hr of AM exposure, and there was increased binding of the transcription factor Sp3. At a later time, 24 hr after AM treatment there was enhanced binding of p53 in the distal enhancer region of the *P21WAF1* gene promoter. These findings suggest a primary role for Sp3 in driving *P21* gene expression after HDAC inhibition by AM, followed by the subsequent recruitment of p53. Induction of $p21^{Waf1}$ protein expression was detected at time-points between 3 and 72 hours after AM treatment, and coincided with growth arrest in G_1 of the cell cycle. The results are discussed in the context of other anti-carcinogenic mechanisms ascribed to garlic organosulfur compounds, and the metabolic conversion of such compounds to HDAC inhibitors *in situ*.

3.2 Introduction

Epigenetic changes play a pivotal role in the deregulation of gene expression during cancer development (241). For example, the silencing of tumor suppressor genes has been associated with aberrant patterns of histone acetylation in HT29 and other human colon cancer cells (304, 305). Histone acetylation and deacetylation is catalyzed, respectively, by histone acetyltransferases (HATs) and histone deacetylases (HDACs). Histone deacetylation typically produces a compact chromatin configuration that restricts transcription factor access to DNA and represses gene expression (248). HDAC inhibitors are gaining interest as potential anti-cancer drugs due to their ability to de-repress epigenetically-silenced genes in cancer cells, resulting in growth arrest, apoptosis, and differentiation(250, 306, 307).

Microarray analyses revealed that about 2-5% of genes were de-repressed within the initial hours of HDAC inhibitor treatment (253, 254), and the cell cycle regulator $p21^{WAF1}$ (p21) was an early target for upregulation (255-257).

Unsilencing of p21 has been reported in cancer cells treated with potent HDAC inhibitors (9,10), such as trichostatin A (TSA) and suberoylanilide hydroxamic acid (SAHA). The latter compound, marketed under the name Vorinostat, has shown promise in the treatment of advanced cutaneous T-cell lymphoma (262). Recently, attention has shifted to dietary agents that act as inhibitors of HDAC activity, including butyrate, sulforaphane, and organosulfur compounds from garlic (reviewed in (234, 288)).

Garlic, onions, leeks, and other *Allium* vegetables have numerous purported health benefits, including anti-cancer properties (45, 308-310). A recent study, for example, found odds ratios among persons with high *versus* low intakes of onions and garlic that were significantly associated with a lower risk of colorectal adenoma (239). Much interest has focused on garlic-derived organosulfur compounds. These compounds include oil-soluble constituents diallyl sulfide (DAS), diallyl disulfide (DADS), diallyl trisulfide (DATS), dithiins, and ajoene; water-soluble derivatives S-allyl cysteine (SAC) and S-allyl mercaptocysteine (SAMC); and metabolites allyl mercaptan (AM) and allyl methyl sulfide (AMS) (54, 292, 311). Such compounds can alter xenobiotic drug metabolizing enzymes and inhibit the formation of carcinogen-DNA adducts (74, 312). Garlic organosulfur compounds also produce anti-proliferative effects in cancer cells, leading to cell cycle arrest and/or apoptosis(84, 313) Interestingly, histone hyperacetylation associated with growth inhibition was reported in cancer cells treated with DADS (290) and SAMC (291), suggesting that these compounds may alter HDAC enzymes. In primary rat hepatocytes, DADS was metabolized to AM within 30 min (292), and AM was more effective than its precursors (DADS and SAMC) at inhibiting HDAC activity under cell-free conditions (164).

Based on these findings, we screened several garlic organosulfur compounds *in vitro* and identified AM as the most potent inhibitor of HDAC activity. In human colon cancer cells, AM induced the accumulation of acetylated histones and enhanced the binding of Sp3 and p53

transcription factors to the *P21WAF1* gene promoter. There was a corresponding increase in p21 mRNA and protein expression, resulting in cell cycle arrest and growth inhibition.

3.3 Materials and methods

Cell culture and reagents The HT29 human colon adenocarcinoma cell line was obtained from American Type Culture Collection and cultivated in McCoy's 5A medium (Life Technologies, Inc.) supplemented with 1% penicillin/streptomycin and 10% fetal bovine serum. TSA, AM, AMS, and DADS were purchased from Sigma-Aldrich (St. Louis, MO). SAC and SAMC were synthesized by Wakunaga of America Co. (Mission Viejo, CA). Cells (0.4×10^6) were seeded in 60 mm dishes 36 h prior to treatment. AM and TSA were dissolved in 0.1% dimethylsulfoxide (DMSO), and mixed with culture medium prior to addition to the cells. Control cultures were treated in parallel with 0.1% DMSO alone.

HDAC activity HDAC activity was determined using the Fluor-de-Lys HDAC activity assay kit (Biomol, Plymouth Meeting, PA), as reported before (282, 283, 285, 286). Incubations were performed at 37^0C with purified human HDAC8, HeLa nuclear extract (supplied with the kit), or HT29 cellular extract. Fluorescence was measured using a Spectra MaxGemini XS fluorescence plate reader (Molecular Devices), with excitation at 360 nm and emission at 460 nm.

Molecular modeling Molecular docking was carried out using MacroModel® software v8.5 (Schrödinger Inc., Portland, OR). Maestro GUI (Schrödinger Inc.) was used to set up and submit energy calculations to MacroModel®. AMBER* force field and MCMM applications within MacroModel® were used to execute flexible docking simulations. For these studies, we used the crystal structure of human HDAC8 with MS-344 inhibitor bound to the catalytic site (1T67 from the Protein Databank). Force field parameters for the zinc atom were taken from previous work on thermolysin (314). The covalent geometry of AM was generated using Maestro, and energy-minimization was performed prior to docking simulation. The flexible docking procedure consisted of iterative torsional sampling searches with structural perturbation followed by energy minimization. The AM molecule was fully flexible, whereas residues within the HDAC8 active site (including zinc) were held fixed in their original positions. A non-bonded model, in which van der Waals and electrostatic interactions alone

were considered, was used for preliminary docking work. The initial docking search started with AM positioned 10Å distance from the enzyme. The lowest-energy structure then was used to derive a truncated zinc-ligand model, which included the binding site residues Asp 178, Asp 167, and His 180 and the nearby AM molecule. Jaguar software v5.5 (Schrödinger Inc.) was used to compute the zinc electric charge distribution by fitting the partial charges to the electrostatic potential calculated at the B3LYP density function level with the LACVP* basis set. After obtaining the optimized stretching and bending parameters of zinc-heteroatom bonds, we fixed zinc-ligand bond lengths and angles and performed another round of conformational searches as described above. The overall lowest-energy structure was determined by considering QM energy of Zn-ligands and the potential energy of AM-HDAC without zinc.

MTT assay Cell growth was determined by assaying for the reduction of 3-(4,5-dimethylthiazol-2-yl)-2,5-diphenyltetrazolium bromide (MTT) to formazan. Briefly, after 24 hr and 48 hr of incubation with AM, TSA, or vehicle alone, 45 µl MTT (5 µg/µl) were added to cells (4×10^4/well) in 96-well plates. Cells were incubated at 37^0C for 4 hr, and a Spectra MaxGemini XS fluorescence plate reader (Molecular Devices) was used to measure absorbance at 620 nm for each well. Growth rate was calculated as follows: Cell growth = [A_{620} treated cells/A_{620} control cells] ×100%.

Flow cytometry Cells treated with vehicle, AM, or TSA for 24 hr were harvested in cold PBS, fixed in 70% ethanol, and stored at 4^0C for at least 48 hr. Fixed cells were washed with PBS once and resuspended in propidium iodide/Triton X-100 staining solution containing RNase A. Samples were incubated in the dark for 30 min before cell cycle analysis. The DNA content of the cells was detected using EPICS XL Beckman Coulter and analyses of cell distribution in the different cell cycle phases were performed using Multicycle Software (Phoenix Flow Systems, San Diego, CA).

Immunoblotting Protein concentration of cell lysates was determined using the BCA assay (Pierce, Rockford, IL). Proteins (20 mg) were separated by SDS-PAGE on 4-12% Bis-Tris gel (Novex, San Diego, CA) and transferred to nitrocellulose membranes (Invitrogen, Carlsbad, CA). Membranes were saturated with 2% BSA for 1 hr, followed by an overnight incubation

at 4^0C with primary antibodies against acetylated histone H3 (1:200, Upstate, #06-599), histone H3 (1:200, Upstate, #06-755), acetylated histone H4 (1:2000, Upstate, #06-866), histone H4 (1:2000, Upstate, #05-858), or p21 (1:1000, Cell Signaling, #2947). Membranes were incubated with peroxidase-conjugated secondary antibodies (Bio-Rad, Hercules, CA) for 1 hr. Immunoreactive bands were visualized by using Western Lightning Chemiluminescence Reagent Plus (PE Life Sciences, Boston, MA) and detected with an AlphaInnotech imager system. To ensure equal loading, all blots were re-probed for β-actin (Sigma, A5441).

RT-PCR and quantitative real-time PCR Cells treated with AM or TSA were disrupted by using QIAshredder spin column (QIAGEN, Santa Clarita, CA, USA) and total RNA was extracted using the RNeasy® Mini kit (QIAGEN) in accordance with the manufacturer's instructions. Single-strand cDNA was synthesized with 5 μg of total RNA using the High-Capacity cDNA Archive kit (Applied Biosystems, Foster city, CA, USA), according to the manufacturer's standard protocol. Sequences of the gene-specific primers used for RT-PCR are available upon request. A separate set of primers was used for real-time PCR, which was performed on an ABI Prism 7500 Real-Time PCR instrument (Applied Biosystems). Primers and TaqMan probes were obtained from Applied Biosystems (TaqMan® Gene Expression Assays). The PCR conditions were as follows: denaturation for 10 min at 95^0C, followed by 50 cycles at 95^0C for 15 sec and 60^0C for 1 min. The linear range of amplification was determined using serially diluted cDNA (4-fold series). The mRNA expression of the target gene was normalized to the corresponding *GAPDH* internal control.

Chromatin immunoprecipitation (ChIP) assays HT29 cells were cultured with 0.1% DMSO (vehicle), AM, or TSA for 4 hr or 24 hr, and fixed in 1% formaldehyde for 10 min at room temperature. Cross-linking was stopped by adding glycine at a final concentration of 0.125 M. The ChIP kit from Active Motif (Carlsbad, CA) was used according to the manufacturer instructions. Chromatin was incubated with 10 μg anti-acetylated histone H3 (Upstate, #06-599), anti-Sp1 (Santa Cruz, sc-14027x), anti-Sp3 (Santa Cruz, sc-13018x), anti-p53 (Santa Cruz, sc-126x), or anti-polymerase II (included in the kit) antibodies overnight at 4^0C. DNA pull-down was purified by phenol/chloroform extraction followed by ethanol precipitation. DNA was then resuspended in 30 μl DEPC water (or 100 μl for the input controls). Primers used to

amplify different regions of the *P21WAF1* gene promoter and downstream were as follows (F= forward, R = reverse): a: (-3940 to -4346) F-5'-GATGCCAACCAGATTTGCCG-3' and R-5'-CCTGGCTCTAACAACATCCC-3'; b: (-3538 to -3941) F-5'-GAACAGGAAGACCATCCAGG-3' and R-5'-GGTCATCACACCTGCTATGTC-3'; c: (-2029 to -2478) F-5'-CACCACTGAGCCTTCCTCAC-3' and R-5'-CTGACTCCCAGCACACACTC-3'; d: (-1335 to -1688) F-5'-GAAATGCCTGAAAGCAGAGG-3' and R-5'-GCTCAGAGTCTGGAAATCTC-3'; e: (-677 to -981) F-5'-GGAGGCAAAAGTCCTGTGTTC-3' and R-5'-GGAAGGAGGGAATTGGAGAG-3'; f: (-324 to -676) F-5'-CCCGGAAGCATGTGACAATC-3' and R-5'-CAGCACTGTTAGAATGAGCC-3'; g: (+41 to -343) F-5'-GGCTCATTCTAACAGTGCTG-3' and R-5'-TCCACAAGGAACTGACTTCG-3'; h: (+3516 to +3349) F-5'-GTTGATGGGCCTCTCTGGTTA-3' and R-5'-AGGCAACCAAGGCTCAGATA-3'. Immuno-precipitated DNA (4 µl) or input controls (1 µl) were subjected to PCR amplification as follows: pre-incubation for 5 min at 95^0C, 30 s at 95^0C, 30 s at 62^0C, and 30 s at 72^0C (35 cycles), ending with 10 min at 72^0C. PCR products were separated by electrophoresis through 1.5% agarose gel. In subsequent experiments, real-time PCR was used to quantify the outcome from ChIP assays. Primers within regions b and g were further optimized for the real time conditions and designated as regions b' and g', respectively. The corresponding primer sequences were as follows: b': (-3906 to -3756) F-5'-CTGAGGGGAGGCTCATACTG-3' and R-5'-CAGAGCCAGGATGAATTGGT-3'; g': (-171 to -11) F-5'-GCTGGCCTGCTGGAACTC-3' and R-5'-AGCGCGGCCCTGATATAC-3'. Forty-two cycles of PCR were run on an Opticon Monitor 2 system (Finnzymes, Finland), in a 20-µl reaction containing DNA, SYBR Green I dye (DyNAmo master solution, Finnzymes), and primer set. PCR conditions were 30 s at 95^0C, 30 s at 62^0C, and 40 s at 72^0C, ending with 10 min at 72^0C.

Statistical analyses Results were expressed as mean ± SD. Statistical significance was evaluated for data from three independent experiments using Student's *t* test. A p-value <0.05 was considered to be statistically significant.

3.4 Results

AM is a competitive HDAC inhibitor

Compounds that inhibit HDAC enzymes and increase histone acetylation have promising therapeutic potential (315). We first examined whether DADS, SAC, SAMC, or their

metabolites AM and AMS might inhibit HDAC activity in a cell-free system. The compounds were selected based on structural features that might be compatible with the HDAC active site and/or published reports on their ability to induce histone acetylation in cancer cells(164, 290, 291). Under the conditions used here, AM was the only compound to produce a marked, dose-dependent inhibition of HDAC activity (**Figure 3.1A**). The concentration for 50% inhibition (IC_{50}) by AM was ~20 μM. A separate test for quenching showed that AM did not interfere with the fluorescence signal of the assay (data not presented).

To provide structure-function insights, we assessed the ability of AM and three of its structural analogues to inhibit HDAC activity in HeLa nuclear extracts and with purified human HDAC8 (**Figure 3.1B**). The double bond in AM was substituted with a hydroxyl group or a phenyl ring in mercaptoethanol and benzyl mercaptan, respectively, whereas the sulfhydryl moiety was replaced by a hydroxyl group in allyl alcohol. At the concentrations used here, none of the structural analogues inhibited HDAC activity in HeLa nuclear extracts (**Figure 3.1B**, top). However, with 20 μM AM in the assay, HDAC activity was inhibited by 45.6% in HeLa nuclear extracts and by 57.7% using purified human HDAC8 (**Figure 3.1B**, top and bottom, respectively). HDAC8 was inhibited by 15% with 20 μM benzyl mercaptan in the assay, and no effect was observed with 20 μM mercaptoethanol or 20 μM allyl alcohol. At the highest concentration tested (200 μM), all compounds inhibited HDAC8 significantly, except for allyl alcohol, which lacks the sulfhydryl group. Thus, the relative order of inhibitory potency towards HDAC8 was as follows: AM>benzyl mercaptan>mercaptoethanol>>allyl alcohol.

We next investigated the kinetics of HDAC8 inhibition by AM (**Figure 3.1C**). The Cornish-Bowden plot of S/V *versus* I generated a series of parallel lines, and the Dixon plot of 1/V *versus* I had lines that intersected above the *x*-axis, consistent with competitive type inhibition (316). The inhibitor constant (Ki) was estimated to be 24 μM by linear regression analysis of the Dixon plot. The competitive mechanism also was supported by molecular docking studies, based on the available crystal structure of human HDAC8 with bound inhibitor (317). Preliminary docking in a non-bonded model confirmed that AM fit into the

catalytic site of HDAC8 without steric hindrance (**Figure 3.1D**, left). The free energy of AM binding to HDAC8 was estimated to be -30 kcal/mol. Hydrophobic interactions were predicted between various residues of the pocket and AM, which favored localization of the ligand deep within the enzyme active site. Moreover, in an optimized truncated model, a strong interaction was predicted (-120 kcal/mol) between the zinc atom of HDAC8 and the sulfur atom of AM. In the final lowest-energy structure computed, the sulfur atom of AM was located at 2.25Å from the zinc atom (**Figure 3.1D**, right), suggesting that the zinc-sulfur interaction might drive AM binding within the HDAC8 active site.

HDAC inhibition and histone acetylation in HT29 cells treated with AM

The HDAC inhibitory activity of AM was examined in human HT29 colon cancer cells, with TSA as a positive control. When HT29 cell extracts were treated directly with the test agents in a cell-free system, as described above for HeLa extracts, the IC_{50} values for inhibition of HDAC activity by AM and TSA were 20 μM and 5 nM, respectively (**Figure 3.2A**). However, much higher concentrations of AM and TSA were needed with intact cells. Specifically, a 25-100-fold higher dose of AM (0.5-2.0 mM) and a 20-40-fold higher dose of TSA (0.1-0.2 μM) gave comparable HDAC inhibition with the cell-free assay system (**Figure 3.2B**). For both compounds, dose-dependent inhibition of HDAC activity was detected within 10 min of treatment, and the inhibition was significant at various times up to 72 hr in HT29 cells (**Figure 3.2B**).

When normalized to H3, acetylated H3 was induced up to 1.8-fold within 10 min of AM or TSA treatment, as compared with the corresponding vehicle control (**Figure 3.2C**). At 24 hr, acetylated histone H3 was increased 2.4-fold by 2 mM AM and 4.5-fold by 0.2 μM TSA. Acetylated H3 then returned to baseline in cells treated with TSA, but at 72 hr acetylated H3 remained elevated 1.5-fold in cells treated with 1-2 mM AM. When normalized to H4, acetylated H4 was increased up to 1.8-fold within 10 min of AM or TSA treatment. Acetylated H4 was increased 2.1-fold 30 min after treatment with 2 mM AM, and 2.8-fold 3 hr after exposure to 0.2 μM TSA. Increases for acetylated H3 were dose-dependent at various times up to 24 hr after treatment with AM, and at 10 min, 30 min, 3 hr, and 24 hr after treatment with TSA. For acetylated H4, dose-dependent increases were detected at 30

min, 6 hr, and 12 hr after treatment with AM, and at 3, 6, 12, and 24 hr after treatment with TSA.

Histone acetylation and recruitment of Sp3 and p53 to the P21WAF1 promoter

In cancer cells treated with HDAC inhibitors, histone hyperacetylation is commonly associated with the induction of p21 (318). In HT29 cells, p21 expression was induced by AM in both a time- and dose-dependent manner. After 1 hr incubation with 0.5-2.0 mM AM, p21 mRNA was increased 2-fold, and a dose-dependent response was observed at 6 hr, with 8-fold higher levels of p21 mRNA detected in cells treated with 2.0 mM AM (**Figure 3.3A**). A marked ~5-fold increase in p21 mRNA expression was observed at 6 hr in cells treated with 0.1 or 0.2 μM TSA, and a slight increase also was detected at 1 hr in cells treated with 0.2 μM TSA. An increase in p21 protein expression also was observed within 3 hr of AM treatment, and to a lesser extent for TSA at 3 hr (**Figure 3.3B**). However, p21 protein expression was increased markedly by TSA at 6, 12, and 24 hr, and then returned to control levels. For AM, the increase in p21 protein expression was dose-dependent from 6 to 72 hr.

In subsequent experiments, ChIP analyses were performed using anti-acetylated histone H3 antibody followed by primers to selected regions within the *P21WAF1* gene promoter (**Figure 3.4A**). After 4 hr treatment with AM or TSA, there was a marked increase in the level of histone H3 acetylation associated with promoter regions d, f, and g, but only a marginal increase was detected in region h, downstream of the 5' flanking region. The Sp1 family of transcription factors has been implicated in the induction of p21 by HDAC inhibitors (319), and promoter region g contains six potential Sp1/Sp3 binding sites, plus the initiation codon. Within 4 hr of AM or TSA treatment, there was an increase in Sp3, but not Sp1, associated with promoter region g (**Figure 3.4B**).

As illustrated in Figure 4A, the *P21WAF1* promoter also contains p53 binding sites at positions -4001 (region a), -3764 (region b), -2311 and -2276 (region c), and -1391 (region d). For regions a-d, ChIP assays with anti-p53 antibody produced only weak bands at 4 hr (**Figure 3.4C**, upper panels). At 24 hr, however, there was a strong increase in p53 associated with regions a and b after TSA exposure, and for region b after AM treatment. Subsequent experiments used quantitative PCR to assess ChIP signals (**Figure 3.4D**). Four hours after

treatment with AM and TSA, there was a significant increase in acetylated H3 and Sp3 associated with region g', and p53 was increased significantly in region b' at 24 hr. The timing of these changes suggested that AM and TSA increased the binding of Sp3 within 4 hr, followed at a later time by p53 binding to upstream enhancer regions in the *P21WAF1* promoter.

Growth inhibition and cell cycle arrest

Finally, we examined the effects of AM and TSA treatment on the growth of HT29 cells. In the MTT assay (**Figure 3.5A**), AM and TSA inhibited cell growth in a time- and dose-dependent manner. Approximately 50% reduction in cell density was observed with 2 mM AM and 0.2 μM TSA after 48 hr incubation. Analysis of the DNA content by flow cytometry (**Figure 3.5B**) showed that AM and TSA both caused a dramatic decrease in the percentage of cells in S phase. Under the present conditions, AM-treated cells were arrested preferentially in G_1, and a similar finding was obtained using 0.1 μM TSA. At the higher concentration of 0.2 μM TSA, more of the cells were arrested in G_2 *versus* G_1, and virtually none were detected in S phase.

3.5 Discussion

Potent HDAC inhibitors such as TSA and SAHA induce histone acetylation and de-repress target genes such as *P21WAF1* and *BAX*, triggering cell cycle arrest and apoptosis in cancer cells (6, 234). Similar findings have been reported for dietary constituents that act as weak HDAC ligands, such as butyrate and sulforaphane (320). With the exception of trapoxin and depudesin, most HDAC inhibitors block substrate access to the HDAC active site in a reversible fashion (6). We found that AM was a competitive HDAC inhibitor *in vitro*, with a Ki of 24 μM for human HDAC8. Molecular docking studies revealed favorable energetic conditions for AM binding in the HDAC8 active site, with the sulfhydryl group of AM ideally positioned to interact with the catalytic zinc at the base of the HDAC pocket. Thiol compounds are well known to inhibit zinc-dependent enzymes (321, 322), and synthetic agents containing an $–(CH)_2$-SH group were reported to be strong HDAC inhibitors due to –S-Zn- binding within the active site (323). The sulfhydryl group of AM was clearly important, since HDAC inhibition was abolished in assays using allyl alcohol. HDAC inhibition also was

diminished with mercaptoethanol, which contains a thiol group, but has higher water-solubility than AM. We speculate that this lowers the affinity of mercaptoethanol for the hydrophobic pocket of HDAC8, but further work is needed to confirm this possibility. One interesting feature distinguishing HDAC8 from other HDAC enzymes is that it has a wider active site pocket and larger surface opening (324). This might explain why the more bulky benzyl mercaptan molecule was able to inhibit HDAC8, but was less effective with HeLa nuclear extracts containing other HDACs . In contrast to DADS, SAC, and SAMC, the small size of AM makes it a good fit for multiple HDAC enzymes; indeed, the extent of inhibition by AM was similar for HDAC8, HeLa extracts, and HT29 cell lysates.

In HT29 cells, we detected inhibition of HDAC activity and increased histone acetylation within 10 min of AM and TSA treatment. Acetylated histone H3 was increased for up to 24 hr after TSA treatment, and for 72 hr following AM exposure. A similar time-course was observed for p21 protein expression, with 0.1-0.2 μM TSA increasing p21 for up to 24 hr and 1-2 mM AM increasing p21 for up to 72 hr. One interpretation is that TSA is a potent, transient-acting HDAC inhibitor, whereas AM is less potent but exerts a more sustained level of inhibition.

A common target of HDAC inhibitors is p21, which controls transition through the cell cycle via the inhibition of cyclin-dependent kinases (325). In the present study, induction of p21 by AM was associated with arrest in G_1 of the cell cycle. For TSA, the relative distribution of cells in G_1 *versus* G_2 depended on the dose of HDAC inhibitor used in the experiment. This might be explained by mechanisms affecting other cell cycle regulators (326), such as Akt, checkpoint kinase 1, and the c-Jun NH(2)-terminal kinase signaling axis, which have been implicated in prior studies with garlic organosulfur compounds (152, 327, 328).

HDAC inhibitors increase the levels of histone acetylation, which facilitates chromatin remodeling and recruitment of transcription factors to target genes. In prior studies with HDAC inhibitors butyrate and SAHA (329, 330), changes in histone acetylation status and Sp1/Sp3 binding were observed on the promoter region of *P21WAF1*. We confirmed that, within 4 hr of AM and TSA treatment, Sp3 was recruited to the *P21WAF1* promoter, concurrent with increased histone acetylation. No increase was seen for Sp1 under the same

conditions. Further studies are needed to establish the mechanism by which Sp3 was selectively targeted to *P21WAF1*, and whether the acetylation status of the transcription factor itself was altered (331, 332). Although Sp3 acts as a transcriptional repressor in some scenarios, HAT activity acetylates Sp3 leading to promoter activation (332). Thus, Sp1/Sp3 activity may be determined by the dynamic balance between HATs and HDACs in their vicinity. Indeed, while direct interactions between Sp1/Sp3 and p300/CBP were associated with promoter activation upon HDAC inhibitor treatment (333), Sp1/Sp3 also mediated the repression of *P21WAF1* by HDAC1-3 in colon cancer cells (8). Post-translational modifications of Sp1/Sp3 also were implicated in *P21WAF1* transcriptional activation by TSA (334, 335). We did not detect any change in global HAT activity following AM treatment in HT29 cells (data not shown), but the trafficking of transcriptional co-activators to the *P21WAF1* promoter, such as p300/CBP and CBP/p300-associated factor (P/CAF), should be examined in more detail, due to their intrinsic HAT activity (336, 337).

It has been reported that acetylation of wild-type p53 can increase its half-life and binding to the *P21WAF1* promoter (338, 339). The mutant form of p53 which is over-expressed in HT29 cells, namely $p53^{R273H}$, is believed to be responsible for silencing p21, and various strategies have been sought to rescue $p53^{R273H}$ in cancer cells and restore normal p53-target gene expression (340). Recently, Vikhanskaya *et al*. studied functional mutants of p53 and reported that repression of p21 by $p53^{R273H}$ was abolished by TSA treatment (341). Under the present conditions, p53 interaction with the *P21WAF1* promoter was barely detectable in ChIP assays at 4 hr, but it was clearly observed at 24 hr after TSA and AM treatment, localized in the upstream (distal) enhancer region. Little is known about *P21WAF1* promoter regulation by $p53^{R273H}$, but the results of this study and others (341, 342) support the view that p53 mutant-mediated suppression of target genes is dependent on HDAC activity. It is noteworthy that the eventual loss of p21 induction by TSA at 24 hr coincided with increased binding of p53 at two sites in the proximal promoter (a and b, **Figure 3. 4C**), compared with only one site for AM, in which p21 remained elevated for up to 72 hr. Further work is needed to clarify the role of specific p53 mutants, their binding sites in the *P21WAF1* promoter, and the response to various HDAC inhibitors.

Based on the results of the present study, we conclude that the chemopreventive effects of garlic organosulfur compounds may be due, in part, to their metabolic conversion to AM followed by HDAC inhibition. An important issue for future work will be to assess the relevant levels of AM achieved *in situ*, since exogenous application of AM (and TSA) to human colon cancer cells required much higher concentrations to affect HDAC activity than with the cell-free assays. Concentrations in the range 0.2-2 mM were used in prior mechanistic studies with DADS, SAMC, AM, and other garlic-derived organosulfur compounds (28-30), although 40 μM DATS was reported to inactivate Akt and trigger caspase-mediated apoptosis in human prostate cancer cells(152). It remains to be determined whether the ingestion of multiple organosulfur compounds in garlic might generate intracellular concentrations of AM on the order ~20 μM, which could inhibit HDAC activity in colonic epithelial cells or systemic tissues such as prostate, for which anti-carcinogenic effects have been reported(69, 74, 84, 152, 164, 290-292, 312, 313, 326-328).

In summary, we provide here the first evidence that AM acts a competitive HDAC inhibitor *in vitro*, with a Ki on the order of 24 μM for human HDAC8. In HT29 cells, inhibition of HDAC activity by AM coincided with increased global histone acetylation, as well as localized hyperacetylation of histone H3 on the *P21WAF1* promoter. Recruitment of Sp3 to the *P21WAF1* promoter occurred within 4 hr of AM exposure, and was followed by the subsequent binding of p53 to the distal enhancer region. Induction of p21 was both rapid and sustained, and was associated with a dose-dependent G_1 arrest in AM-treated HT29 cells. It will be interesting to examine the cooperative effects of garlic organosulfur compounds, and other reported dietary HDAC inhibitors(6, 288, 343), in combination with drugs that reverse DNA methylation and epigenetic gene silencing, with the potential for improved therapeutic efficacy(344, 345).

A

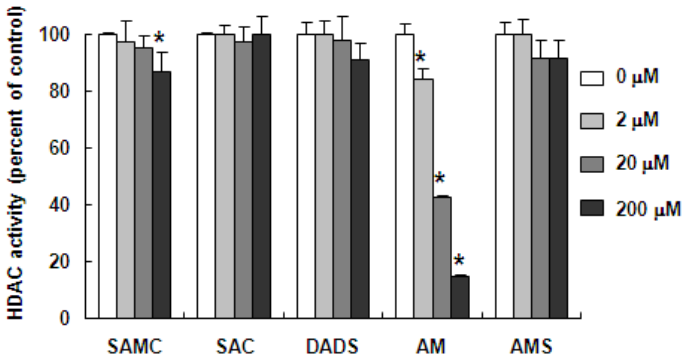
HDAC activity (percent of control)
100
80
60
40
20
0
SAMC
SAC
DADS
AM
AMS
0 μM
2 μM
20 μM
200 μM

B

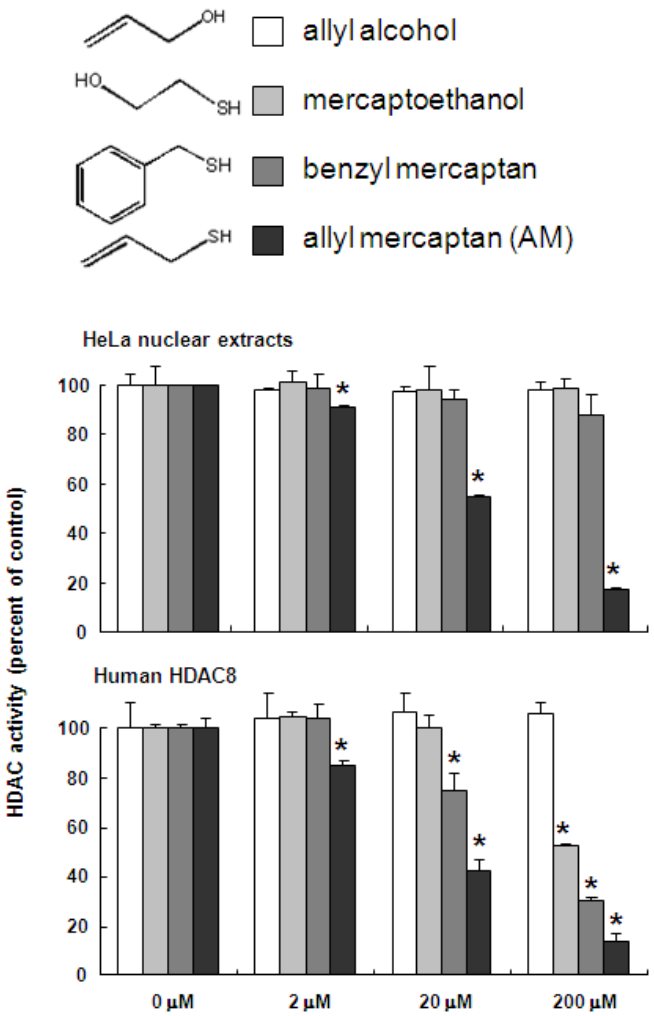
OH
allyl alcohol
HO
SH
mercaptoethanol
SH
benzyl mercaptan
SH
allyl mercaptan (AM)
HeLa nuclear extracts
Human HDAC8
HDAC activity (percent of control)
100
80
60
40
20
0
0 μM
2 μM
20 μM
200 μM

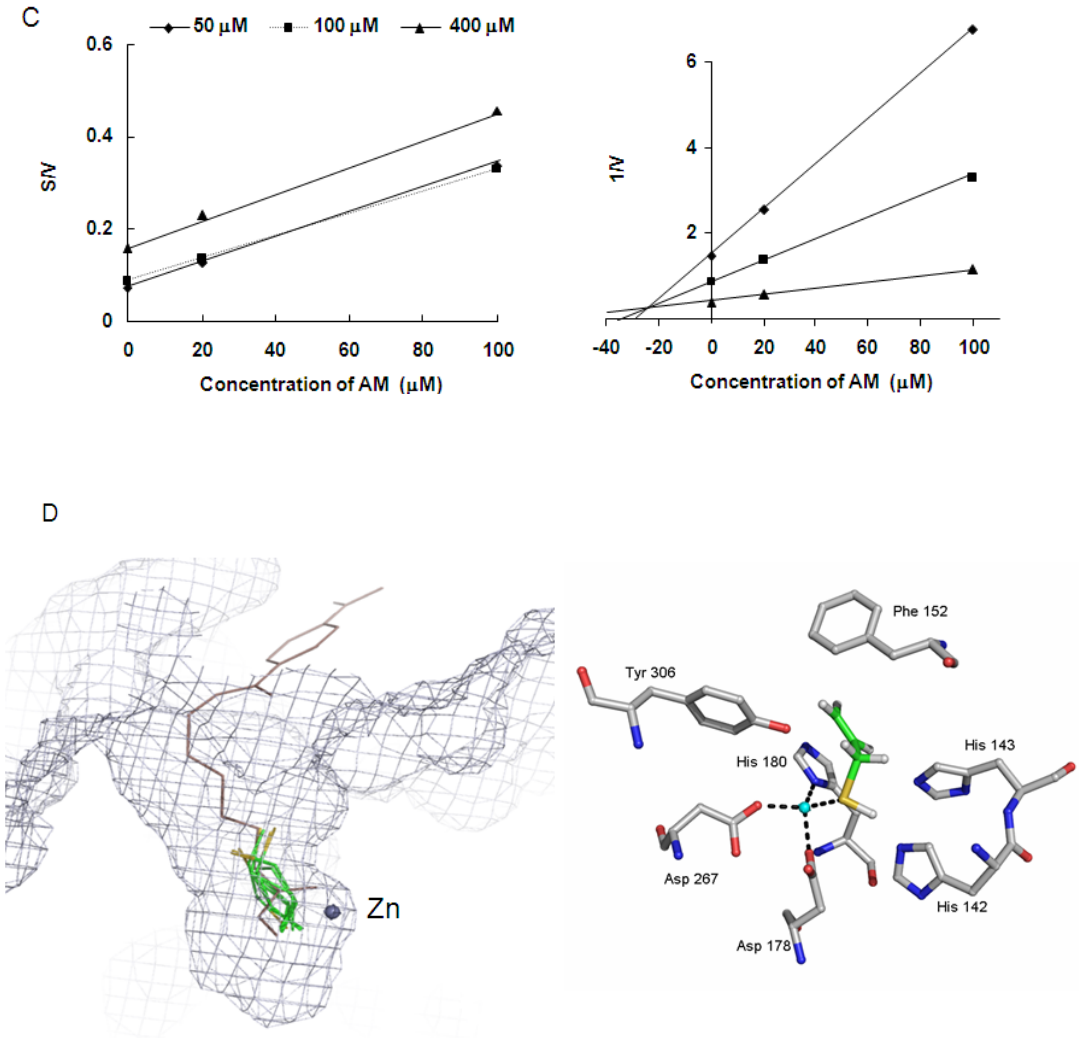

Figure 3.1 AM is a competitive HDAC inhibitor. (**A**) HDAC activity was evaluated using HeLa nuclear extracts in the presence of 2, 20, and 200 µM SAMC, SAC, DADS, AM, and AMS. Data (mean±SD, n=3; *P<0.05) were expressed as percent of DMSO control. (**B**) Inhibition of HDAC activity by AM and three structural analogues, allyl alcohol, benzyl mercaptan, and mercaptoethanol. HDAC activity was assayed with HeLa nuclear extracts (top) or human HDAC8 (bottom). Data = mean±SD, n=3 (*P<0.05). (**C**) Cornish-Bowden plot (left) and Dixon plot (right) of HDAC8 inhibition by AM, indicating competitive binding (Ki = 24 µM). (**D**) Modeling of the HDAC8-AM complex, using MacroModel® v8.5 (Schrödinger Inc.). Left: lowest-energy configurations of AM in the active site of human HDAC8, based on a non-bonded model docking search. Enzyme-bound inhibitor MS-344 (brown) and the active zinc atom (blue sphere) are shown from a prior report (47), which highlights the favorable orientation of AM (green). Right: AM docked in the HDAC8 catalytic core in the lowest-energy structure after Jaguar calculation (Schrödinger Inc.). The sulfur of AM (yellow) was oriented 2.25Å from the zinc atom (blue sphere), and hydrophobic interactions with adjacent residues were predicted to further stabilize AM binding in the HDAC8 pocket.

A

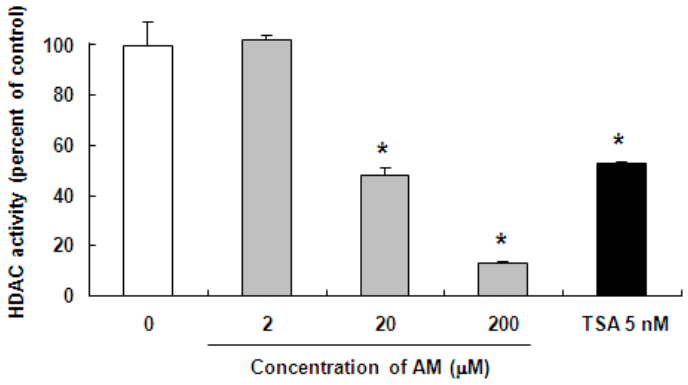
HDAC activity (percent of control)
100
80
60
40
20
0
0
2
20
200
TSA 5 nM
Concentration of AM (μM)

B

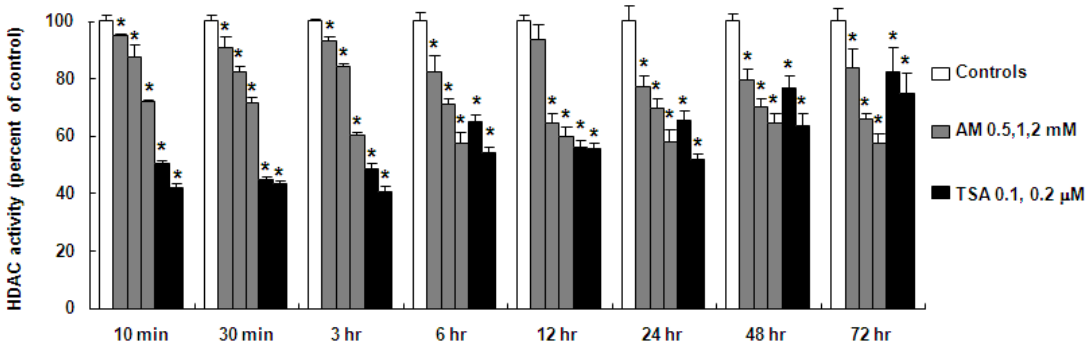
HDAC activity (percent of control)
100
80
60
40
20
0
10 min
30 min
3 hr
6 hr
12 hr
24 hr
48 hr
72 hr
Controls
AM 0.5,1,2 mM
TSA 0.1, 0.2 μM

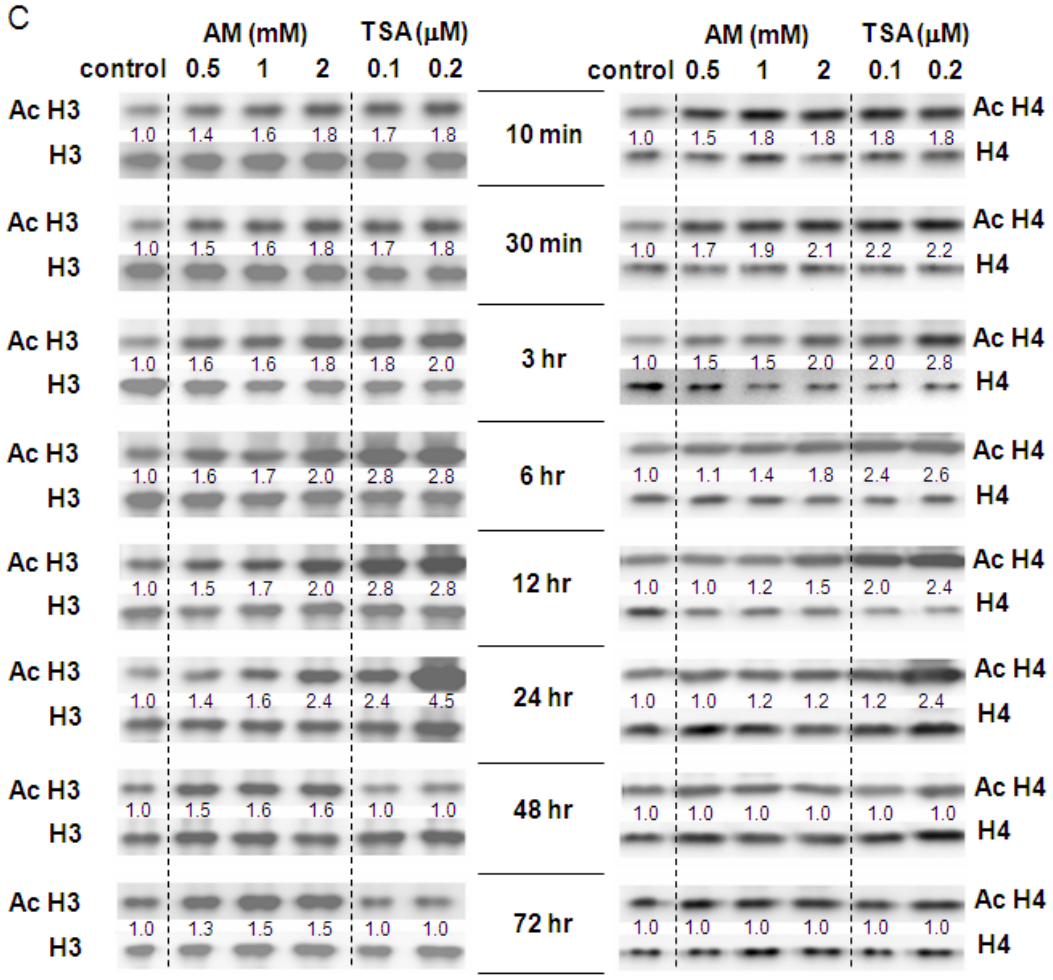

Figure 3.2 HDAC inhibition and histone acetylation in AM-treated HT29 cells. (**A**) Whole cell extracts from human HT29 colon cancer cells were treated directly with the test agents and assayed for HDAC activity (BioMol kit). The IC_{50} for AM and TSA was 20 μM and 5 nM, respectively. Data=mean±SD (n=3), *P<0.05. (**B**) HT29 cells were treated with AM (0.5, 1, 2 mM) or TSA (0.1, 0.2 μM) for selected times, from 10 min to 72 hr, and whole cell extracts were tested for HDAC activity. Data=mean±SD (n=3), *P<0.05. (**C**) In the same cell lysates as (B), acetylated histones H3 and H4 were analyzed by immunoblotting. At each time-point, acetylated histone expression was normalized to the corresponding non-acetylated histone, and this ratio was assigned an arbitrary value of 1.0 for the vehicle controls.

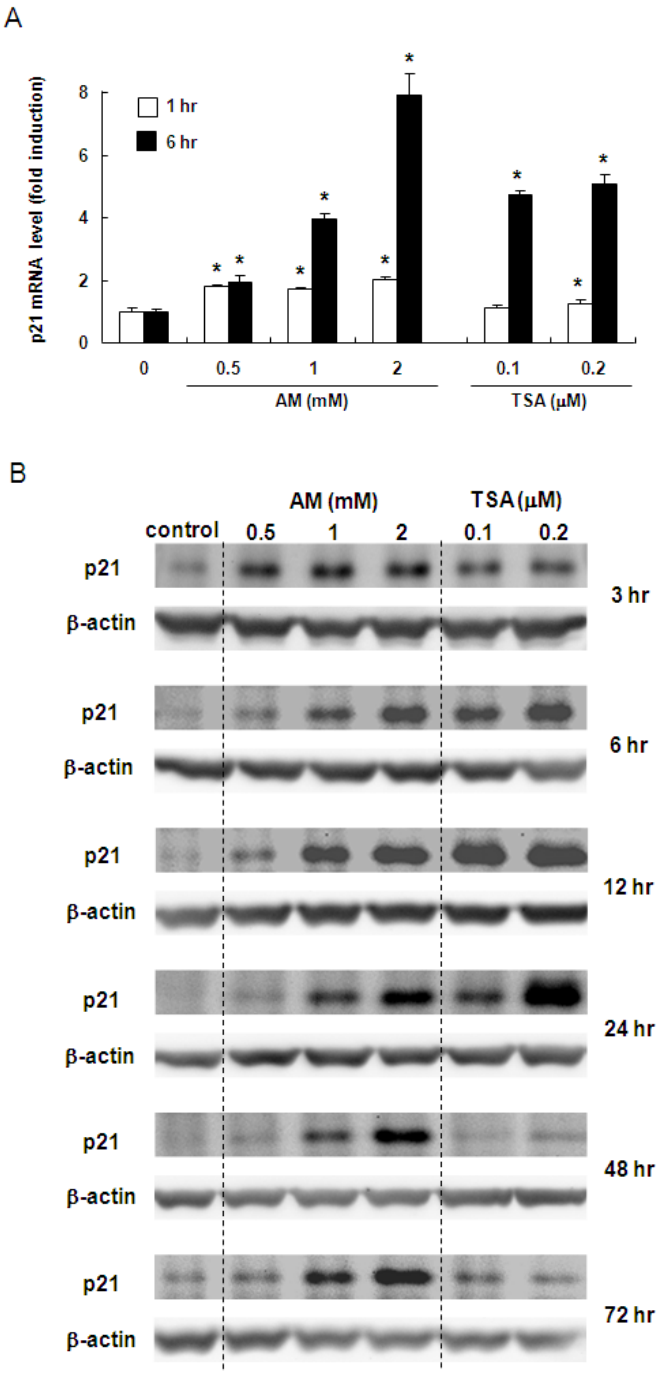

Figure 3.3 AM and TSA induce p21 expression in HT29 cells. (**A**) Real-time RT-PCR was used quantify p21 mRNA expression after 1 and 6 hr of treatment with AM (0.5, 1, 2 mM) or TSA (0.1, 0.2 μM). *GAPDH* was used as internal control. Results are shown as fold induction, relative to the corresponding vehicle controls; mean±SD, n=3 (*P<0.05). (**B**) Immunodetection of p21 protein expression, with β-actin as loading control.

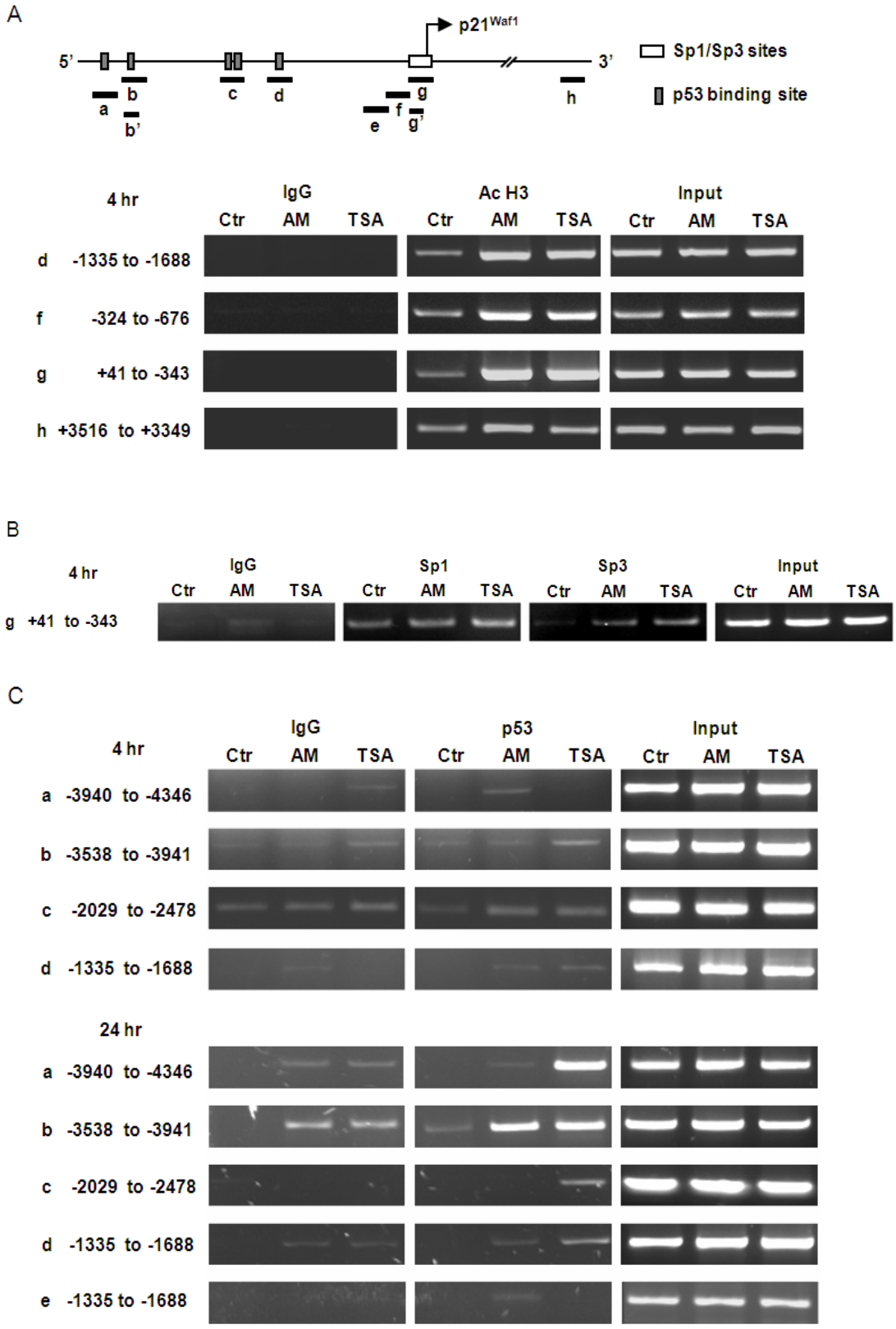
A
p21Waf1
5'
3'
Sp1/Sp3 sites
p53 binding site
a
b
b'
c
d
e
f
g
g'
h
4 hr
IgG
Ac H3
Input
Ctr
AM
TSA
d -1335 to -1688
f -324 to -676
g +41 to -343
h +3516 to +3349
B
4 hr
IgG
Sp1
Sp3
Input
Ctr
AM
TSA
g +41 to -343
C
4 hr
IgG
p53
Input
Ctr
AM
TSA
a -3940 to -4346
b -3538 to -3941
c -2029 to -2478
d -1335 to -1688
24 hr
a -3940 to -4346
b -3538 to -3941
c -2029 to -2478
d -1335 to -1688
e -1335 to -1688

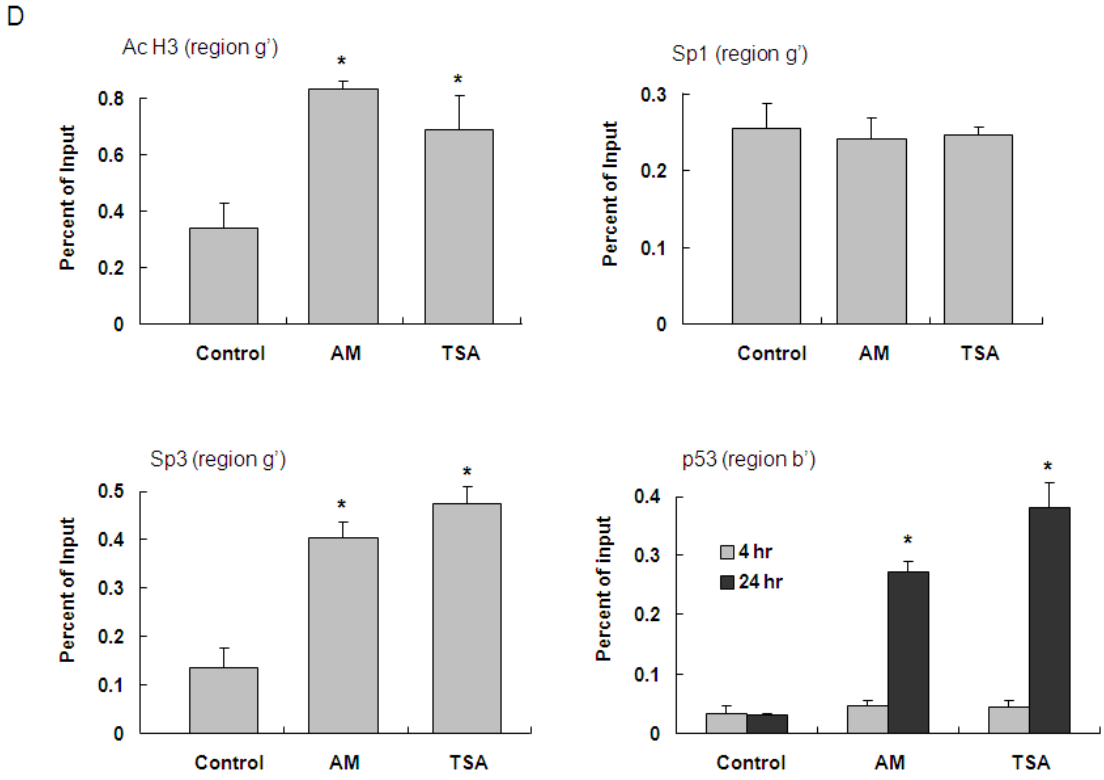

Figure 3.4 Histone acetylation and transcription factor binding to *P21WAF1*. (**A**) Schematic representation of the *P21WAF1* promoter, showing p53 and Sp1/Sp3 binding sites, and regions amplified by PCR after chromatin immunoprecipitation (ChIP). HT29 cells were treated with DMSO (controls, Ctr), AM, or TSA for 4 hr and ChIP was performed with anti-acetylated H3 antibody followed by primers to regions d, f, and g in the 5' promoter, or region h further downstream. IgG was used as negative control, and input samples were used as positive controls for PCR amplification. (**B**) The ChIP assay in (A) was repeated using anti-Sp1 or anti-Sp3 antibodies, and primers to region g (-343 to +41), which contains multiple Sp1/Sp3 binding sites. (**C**) The ChIP assay was repeated at 4 and 24 hr after TSA or AM treatment, using anti-p53 antibody, followed by primers to regions a-d, as shown. Region e, which lacks a p53 binding site, was used as a control in some experiments. (**D**) Acetylated H3, Sp1, Sp3, and p53 DNA pull-downs from the ChIP assay were quantified by real-time PCR. Region b': -3906 to -3756; region g': -171 to -11. Data=mean±SD (n=3), *P<0.05.

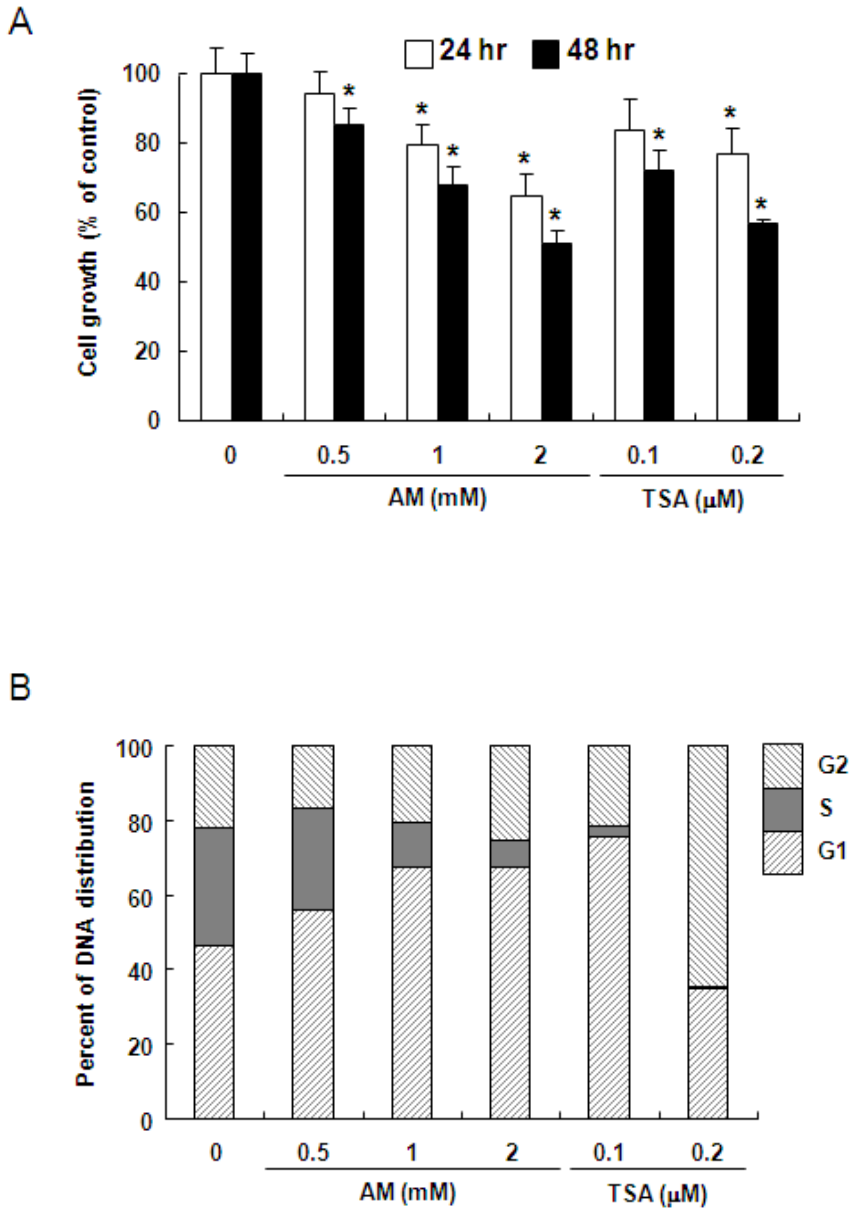

Figure 3.5 AM and TSA inhibited cell proliferation and induced cell cycle arrest. (**A**) Growth arrest in HT29 cells treated with AM or TSA, detected using the MTT assay. Data = mean±SD, n=3, *P<0.05. (**B**) DNA content as determined by flow cytometry (see Material and Methods). Results are representative of the findings from three independent experiments. For clarity, statistical outcomes associated with AM- or TSA-induced changes in G1, S, and G2 cell cycle distribution *versus* vehicle control were omitted from the figure (*P<0.05, all treatments).

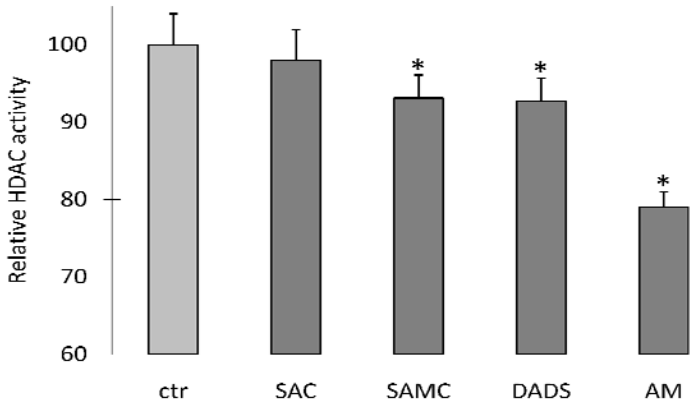

Figure 3S.1 SAMC, DADS and AM decreased cellular HDAC activities. HT29 cells were treated with 500μM SAC, SAMC, DADS or AM for 12 hours, and the HDAC activities in the cellular extracts were measured using HDAC assay as described in Materials and methods.

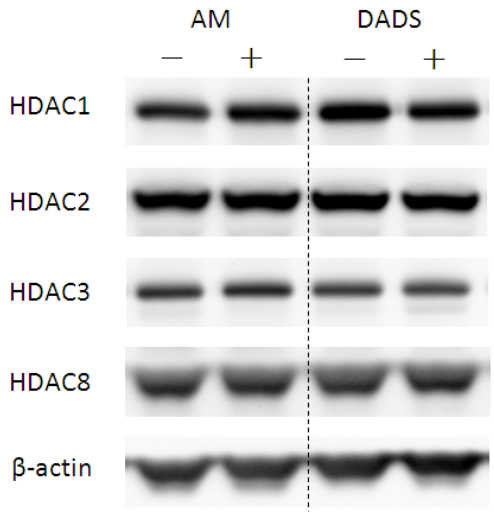

Figure 3S.2 AM and DADS did not change the protein levels of class I HDACs. HT29 cells were treated with 2mM AM or 0.5mM DADS for 12 hours, and whole cell lysate were immune-blotted against indicated HDAC proteins. β-actin was blotted as loading control.

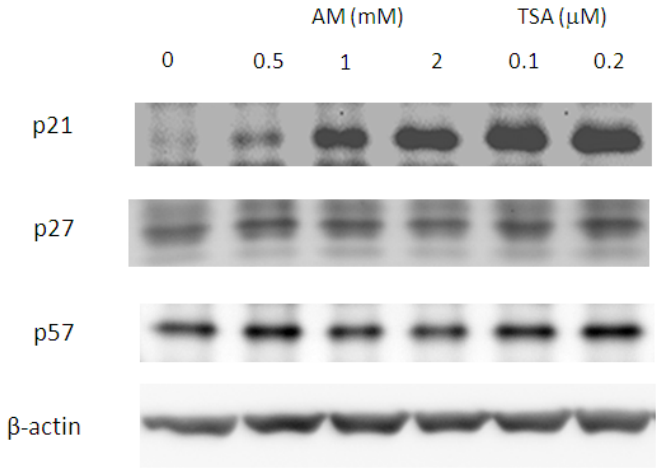

Figure 3S.3 The effect of AM on the protein levels of cell cycle inhibitors. HT29 cells were treated with AM or TSA of indicated concentrations for 12 hours, and the expression level of cell cycle inhibitors p21, p27 and p57 were examined using immunoblot. β-actin was blotted as loading control.

Figure 3S.4 Induction of histone acetylation *in vivo* by garlic organosulfur compounds. AM(200mg/kg body weight), DADS(100mg/kg body weight), garlic oil(Sigma W250317, 200mg/kg body weight), AGE(*Kyolic* aged garlic extract, 200mg/kg body weight), FGE(fresh garlic extract, 750mg/kg body weight), or garlic powder(*Natrol* garlic powder, 200mg/kg body weight) were orally administrated to 6-week-old ICR mice. Corn oil (in which AM, DADS and garlic oil were dissolved) and saline solution (in which AGE, FGE and garlic powder were dissolved) were also orally administrated as controls. 6 hours and 24 hour after administration, mice were sacrificed and acetylation levels of histones in livers(A) and intestines(B) were examined by immunoblotting. * p-value < 0.05.

α-Keto acid metabolites of organoselenium compounds inhibit histone deacetylase activity in human colon cancer cells

Hui Nian, William H. Bisson, Wan-Mohaiza Dashwood, John T. Pinto
and Roderick H. Dashwood

Carcinogenesis

2001 Evans Road, Cary, NC 27513

Vol.30 no.8 pp1416-1423, 2009

4.1 Abstract

Methylselenocysteine (MSC) and selenomethionine (SM) are two organoselenium compounds receiving interest for their potential anti-cancer properties. These compounds can be converted to β-methylselenopyruvate (MSP) and α-keto-γ-methylselenobutyrate (KMSB), α-keto acid metabolites that share structural features with the histone deacetylase (HDAC) inhibitor butyrate. We tested the organoselenium compounds in an *in vitro* assay with human HDAC1 and HDAC8; whereas SM and MSC had little or no activity up to 2 mM, MSP and KMSB caused dose-dependent inhibition of HDAC activity. Subsequent experiments identified MSP as a competitive inhibitor of HDAC8, and computational modeling supported a mechanism involving reversible interaction with the active site zinc atom. In human colon cancer cells, acetylated histone H3 levels were increased during the period 0.5-48 h after treatment with MSP and KMSB, and there was dose-dependent inhibition of HDAC activity. The proportion of cells occupying G2/M of the cell cycle was increased at 10-50 μM MSP and KMSB, and apoptosis was induced, as evidenced by morphological changes, Annexin V staining, and increased cleaved caspase-3, -6, -7, -9, and poly(ADP-ribose)polymerase. *P21WAF1*, a well-established target gene of clinically-used HDAC inhibitors, was increased in MSP- and KMSB-treated colon cancer cells at both the mRNA and protein level, and there was enhanced *P21WAF1* promoter activity. These studies confirm that in addition to targeting redox-sensitive signaling molecules, α-keto acid metabolites of organoselenium compounds alter HDAC activity and histone acetylation status in colon cancer cells, as recently observed in human prostate cancer cells.

4.2 Introduction

Methylselenocysteine (MSC) and selenomethionine (SM) are two major organoselenium compounds present in selenium-enriched plants and yeast(346). Both of these compounds have reported anticancer properties, including in breast, prostate, and colon cancer cells (200, 203, 210, 347-350). For example, in mouse mammary epithelial tumor cells *in vitro*, MSC attenuated phosphatidylinositol 3-kinase activity, reduced the phosphorylation of p38, and inhibited the Raf-MEK-ERK signaling pathway(200). In human colon cancer cells, SM regulated cyclooxygenase-2 expression via nuclear factor-κB, and apoptosis induction was

p53 dependent and mediated by superoxide(348, 349). It has been suggested that methylselenol (MS), a β- or γ-elimination product of MSC and SM, may be a key metabolite for cancer chemoprevention, acting to redox-modify proteins and regulate key signaling pathways (351). However, MS may not be the only metabolite with important biological activity. In the liver, MSC and SM undergo transamination reactions to generate β-methylselenopyruvate (MSP) and α-keto-γ-methylselenobutyrate (KMSB), respectively (**Figure 4.1**). The widely-distributed enzyme glutamine transaminase K (GTK) also efficiently converts MSC to MS and MSP (352).

MSP and KMSB share structural features with butyrate, a short-chain fatty acid reported to competitively inhibit histone deacetylase (HDAC) activity (269). HDAC inhibitors have received increasing interest as cancer therapeutic agents, due to their potential to de-repress epigenetically-silenced genes via changes in histone acetylation status (250, 253-256). Interestingly, the human diet contains several chemopreventive agents that also inhibit HDAC activity, helping to trigger cell cycle arrest/apoptosis in cancer cells through chromatin remodeling (164, 234, 282, 285, 288, 290, 291, 353). We reported previously on the HDAC inhibitory effects of sulforaphane from broccoli and garlic-derived organosulfur compounds(282, 285, 353) The search continues for novel dietary agents that might be used alone or in combination with HDAC inhibitor drugs being developed as candidates for cancer therapy(250, 253-256). There also is interest in learning, from a basic mechanistic standpoint, how different dietary agents influence HDAC activity, histone acetylation status, and the expression of cell cycle regulators, such as $p21^{WAF1}$ (p21). In this report, we describe for the first time the HDAC inhibitory effects of organoselenium compounds in human colon cancer cells, and the corresponding changes in cell growth, apoptosis, and p21 expression.

4.3 Materials and methods

Cell culture and reagents Human HT29 and HCT116 colon cancer cell lines were obtained from American Type Culture Collection (Manassas, VA) and cultivated in McCoy's 5A medium (Life Technologies, Carlsbad, CA) supplemented with 1% penicillin-streptomycin and 10% fetal bovine serum. In some experiments, HCT116 ($p53^{-/-}$) and HCT116 ($p53^{+/+}$) cells were

used, kindly provided by Dr. Bert Vogelstein (Johns Hopkins University, Baltimore, MD). MSC, SM, MSP and KMSB were generated as reported elsewhere (352).

HDAC activity HDAC activity was determined using the Fluor-de-Lys HDAC activity assay kit (Biomol, Plymouth Meeting, PA), as reported before (353). Incubations were performed at 37°C with purified human HDAC8, human HDAC1, or nuclear extracts from colon cancer cells. Fluorescence was measured using a Spectra MaxGemini XS fluorescence plate reader (Molecular Devices), with excitation at 360 nm and emission at 460 nm.

Molecular modeling Coordinates of the human HDAC8 catalytic domain were taken from the crystal structures available in the Protein Data Bank (Pdb) 1T67 (MS-344/HDAC-8) (354). The model was energetically refined in the internal coordinate space with Molsoft ICM v3.5-1p (355). The docking was represented by five types of interaction potentials: (i) van der Waals potential for a hydrogen atom probe; (ii) van der Waals potential for a heavy-atom probe (generic carbon with 1.7 Å radius); (iii) optimized electrostatic term; (iv) hydrophobic terms; and (v) loan-pair-based potential, which reflects directional preferences in hydrogen bonding. The energy terms were based on the all-atom vacuum force field ECEPP/3 with appended terms from the Merck Molecular Force Field to account for solvation free energy and entropic contribution. Modified inter-molecular terms such as soft van der Waals and hydrogen-bonding as well as a hydrophobic term were included. Conformational sampling was based on the biased probability Monte Carlo procedure, with full local minimization after each randomization step. In the ICM-VLS (Molsoft ICM v3.5-1p) screening procedure, ligand scoring was optimized to obtain maximal separation between bound and unbound species. Each selenium compound was assigned a score according to fit within the pocket, accounting for electrostatic, hydrophobic, and entropy parameters (356).

MTT assay Cell growth was determined by assaying for the reduction of dimethyl thiazolium bromide (MTT) to formazan. Briefly, after 48 h incubation with MSP or KMSB, 10 μl MTT (5 μg/μl) were added to cells in 96-well plates. Cells were incubated at 37°C for 4 h, and a Spectra MaxGemini XS fluorescence plate reader (Molecular Devices) was used to measure absorbance at 620 nm for each well. Growth rate was calculated as follows: Cell growth = [A_{620} treated cells/A_{620} control cells] ×100%.

Flow cytometry Cells treated with MSP or KMSB for 8 h and 24 h were harvested in cold PBS, fixed in 70% ethanol, and stored at 4°C for at least 48 h. Fixed cells were washed with PBS once and resuspended in Propidium iodide (PI)/Triton X-100 staining solution containing RNase A. Samples were incubated in the dark for 30 min before cell cycle analysis. The DNA content of the cells was detected using EPICS XL Beckman Coulter and analyses of cell distribution in the different cell cycle phases were performed using Multicycle Software (Phoenix Flow Systems, San Diego, CA).

TUNEL assay Terminal deoxynucleotidyl transferase dUTP nick end labeling (TUNEL) was performed using a Guava TUNEL kit (Hayward, CA), in accordance with the manufacturer's protocol. Briefly, cells were treated with 0-50 μM MSP or KMSB for 48 h and then fixed with 1 % paraformaldehyde on ice for 1 h. After washing with PBS twice, 70% ethanol was added to the cell pellet, and incubated at -20°C to permeabilize the cells for 24 h. The cells were washed with Wash Buffer twice and incubated in the DNA labeling Solution (including TdT enzyme and BrdU-UTP) for 60 min at 37°C in a water bath. Cells were rinsed and collected by centrifugation, and incubated in anti-BrdU-Staining Mix for 45 min at room temperature. Data were acquired on a Guava PCA instrument.

Annexin V assay Annexin V staining was performed using the Guava Nexin kit (Hayward, CA), in accordance with the manufacturer's protocol. Briefly, cells were treated with 0-50 μM MSP or KMSB for 24 h and collected by centrifugation. After washing with PBS, the cells were incubated in Nexin buffer containing Annexin V and 7-AAD on ice for 20 min. Data were acquired on a Guava PCA instrument.

Immunoblotting Protein concentration of cell lysates was determined using the BCA assay (Pierce, Rockford, IL). Proteins (20 mg) were separated by SDS-PAGE on 4-12% Bis-Tris gel (Novex, San Diego, CA) and transferred to nitrocellulose membranes (Invitrogen, Carlsbad, CA). Membranes were saturated with 2% BSA for 1 h, followed by overnight incubation at 4°C with primary antibodies against acetylated histone H3 (1:200, Upstate, #06-599), histone H3 (1:200, Upstate, #06-755), p21 (1:1000, Cell Signaling, #2947) or β-actin (A5441, 1;5000, Sigma). Membranes were then incubated with peroxidase-conjugated secondary antibodies (Bio-Rad, Hercules, CA) for 1 h. Immunoreactive bands were visualized by using Western

Lightning Chemiluminescence Reagent Plus (PE Life Sciences, Boston, MA) and detected with an AlphaInnotech imaging system.

RT-PCR and quantitative real-time PCR Cells treated with MSP or KMSB were disrupted by using QIAshredder spin column (QIAGEN, Santa Clarita, CA, USA) and total RNA was extracted using the RNeasy® Mini kit (QIAGEN) in accordance with the manufacturer's instructions. Single-strand cDNA was then synthesized with 5 μg of total RNA using the High-Capacity cDNA Archive kit (Applied Biosystems, Foster city, CA, USA), according to the manufacturer's protocol. Real-time amplification was achieved using an ABI Prism 7500 Real-Time PCR instrument (Applied Biosystems). Pairs of primers and TaqMan probes were obtained from Applied Biosystems (TaqMan® Gene Expression Assays). PCR was performed as follows: denaturation for 10 min at 95°C, followed by 50 cycles at 95°C for 15 sec and 60°C for 1 min. The linear range of amplification was determined using serially diluted cDNA (4-fold series). The mRNA expression of the target gene was normalized to the corresponding *GAPDH* internal control.

Luciferase assay The effects of MSP and KMSB on *P21WAF1* promoter activity was determined by dual luciferase reporter gene assay. The full-length 5' regulatory region (p21P) and the deletion mutants p21PΔ1.1, p21Psma, p21PsmaΔ1 containing firefly luciferase gene were gifts of Dr. Xiao-Fan Wang (357). pRL-CMV plasmid containing the renilla luciferase gene (Promega, Madison, WI) was used as internal control. HT29 cells were cultured in 60 mm plates for 24 h. Plasmid construct (4 μg), 10 ng pRL-CMV plasmid DNA, and 12 ml TransFast reagent (Promega, Madison, WI) were mixed together in 2 ml media and used to transfect each plate in the absence of serum. After 1 h, 4 ml 10% serum media containing MSP or KMSB were added to the plates. Twenty-four hours later, cells were lysed and luciferase assays were performed using the Dual Luciferase Reporter Assay System (Promega, Madison, WI). The relative luciferase activity reported here is the ratio of firefly luciferase activity over renilla luciferase activity.

Chromatin immunoprecipitation (ChIP) ChIP assays were performed based on a published methodology (24). In brief, HT29 cells were cultured with 10 μM MSP for 4 h and fixed in 1% formaldehyde for 10 min at room temperature. Cross-linking was stopped by adding glycine

at a final concentration of 0.125 M. The ChIP kit from Active Motif (Carlsbad, CA) was used according to the manufacturer's instructions. Chromatin was incubated with anti-RNA polymerase II antibody (provided with the kit), anti-histone H3 (Cell Signaling, #2650, 1:50), anti-acetylated histone H3-Lys9 (Cell Signaling, #9671, 1:50), and anti-acetylated histone H3-Lys18 (Cell Signaling, #9675, 1:25). The corresponding blocking peptide was used to confirm antibody specificity (i.e., acetyl-histone H3 (Lys 9) blocking peptide (Cell Signaling, #1083, 1:500) and acetyl-histone H3 (Lys 18) blocking peptide (abcam, #24003, 1:1000), data not shown). DNA pull down was purified by phenol–chloroform extraction followed by ethanol precipitation. Data were quantified with a LightCycler 480 II (Roche, Indianapolis, IN) for *P21WAF1* gene promoter region -249 to -389, using primers F 5' GTAAATCCTTGCCTGCCAGA and R 5' ACATTTCCCCACGAAGTGAG. PCR conditions were 15 s at 95^0C, 10 s at 60^0C and 10 s at 72^0C.

Statistics Where indicated, results were expressed as mean±SD. Statistical significance was evaluated for data from three independent experiments using Student's *t*-test. A *P*-value <0.05 was considered to be statistically significant, and indicated as such with an asterisk (*) on the corresponding figures. Statistical analyses were performed by Dr. Clifford B. Pereira, Department of Statistics, Oregon State University.

4.4 Results

MSP and KMSB inhibit HDAC activity

We first studied the HDAC inhibitory effects of MSP and KMSB using purified human HDAC1 and HDAC8 enzymes in a cell-free system (**Figure 4.2A**). Both α-keto acids inhibited HDAC activity in a dose-dependent manner over the concentration range 2-2000 μM, with MSP being especially effective against HDAC8 (IC_{50} ~20 μM). Under the same experimental conditions, the parent compounds MSC and SM had little or no effect on HDAC activity (data not presented). Thus, the inhibitory potency towards HDAC8 was in the order: MSP>KMSB>>MSC>SM. By varying the concentrations of substrate and test agent, we examined the kinetics of HDAC8 inhibition by MSP. In the Lineweaver-Burk plot, lines of increasing slope intersected on the y-axis (**Figure 4.2B**); thus, MSP was identified as a competitive inhibitor, with the potential to bind reversibly to the HDAC8 active site. Based

on the available crystal structure with bound inhibitors (317, 354), we simulated the possible interaction between MSP and HDAC8. Molecular modeling indicated that MSP docked in an energetically-favored orientation, with the α-carbonyl group and one of the carboxylate oxygen atoms coordinating with the buried zinc (**Figure 4.2C**, left). KMSB adopted a similar orientation in the HDAC8 active site using the iterative docking procedure (**Figure 4.2C**, right).

MSP and KMSB increase histone acetylation in human colon cancer cells

HCT116 and HT29 human colon cancer cells were used to investigate the cellular effects of MSP and KMSB. Cells were exposed to 2, 10, and 50 μM KMSB or MSP for selected times, and the levels of global histone H3 acetylation were examined by immunoblotting of whole cell lysates (**Figure 4.3A**). Dose-dependent increases in acetylated histone H3 were detected as early as 30 min after MSP and KMSB treatment, which persisted for at least 48 h. For example, in HT29 cells treated with 2, 10 and 50 μM MSP (**Figure 4.3A**, right), acetylated histone H3 levels were increased 1.2-, 1.3-, and 1.9-fold at 0.5 h and 4.2-, 9.4-, and 9.4-fold at 48 h, compared with 0 μM MSP. At the highest concentration of 50 μM MSP and KMSB, HDAC inhibition was evident in nuclear extracts at 30 min (data not shown), and dose-dependent loss of HDAC activity was detected by 3 h (**Figure 4.3B**). MSC and SM parent compounds, however, had no effect on histone H3 acetylation or HDAC activity up to 5 h after treatment (data not shown). By 24 h, MSC at the highest concentration tested (200 μM) increased histone H3 acetylation in both cell lines, whereas SM had no effect after normalizing to total histone H3 levels in the whole cell lysates (**Figure 4.3C**).

MSP and KMSB inhibit cell growth and induce cell cycle arrest/apoptosis

In human colon cancer cells, treatment with MSP or KMSB resulted in dose-dependent loss of cell viability. For example, 48 h after exposure to 50 μM MSP or KMSB, ~60% of HCT116 cells and ~40% of HT29 cells remained viable (**Figure4.4A**). The two highest concentrations of 10 and 50 μM MSP and KMSB increased the proportion of cells occupying the G2 phase of the cell cycle, most notably in HCT116 cells at 8 and 24 h (**Figure 4.4B**). At 24 h, the lowest concentration of 2 μM MSP increased the proportion of cells in G1 and decreased the

proportion in S phase, but this was not evident for 2 μM KMSB. We recently reported similar findings for trichostatin A, such that arrest in G1 *versus* G2 of the cell cycle was dependent on the dose of the HDAC inhibitor (353).

Colon cancer cells treated with MSP or KMSB developed a rounded morphology and detached from the plate, indicative of apoptosis (data not shown). In the Annexin V assay, there was a dose-dependent increase in positively-labeled cells after treatment with MSP or KMSB (**Figure 4.5A**). At the highest concentration of MSP and KMSB (50 μM), more than 50% HCT116 cells and 20% HT29 cells were Annexin-positive, compared with ~7% for the controls. In the TUNEL assay, there was evidence for increased DNA fragmentation (**Figure 4.5B**). For example, 48 h after treatment with 50 μM MSP or KMSB, more than 50% HCT116 cells and 20% HT29 cells were TUNEL-positive. Caspase activation also was examined by immunoblotting (**Figure 4.5C**). Cleaved caspases -3, -6, -7, and -9, as well as cleaved PARP, were increased in a dose-dependent manner 24 h after treatment with MSP or KMSB. No corresponding changes were detected for cleaved caspase-8 (data not shown).

MSP and KMSB induce p21

The cell cycle regulator p21 is a well-established target of HDAC inhibitor drugs (256, 257) and dietary HDAC inhibitors (234, 282, 285). HT29 cells have low endogenous levels of p21, but p21 protein expression was elevated for at least 24 h after MSP- or KMSB-treatment (**Figure 4.6A**). Quantitative RT-PCR analyses revealed that MSP and KMSB also increased *p21* mRNA levels in HT29 cells (**Figure 4.6B**). For example, 2, 10, and 50 μM concentrations of KMSB increased *p21* mRNA expression 1.5-, 6-, and 13-fold, respectively.

Chromatin immunoprecipitation assays of the *P21WAF1* promoter revealed a slight decrease in Pol II and histone H3 levels, and a 2- to 3-fold increase in acetylated histone H3 K9 and acetylated histone H3 K18 levels, 4 h after HT29 cells were treated with 10 μM MSP (**Figure 4.6C**). No significant changes were detected for the promoter region of a control gene (*ACTB*) under the same experimental conditions (data not presented).

In HT29 cells transfected with a *P21WAF1* promoter-reporter containing p53 and Sp1/Sp3 sites, 10 μM MSP or KMSB increased the luciferase activity significantly (**Figure 4.6D**).

Deletion of the p53 and Sp1/Sp3 sites decreased the basal reporter activity (compare white bars in Figure 4.6D), but as long as the Sp1/Sp3 sites were present, MSP and KMSB both increased the reporter activity compared with the corresponding control. Deletion of the Sp1/Sp3 sites (in p21PSmaΔ1) completely abrogated the response to MSP and KMSB.

To examine the role of p53, HCT116 ($p53^{-/-}$) and HCT116 ($p53^{+/+}$) cells were treated with 10 μM MSP and 12 h later the whole cell lysates were immunoblotted for p53, p21, and acetylated histone H3 (**Figure 4.6E**). As expected, p53 was detected in HCT116 ($p53^{+/+}$) but not in HCT116 ($p53^{-/-}$) cells, and MSP had no effect on the basal p53 expression in either cell line. Higher levels of endogenous p21 were detected in HCT116 ($p53^{+/+}$) than HCT116 ($p53^{-/-}$) cells, but in both cell lines MSP strongly induced p21, as well as acetylated histone H3. Histone H3 and β-actin, which served as loading controls, were unaffected by MSP treatment.

4.5 Discussion

We report here, for the first time, that MSP and KMSB inhibited human HDAC1 and HDAC8 activities in a concentration-dependent manner *in vitro*. Enzyme kinetics studies coupled with molecular modeling supported a mechanism involving reversible competitive inhibition, as seen for other small molecule inhibitors, such as butyrate and allyl mercaptan (269, 353). The predicted orientation of MSP and KMSB in the HDAC pocket resembled that of known HDAC inhibitor drugs, which coordinate with the zinc atom and establish H-bond partners with buried polar residues. Considering the conserved nature of the HDAC active site, it is likely that MSP and KMSB will inhibit other class I and class II HDACs by competing with substrate for binding to the enzyme. An important distinction, however, is that nM Ki values are typical for the more potent HDAC inhibitors used in the clinical setting, whereas butyrate, allyl mercaptan, and MSP have inhibitor constants on the order of 46 μM, 24 μM, and 35 μM, respectively ((269, 353), and this study). As discussed elsewhere (353, 358), dietary HDAC inhibitors typically produce a more sustained level of histone hyperacetylation with lower toxicity than HDAC inhibitor drugs. Thus, dietary isothiocyanates, organosulfur compounds, and organoselenium metabolites might be combined with lower doses of clinically-used HDAC inhibitors to minimize toxicity and augment the therapeutic efficacy.

Colon cancer cells treated with MSP or KMSB had increased levels of p21 mRNA and protein expression, and there was increased histone acetylation associated with the *P21WAF1* promoter region. Previous studies implicated p21 as a downstream target of HDAC inhibitor drugs (256, 257). We have reported that dietary HDAC inhibitors, such as sulforaphane and allyl mercaptan, increase p21 mRNA and protein expression in human cancer cells, with evidence for histone hyperacetylation on the *P21WAF1* promoter, and enhanced binding of the transcription factor Sp3 (282, 285, 353). Consistent with the latter findings, MSP and KMSB increased the activity of a *P21WAF1* luciferase reporter in HT29 cells, except when the Sp1/Sp3 sites were eliminated, and p21 mRNA and protein levels were elevated markedly. Deletion of the p53 binding sites did not interfere with the ability of KMSB or MSP to induce *P21WAF1* reporter activity. We also observed that in p53-null HCT116 ($p53^{-/-}$) cells, MSP strongly increased the expression of acetylated histone H3, as well as p21 (Figure 4.6E). These findings suggest that the mechanism of p21 induction is likely to be p53-independent, although in cells that contain p53 (wild type or mutant) there may be a role for p53 at later time points, as reported for allyl mercaptan(353). In addition to p21, we are interested in studying other potential targets, and several interesting candidates have been implicated in prior studies with HDAC inhibitor drugs (304, 359, 360). Given the level of apoptosis induction in response to MSP and KMSB treatment (Figure 4.5), bax and related Bcl-2 family members may be worthy of investigation (285).

Much interest of late has focused on the anticancer effects of selenium-enriched yeast and SM. However, selenium-enriched broccoli florets and broccoli sprouts containing high levels of MSC inhibited colon tumor development in several preclinical studies (183, 184, 361). Interestingly, SM produced negative or equivocal results in colon cancer models (175, 362, 363), and addition of inorganic selenite to regular broccoli florets or broccoli sprout powder proved ineffective for the reduction of colon tumors. In a side-by-side comparison, selenium-enriched garlic was more than twice as effective as selenium-enriched yeast for mammary cancer chemoprevention (364). Collectively, these studies clearly indicate that the chemical form of selenium impacts significantly on the potential for cancer chemoprevention.

It has been suggested that MS may be a key active metabolite of MSC, SM, and other selenocompounds (351). The working hypothesis is that MS can redox-modify cysteine-rich regions in proteins, altering their conformation and activity, thereby regulating signaling pathways and gene expression (365). Protein kinase C (PKC) has been postulated as a direct target for redox modification by MS (366). The variation in chemopreventive efficacy between different selenocompounds was presumed to be associated with their different abilities to generate MS. However, this may not be the entire story. MSC is a good substrate for GTK, an enzyme that is widely distributed in mammalian tissues, but which has low activity towards SM (367). We observed histone hyperacetylation after 24 h in colon cancer cells treated with 200 μM MSC, but not SM, and at 5 h no change in histone acetylation status was detected for either compound. Also, in experiments with the *P21WAF1* promoter-reporter, MSC increased the transcriptional activity after 24 h, whereas SM had no effect (data not shown). We interpret these findings as indirect evidence for the conversion of MSC, but not SM, to the α-keto acid metabolite in human colon cancer cells. Support for this idea comes from experiments in human prostate cancer cells, which contain endogenous GTK and convert MSC, but not SM, to the α-keto acid metabolite(368). Given the disappointing news from the Selenium and Vitamin E Cancer Prevention Trial, in which selenium supplements were provided as SM(369), we believe it is now timely to consider a new chemoprevention paradigm for organoselenium compounds. Specifically, MSC and other organoselenium compounds might generate α-keto acid metabolites as HDAC inhibitors, with the potential to affect histone status and chromatin remodeling, leading to de-repression of silenced tumor suppressor genes.

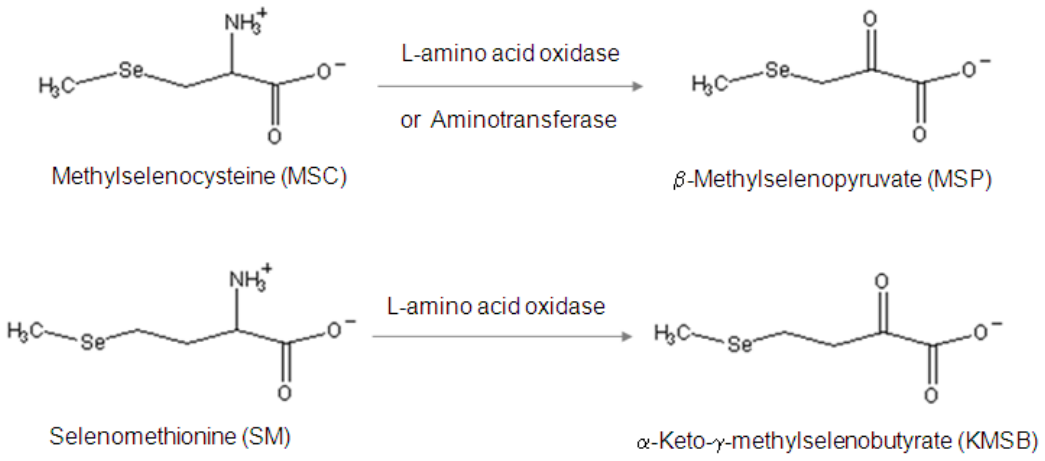

Figure 4.1 Deamination reactions of organoselenium compounds MSC and SM to generate α-keto acid metabolites, MSP and KMSB, respectively.

(A)

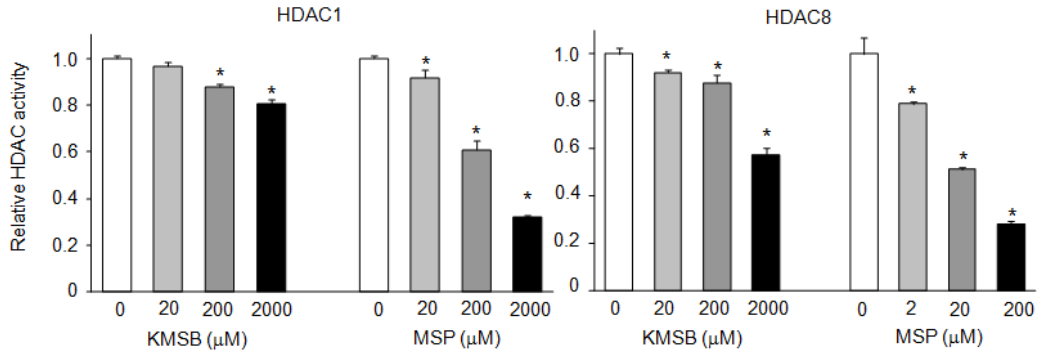
HDAC1
HDAC8
Relative HDAC activity
1.0
0.8
0.6
0.4
0.2
0
0 20 200 2000
KMSB (μM)
0 20 200 2000
MSP (μM)
0 20 200 2000
KMSB (μM)
0 2 20 200
MSP (μM)

(B)

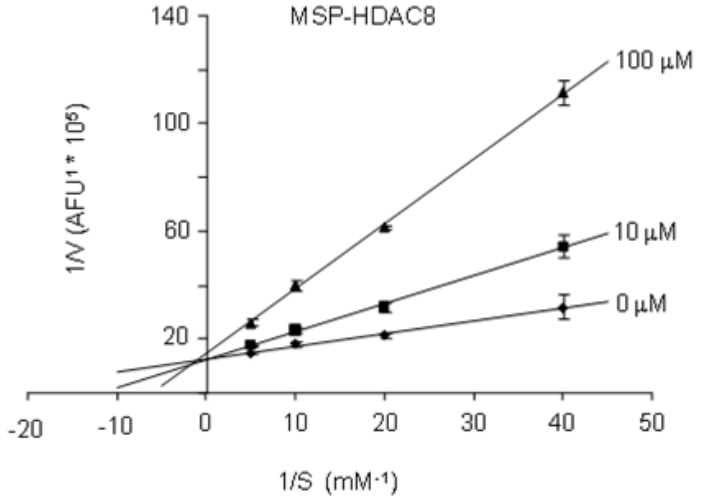
MSP-HDAC8
100 μM
10 μM
0 μM
1/V (AFU¹ * 10⁵)
140
100
60
20
-20
-10
0
10
20
30
40
50
1/S (mM⁻¹)

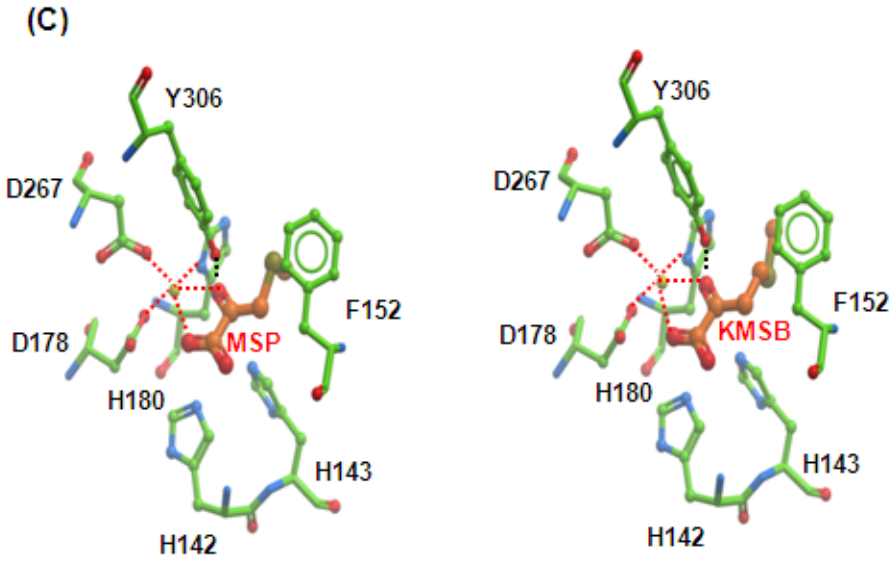

Figure 4.2 KMSB and MSP inhibit HDAC activity. (A) HDAC assays were performed with purified human HDAC1 and HDAC8, in the presence of different concentrations of MSP or KMSB. Data = mean±SD, n=3, *P <0.05. (B) Kinetics of HDAC8 inhibition by MSP. Reaction velocities were measured at different concentrations of substrate, in the presence of 0, 10, and 100 μM MSP. The Lineweaver-Burk plot indicated competitive inhibition (K_i = 35 μM). (C) Docking of MSP (left) and KMSB (right) into human HDAC8 catalytic domain (ICM v3.5-1p). Zinc coordination is represented by red dashed lines. H-bonds are represented by black dashed lines between donor (D) and acceptor (A) atoms, defined as follows: Distance D---A: 2.8-3.2 Å; Angle D-H---A: 140-180˚.

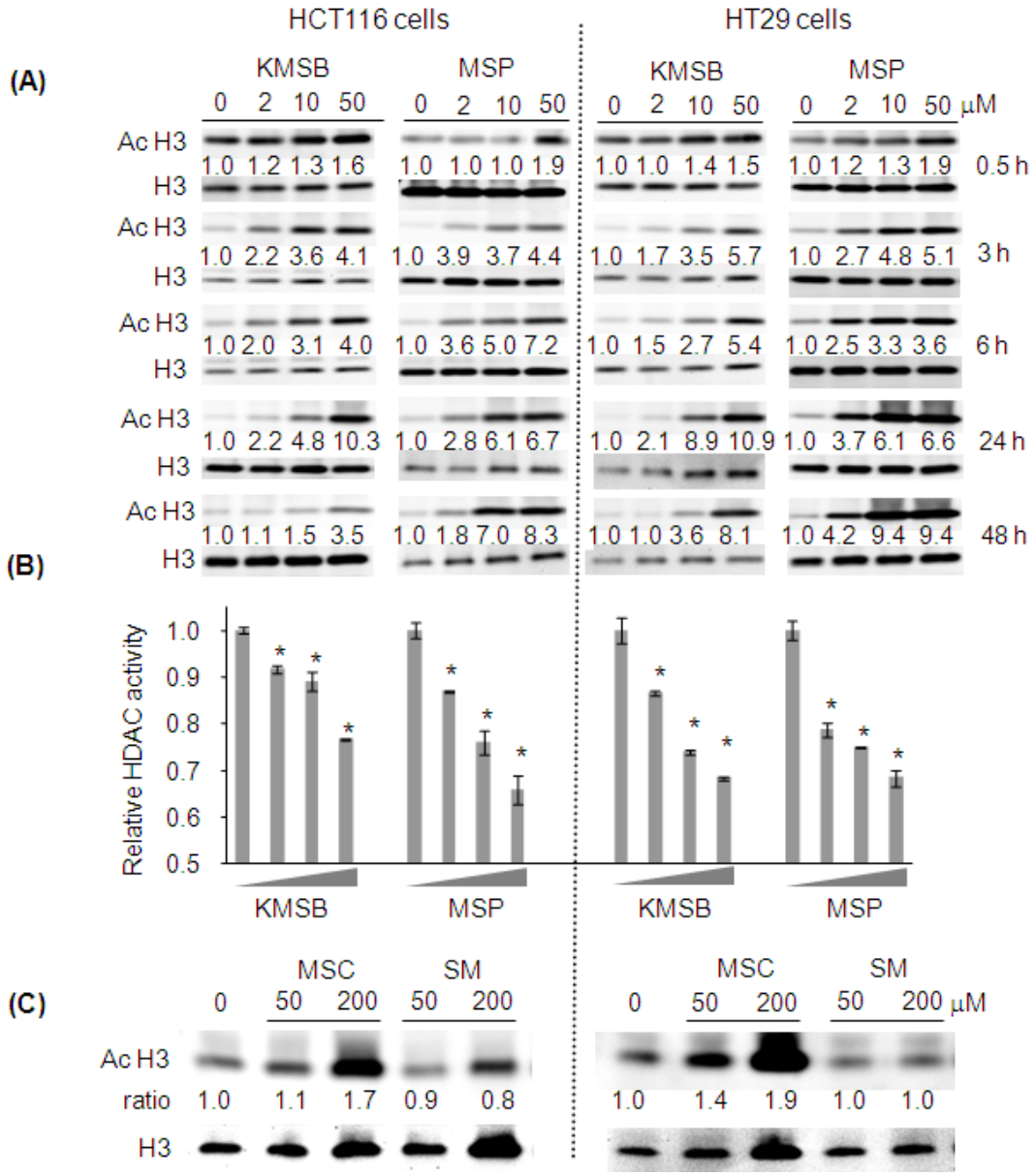

Figure 4.3 Histone acetylation induced by KMSB and MSP in human colon cancer cells. (A) HT29 and HCT116 cells were exposed to 0, 2, 10, and 50 μM KMSB or MSP, and at the times shown acetylated histone H3 (Ac H3) levels were assessed by immunoblotting. Total histone H3 (H3) expression was used as reference control. The ratio of Ac H3:H3 expression is shown for each lane, with the 0 μM treatment control assigned an arbitrary value of 1.0. (B) HDAC activities in nuclear extracts of HCT116 and HT29 cells 3 h after treatment with 0, 2, 10, and 50 μM KMSB or MSP (wedge symbol). Data = mean±SD, n=3, *P <0.05. (C) HCT116 and HT29 cells were exposed to 0, 50, or 200 μM MSC or SM (selenium parent compounds, see Figure 1), followed by immunoblotting for Ac H3 and H3 at 24 h.

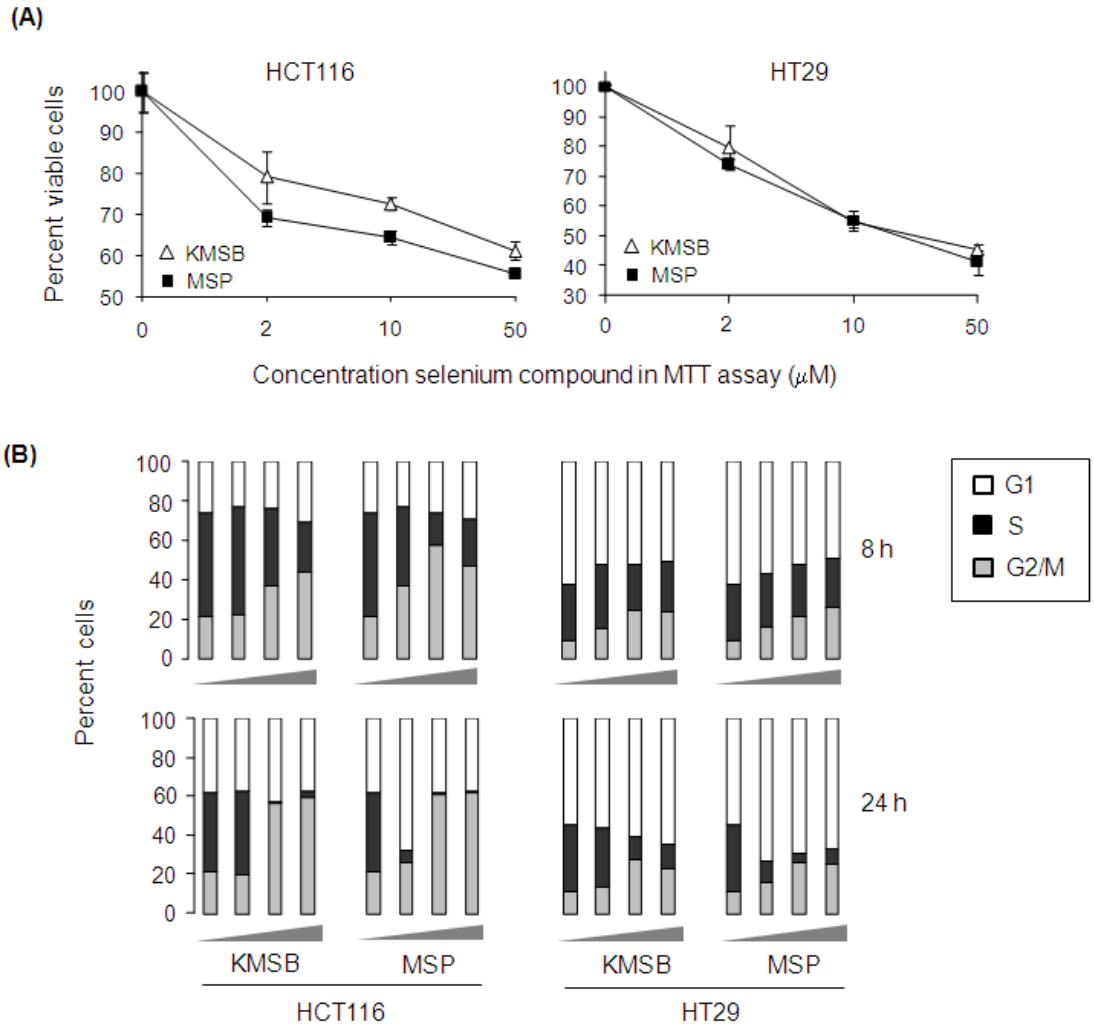

Figure 4.4 KMSB and MSP suppress cell growth and induce cell cycle arrest. (A) In the MTT assay, HCT116 and HT29 cells treated with 0, 2, 10, and 50 μM KMSB or MSP displayed dose-dependent loss of cell viability at 48 h. Data = mean±SD, n=3. (B) HCT116 and HT29 cells were exposed to 0, 2, 10, and 50 μM KMSB or MSP (wedge symbol). The percentage of cells occupying G1, S, and G2/M phases of the cell cycle was determined by flow cytometry. Results are shown for cells collected 8 and 24 h after treatment, and are representative of three independent experiments.

(A)

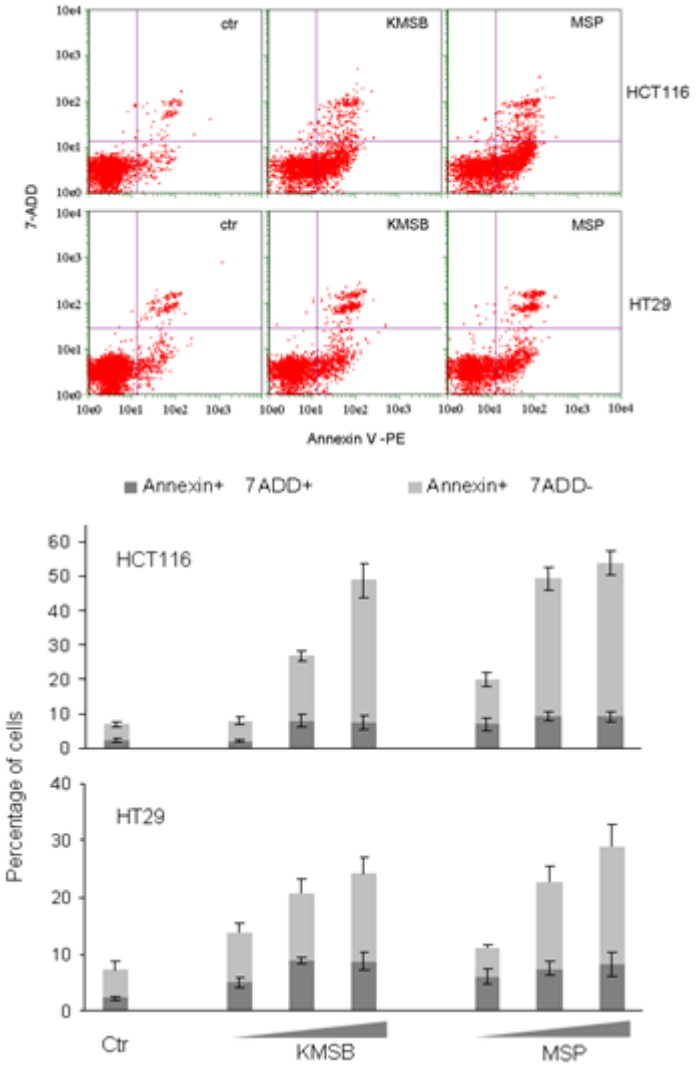
ctr
KMSB
MSP
HCT116
HT29
7-ADD
Annexin V -PE
Annexin+ 7ADD+
Annexin+ 7ADD-
Percentage of cells
Ctr
KMSB
MSP

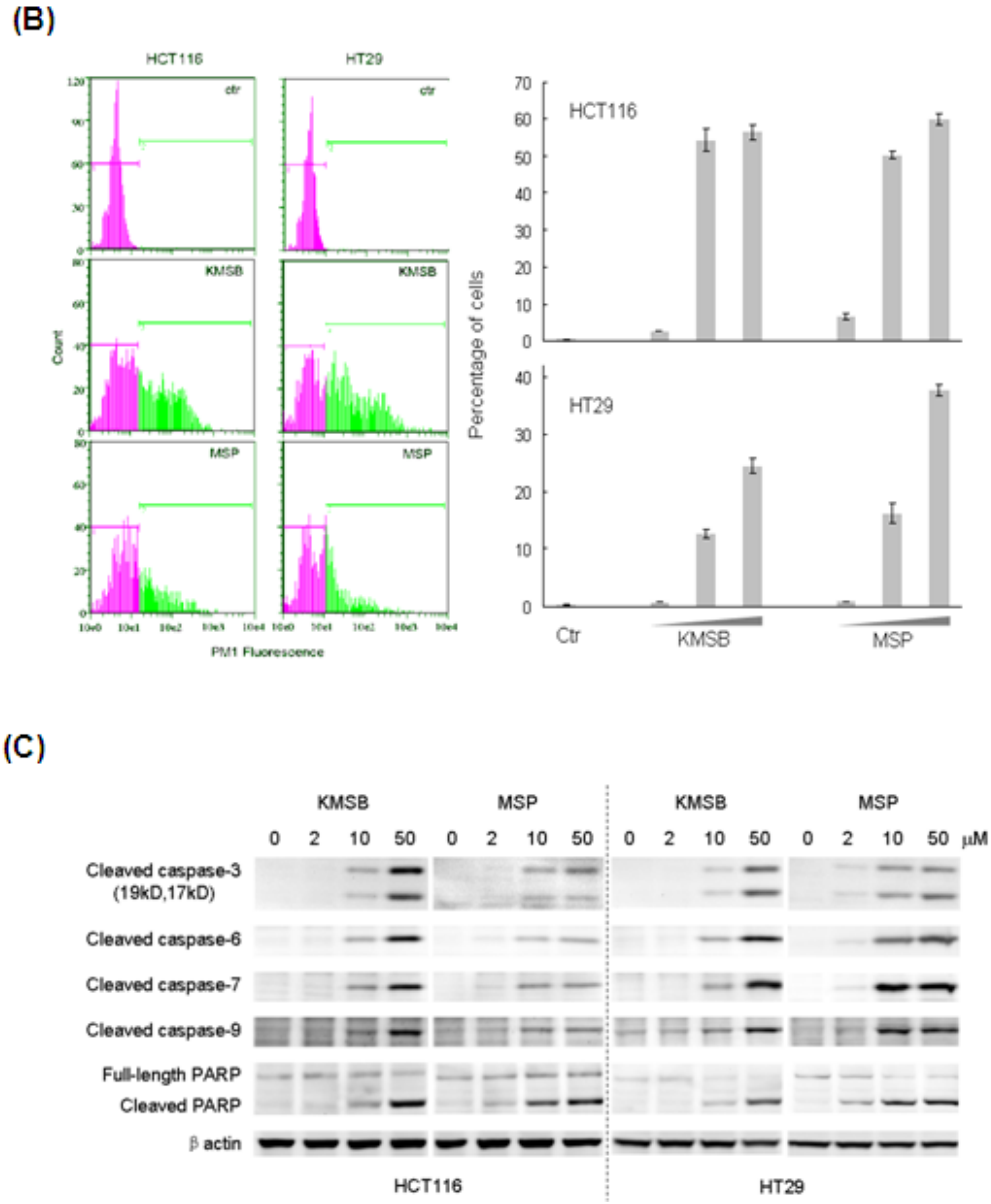

Figure 4.5 KMSB and MSP induce apoptosis in colon cancer cells. (A) HCT116 and HT29 cells were exposed to 2, 10, and 50 μM KMSB or MSP (wedge symbol), or vehicle alone (control, Ctr). Cells were stained 24 h later with Annexin V-PE and 7-AAD (top). Annexin V (+) and 7-AAD (-) indicates early apoptotic cells, whereas Annexin v (+) and 7-AAD (+) indicates late-stage apoptotic cells. The percentage of cells in each population is summarized as mean±SD, n=3 (bottom). (B) Cells were fixed 48 h after treatment with 2, 10, and 50 μM KMSB or MSP (wedge symbol), or vehicle alone (control, Ctr), and TUNEL-positive cells were quantified, see Materials and Methods. Data bars=mean±SD, n=3 (right). (C) Cells were treated with KMSB or MSP and immunoblotted 24 h later for cleaved caspase-3 (two cleaved products of 19 and 17 kD), -6, -7, -9, and PARP (full-length and cleaved bands). β-Actin, loading control.

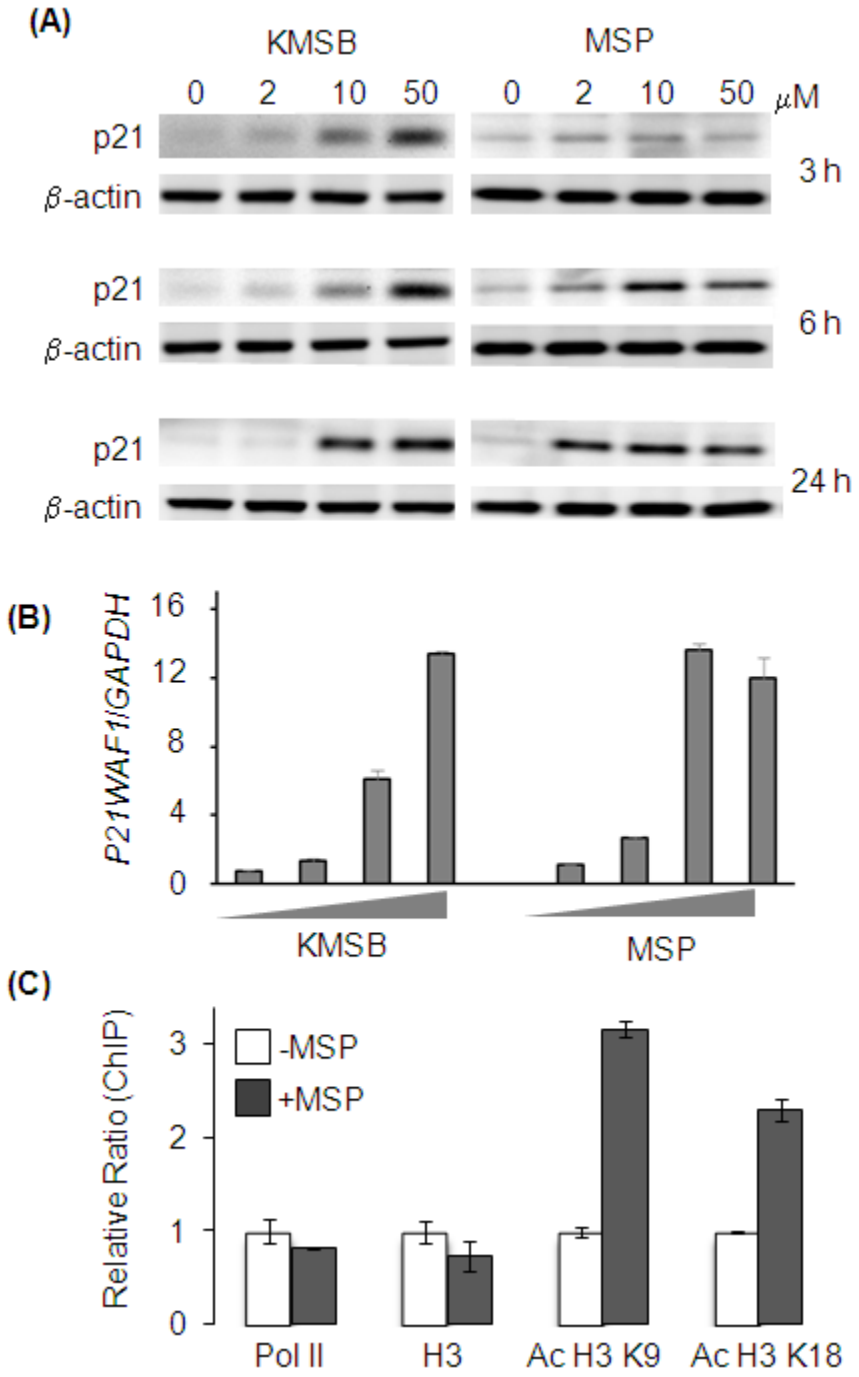
(A)
KMSB
MSP
0 2 10 50 0 2 10 50 μM
p21
β-actin
3 h
6 h
24 h
(B)
P21WAF1/GAPDH
16
12
8
4
0
KMSB
MSP
(C)
Relative Ratio (ChIP)
3
2
1
0
-MSP
+MSP
Pol II
H3
Ac H3 K9
Ac H3 K18

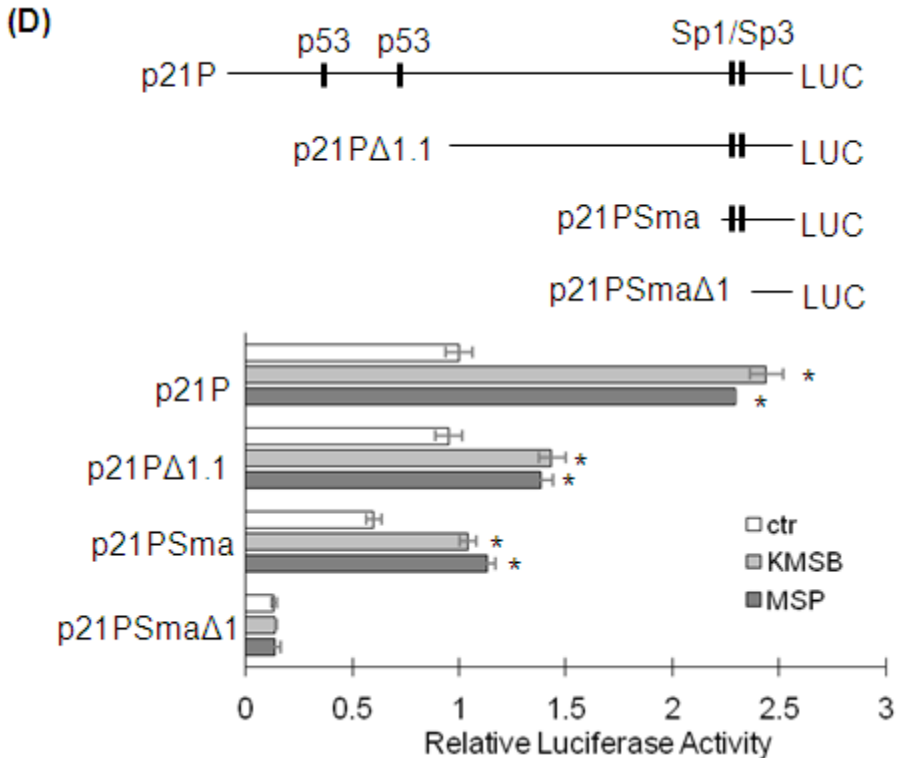
(D)
p53
p53
Sp1/Sp3
p21P
LUC
p21PΔ1.1
LUC
p21PSma
LUC
p21PSmaΔ1
LUC
p21P
p21PΔ1.1
p21PSma
p21PSmaΔ1
ctr
KMSB
MSP
0
0.5
1
1.5
2
2.5
3
Relative Luciferase Activity

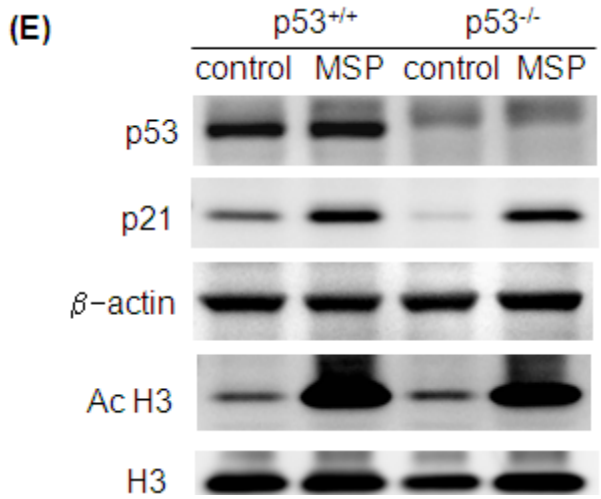

Figure 4.6 Induction of p21 by KMSB and MSP. (A) HT29 cells were exposed to 0, 2, 10, and 50 μM KMSB or MSP, and 3, 6, or 24 h later p21 expression was determined by immunoblotting. (B) Quantitative RT-PCR data for *p21* mRNA expression (normalized to *GAPDH*), 6 h after HT29 cells were treated with 0, 2, 10 and 50 μM KMSB or MSP (wedge symbol). Data bars=mean±SD, n=3. (C) ChIP assays of the *P21WAF1* promoter were performed 4 h after treatment with 10 μM MSP, using the indicated antibodies, and output was quantified by Q-PCR and normalized to input (relative ratio). Data=mean±SD, n=3, from a single experiment, and are representative of findings from three independent experiments. (D) HT29 cells were treated with 10 μM KMSB or MSP, and 24 h later *p21* transcriptional activity was determined using a luciferase (LUC) reporter, as described in Methods. Results are expressed as relative luciferase activity, mean±SD, n=3; *P<0.05 vs control (Ctr). Upper diagram illustrates constructs that contained full-length 5'-regulatory region harboring both p53 and Sp1/Sp3 sites (p21P), deletion of p53 sites (p21PΔ1.1), or the minimal promoter with (p21PSma) or without (p21PSmaΔ1) Sp1/3 sites. (E) HCT116 ($p53^{+/+}$) and HCT116 ($p53^{-/-}$) cells were treated with 10 μM MSP, and 12 h later the whole cell lysates were immunoblotted for p53, p21, and acetylated histone H3 (Ac H3), with histone H3 and β-actin as loading controls. Data are representative of the findings from two separate experiments.

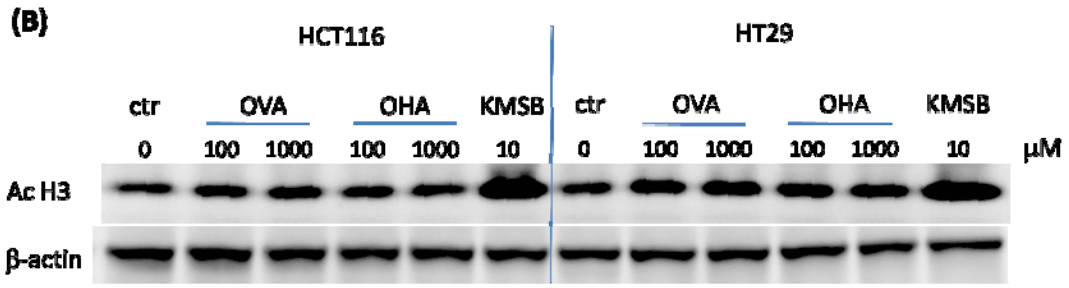

Figure 4S.1 Selenium atom is important for KMSB and MSP's HDAC inhibitory capabilities. (A) HDAC assays were performed in the presence of KMSB, MSP and their analogues 2-oxohexanoic acid and 2-oxovaleric acid within the indicated concentration ranges. (B) HCT116 and HT29 cells were treated with 100μM or 1000μM 2-oxovaleric acid (OVA) or 2-oxohexanoic acid (OHA) for 6 hours, and the levels of acetylated histone H3 in the cell lysates were examined by immunoblot. Cells treated with 10μM KMSB were used as positive controls. β-actin was blotted as loading control.

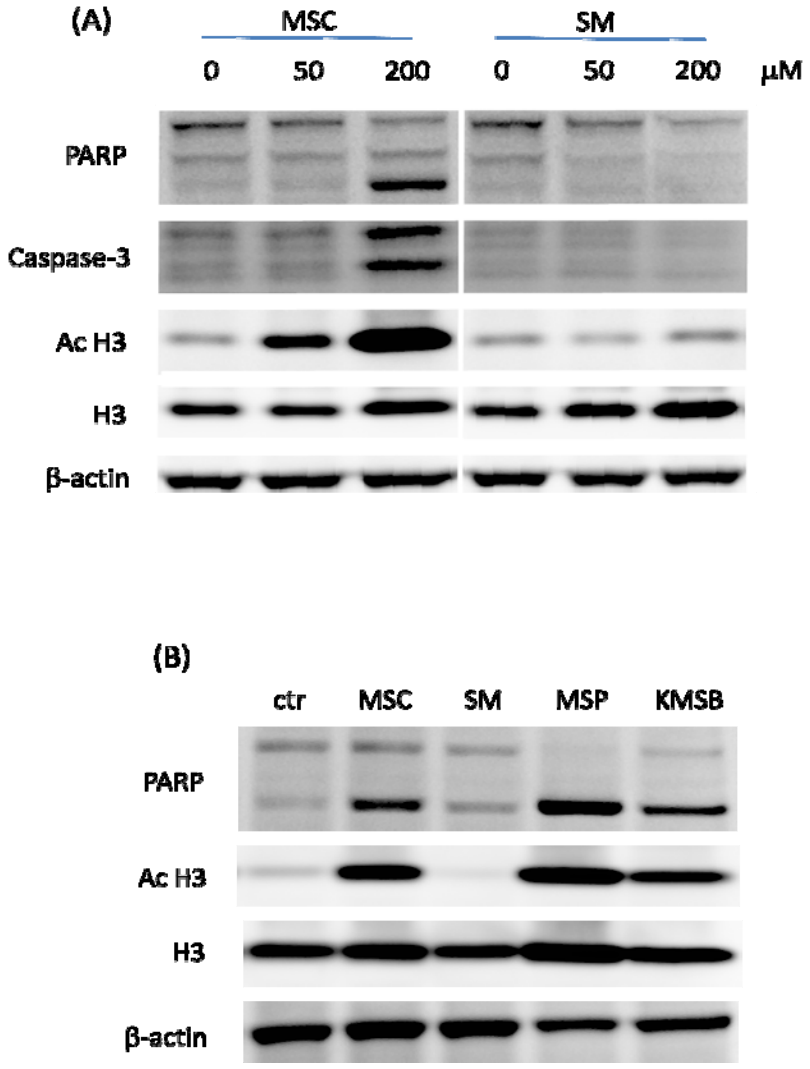

Figure 4S.2 Differential effects of MSC and SM in cancer cell lines. (A) HT29 human colon cancer cells were treated with MSC or SM of indicated concentrations for 36 hours, and the levels of PARP cleavage, activated caspase-3, and acetylated histone H3 were examined using immuoblot. Total histone H3 and β-action were also blotted as loading controls. (B) CCRF-CEM human T-cell leukemia cells were treated with MSC (200μM), SM (200μM), MSP(10μM) or KMSB(10μM) for 36 hours, and the levels of PARP cleavage and acetylated histone H3 were examined using immuoblot. Total histone H3 and β-action were also blotted as loading controls.

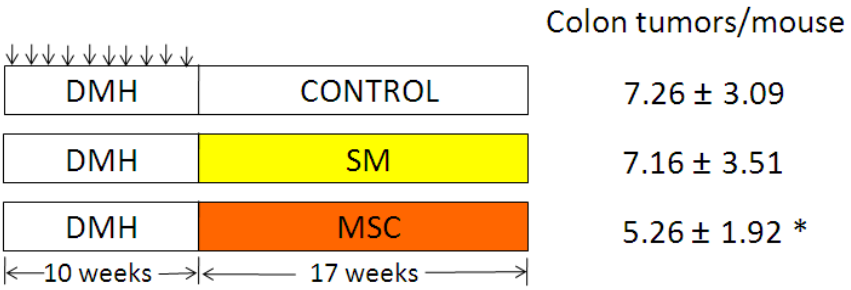

Figure 4S.3 Inhibition of DMH-induced colon tumors by MSC. ICR mice were injected *i.p.* with 20 mg 1,2-dimethyl hydrazine (DMH)/kg body wt, once/wk for 10 wks, then distributed randomly into three groups. One group was fed with standard AIN93M diet (control). The other two groups were fed with 8.6 mg selenium/kg diet in the form of SM or MSC. Mice were euthanized 17 wks later, and the colon tumors were enumerated. *P-value < 0.05, two sample *t*-test (n=19).

Bmf mediates methylselenocysteine-induced apoptosis in colon cancer cells

Hui Nian, Alan Taylor, Mohaiza W. Dashowood, John T. Pinto and Roderick H. Dashwood

Manuscript formatted

5.1 Abstract

Methylselenocysteine has shown chemopreventive efficacy in several cancers, both *in vitro* and *in vivo*, but the molecular mechanisms underlying its anticancer effects are still unclear. Our previous studies have shown that in the presence of glutamine transaminase K, MSC can be converted to its deaminated metabolite, MSP, and MSP is a competitive HDAC inhibitor and induced apoptosis in colon cancer cells. In this paper, we further investigated the role of MSP in MSC's chemopreventive effects in colon cancer cells. First, formation of MSP was detected directly from the cells incubated with MSC. Pretreatment of colon cancer cells with transaminase inhibitor aminooxyacetic acid (AOAA) totally blocked MSC-induced histone hyperacetylation, cell growth inhibition, caspase activation and PARP cleavage. To investigate the molecular mechanisms underlying MSP's anticancer effects, we examined the expression levels of some important apoptosis regulatory proteins. MSP upregulated pro-apoptotic genes Apaf, Bmf, Bim and Bak while downregulated anti-apoptotic gene BCL-xL, among which Bmf was the most dramatically induced gene. Like p21, Bmf mRNA was induced within 1 hour of MSP treatment, and reached the maximal level at 4 hour. MSP induced cell growth inhibition and caspase activation in both p21 wild-type and p21 knock-out cells. However in Bmf mRNA knockdown cells, MSP-induced caspase activation and cell growth inhibition was significantly repressed. Bmf expression was also increased in MSC-treated colon cancer cells, and Bmf knockdown significantly decreased MSC-induced caspase cleavage and cell growth inhibition. These studies confirm that MSP is an active metabolite of MSC in colon cancer cells and contributes to MSC-mediated apoptosis by Bmf induction.

5.2 Introduction

Methylselenocysteine (MSC) is the major organoselenium compound present in selenium-enriched plants, and has reported anticancer properties in several types of cancer *in vivo* and *in vitro*. It has been suggested that methylselenol (MS), a β-elimination product of MSC may be a key metabolite for cancer chemoprevention, acting to redox-modify proteins and regulate key signaling pathways (351). Our previous studies have shown that methylselenopyruvate (MSP) could be another metabolite of MSC after a deamination reaction in the presence of enzymes like glutamine transaminase K. MSP acts as a

competitive HDAC inhibitor and has exhibited anticancer effects in colon cancer cells by inducing cell cycle arrest and apoptosis (370).

Most studies to date indicated that HDAC inhibitors induced apoptosis in colon cancer cells via the intrinsic/mitochondrial pathway(251). This involves a cascade of events including a decrease in mitochondrial membrane potential, cytochrome c release and activation of caspase-9 and 3. Inhibitors of caspase-3 and 9, but not 8, inhibit HDACi-induced apoptosis in colon cancer cells, indicating the importance of the intrinsic apoptotic pathway(32). Previous studies have shown that the transcriptional alteration in the balance between expressions of pro- and anti-apoptotic Bcl-2 family members often initiated HDACi-induced apoptosis via regulating mitochondrial membrane integrity. Global and candidate studies demonstrate increased expression of pro-apoptotic genes including Bim, Bmf and Bak and decreased expression of anti-apoptotic genes including Bcl-2, Bcl-xL and MCL1 in response to HDAC inhibitor treatment (371). Particularly, Bmf is one of the BH3-only Bcl-2 family proteins and regulate activation the intrinsic apoptotic pathway through binding to Bcl-2. Transcriptional activation of Bmf in response to HDACi probably results from hyperacetylation of histones in the Bmf promoter (372). In this study, we report that MSP regulates the expression of Bcl-2 family genes, among which Bmf may play an important role in MSP- and MSC-induced apoptosis.

5.3 Materials and methods

Cell culture and reagents Human HT29 and HCT116 colon cancer cell lines were obtained from American Type Culture Collection (Manassas, VA) and cultivated in McCoy's 5A medium (Life Technologies, Carlsbad, CA) supplemented with 1% penicillin-streptomycin and 10% fetal bovine serum. In some experiments, HCT116 ($p21^{-/-}$) and HCT116 ($p21^{+/+}$) cells were used, kindly provided by Dr. Bert Vogelstein (Johns Hopkins University, Baltimore, MD). MSC was purchased from Sigma (M6680). MSP was generated as reported elsewhere (352).

HPLC-MS-MS analysis of MSC and MSP in the cells HT29 cells were treated with MSC and harvested at 6hr. Cell pellets were sonicated in 250µl water and mixed with 750µl of acetonitrile, and then centrifuged at 16,100 x g for 5 min. The supernatant was transferred to HPLC vials. Standard stocks of MSC and MSP were diluted to 100 µM, then diluted with 3

volumes of acetonitrile, and transferred to HPLC vials. Chromatographic separation was performed on a Shimadzu HPLC system (two LC-10ADvp pumps, a DGU-14A degasser, a SIL-HTc autosampler/system controller, and a CTO-10Avp column oven; Columbia, MD, USA) and a Luna HILIC column (150 x 2 mm) with SecurityGuard HILIC guard cartridge (4 x 2 mm) (both from Phenomenex, Torrance, CA, USA). Both sample (10° C) and column (30° C) temperatures were controlled. The mobile phase contained 0.01% (v/v) formic acid and 10 mM ammonium formate with a gradient of mobile phases A (95:5 acetonitrile:water) and B (Milli-Q water) at a flow rate of 200 μL per minute, with a 5 min equilibration at 5% B prior to each sample. Following sample injection, the mobile phase mix was held at 5% B for 2 min, then increased to 30% B over 8 min, then held at 30% B for 3 min, then returned to 5% B over 1 min, and maintained at 5% B until the end of the run at 20 min. The HPLC system was coupled to a triple quadrupole mass spectrometer with TurboIon Spray source operated in negative mode (Applied Biosystems/MDS Sciex API 3000, Foster City, CA, USA). Nebulizer, curtain, and collision (CAD) gas parameters were set at 7, 7, and 5, respectively. Heater gas was supplied at 6 L/min at 400°C. All gases were high purity nitrogen supplied by a custom liquid nitrogen system (Polar Cryogenics, Portland, OR, USA). The ionizing voltage was –4200 V, and the declustering, focusing, entrance, and exit potentials were –30, –250, –10, and –11 V, respectively. Selective reaction monitoring (SRM) of *m/z* 182.0 to 95.0 and *m/z* 181.0 to 95.0 was used for detecting MSC and MSP, at collision energies of -10 and -13V, respectively. Quantitation was determined from sample-to-standard peak area ratios of MSC and MSP peaks.

MTT assay Cell growth was determined by assaying for the reduction of dimethyl thiazolium bromide (MTT) to formazan. Briefly, after 48 h incubation with MSP or MSC, 10 μl MTT (5 μg/μl) were added to cells in 96-well plates. Cells were incubated at 37°C for 4 h, and a Spectra MaxGemini XS fluorescence plate reader (Molecular Devices) was used to measure absorbance at 620 nm for each well. Growth rate was calculated as follows: Cell growth = [A_{620} treated cells/A_{620} control cells] ×100%.

Immunoblotting Protein concentration of cell lysates was determined using the BCA assay (Pierce, Rockford, IL). Proteins (20 μg) were separated by SDS-PAGE on 4-12% Bis-Tris gel

(Novex, San Diego, CA) and transferred to nitrocellulose membranes (Invitrogen, Carlsbad, CA). Membranes were saturated with 2% BSA for 1 h, followed by overnight incubation at 4°C with primary antibodies against acetylated histone H3 (1:200, Upstate, #06-599), histone H3 (1:200, Upstate, #06-755), p21 (1:1000, Cell Signaling, #2947), PARP (1:1000, cell signaling, #9532), cleaved caspase-3(1:1000, cell signaling, #9661), cleaved caspase-6(1:1000, cell signaling, #9761), cleaved caspase-9(1:1000, cell signaling, #9505), or β-actin (A5441, 1;5000, Sigma). Membranes were then incubated with peroxidase-conjugated secondary antibodies (Bio-Rad, Hercules, CA) for 1 h. Immunoreactive bands were visualized by using Western Lightning Chemiluminescence Reagent Plus (PE Life Sciences, Boston, MA) and detected with an AlphaInnotech imaging system.

RT-PCR and quantitative real-time PCR Cells treated with MSP or MSC were disrupted by using QIAshredder spin column (QIAGEN, Santa Clarita, CA, USA) and total RNA was extracted using the RNeasy® Mini kit (QIAGEN) in accordance with the manufacturer's instructions. Single-strand cDNA was then synthesized with 2 μg of total RNA using the SuperScript™ III First-Strand Synthesis kit (Invitrogen, Carlsbad, CA, USA), according to the manufacturer's protocol. Real-time amplification was achieved using Roche LightCycler 480 Real-Time PCR instrument with standard temperature protocol and 2*LightCycler 480 SYBR Green I Master in 10μl volume, in triplicates. 500nM concentrations of the following primer pairs were used for the reations: p21: F-5'-ATGAAATTCACCCCCTTTCC-3' and R-5'-CCCTAGGCTGTGCTCACTTC-3'; Bax: F-5'-TCTGACGGCAACTTCAACTG-3' and R-5'-CACTGTGACCTGCTCCAGAA-3'; Bcl-2: F-5'-GTCTGGGAATCGATCTGGAA-3' and R-5'-AATGCATAAGGCAACGATCC-3'; Bmf: F-5'-CTGGGAAGTGGACTGTGGTT-3' and R-5'-GGCAGGTACTGGCTGAGAAG-3'; Bim: F-5'-GAGATATGGATCGCCCAAGA-3' and R-5'-GTGCTGGGTCTTGTTGGTTT-3'; Bcl-xL: F-5'-TCTGGTCCCTTGCAGCTAGT-3' and R-5'-TCCTTTCTGGGGAAGAGGTT-3'; Apaf: F-5'-TGGCCTTCAGCAGTTCTTTT-3' and R-5'-ATTAAAATTGGCCCCACCTC-3'; Bak: F-5'-GGGTCTATGTTCCCCAGGAT-3' and R-5'-GCACCCCTAGAGTTGAGCAG-3'; Caspse-9: F-5'-GCTTAGGGTCGCTAAATGCTG-3' and R-5'-TGTCGTCAATCTGGAAGCTG-3'. The mRNA expression of the target gene was normalized to the corresponding *GAPDH* internal control.

Small RNA interference The duplex siRNAs for Bmf (target sequences: 5'-CAACCUUGCUUUGAAUGGA-3', 5'-GAGUAACAGAUAACGAUUA-3', 5'-GAAUCUACCAGUUG UCGAA-3', 5-GGAAAUAGGAGGAGUCUAG-3') were synthesized by Dharmacon. Cells were plated at 105 cells per well in a 6-well plate, incubated for 24 hours, and transfected either with Bmf siRNA or control random siRNA duplexes (100nM each) using DharmaFECT 4 transfection agents according to the manufacturer's instructions.

Statistics Where indicated, results were expressed as mean±SD. Statistical significance was evaluated for data from three independent experiments using Student's *t*-test. A *P*-value <0.05 was considered to be statistically significant, and indicated as such with an asterisk (*) on the corresponding figures.

5.4 Results

Generation of MSP in MSC-treated cells

In our previous studies, we have shown MSP was formed when MSC was incubated with homogenates of prostate cancer cells in a cell-free system. To demonstrate whether MSC can be transformed into MSP in the cells, we incubated HCT116 and HT29 cells with MSC for 6 hours, and the existence of MSP and MSC in the media and cell lysate was examined by HPLC-MS-MS. As is shown in **Figure 5.1**, in the media we detected only MSC, but in the cell lysate extracted from treated cells we also detected MSP, indicating MSP was generated from MSC inside the cells. The relative concentration of MSP in the cell lysate is about one fortieth of that of MSC.

AOAA pretreatment repressed MSC's anticancer effects

To evaluate the role of MSP in MSC's anticancer effects, we used the transaminase inhibitor aminooxyacetic acid (AOAA) to block MSC's conversion to MSP. First we tried different concentrations of AOAA and found that 0.5mM AOAA pretreatment did not change MSP's effect on histone acetylation but completely repressed MSC-induced histone hyperacetylation in the cells (**Figure 5.2 A**). We conclude at this dose, AOAA blocks the generation of MSP from MSC in the cells. Without AOAA, MSC induced significant cell growth inhibition, p21 protein increase, caspase-3 activation and PARP cleavage in HCT116 cells as

we have seen in MSP-treated cells. But with the pretreatment of 0.5mM AOAA, all these MSC's cellular effects were completely repressed, while the presence of AOAA had no effect on MSP's effects (**Figure 5.2 B**, **C**).

P21 induction is not critical for MSP's anticancer effects

MSP can induce cell cycle arrest and caspase-mediated apoptosis in colon cancer cells. Like other HDAC inhibitors, MSP rapidly increased the expression of cell cycle inhibitor p21. Although it has been reported that p21 induction was critical for some HDAC inhibitors' anticancer effects in colon cancer cells, we found that it was dispensible for MSP-induced colon cancer cell growth inhibition and apoptosis. In both p21 +/+ and p21 -/- HCT116 cells, MSP caused similar proliferation inhibition and apoptotic effects indicated by PARP cleavage and caspase-3 activation (**Figure 5.3**).

MSP induces Bmf expression

To investigate the molecular mechanisms underlying MSP-induced apoptosis, we examined the expression levels of several apoptosis-related genes that have been reported to play an important role in cancer cell apoptosis induced by other HDAC inhibitors. As is shown in **Figure 5.4 A**, in HCT116 and HT29 cells, 12 hour treatment of MSP decreased the mRNA level of anti-apoptotic gene Bcl-xL by about 75%, while approximately doubled the expression levels of pro-apoptotic genes Apaf-1, Bak and Bim. In particular, MSP treatment dramatically induced Bmf expression with 14-fold increase in mRNA level in HT29 cells and 18-fold in HCT116 cells. Similar to p21, Bmf induction by MSP occurred very quickly (**Figure 5.4 B**). Within one hour after treatment, Bmf mRNA increased by 5 fold, and at 6 hour, the level of Bmf mRNA reached the maximum. Like p21, Bmf could be an immediate gene regulated by MSP at the transcriptional level.

Bmf mRNA knock-down decreased MSP- and MSC-mediated apoptosis

To evaluate biological significance of the Bmf induction in MSP-mediated apoptosis, we used siRNA to knock down Bmf expression in HT29 cells. Transfection of Bmf siRNA reduced more than 85% of Bmf transcripts in the cells, compared to non-target siRNA-transfected cells (**Figure 5.5 A**). Knocking down Bmf significantly reduced MSP-induced activation of caspase-

3, 6, and 9. Higher level of PARP remained uncleaved upon MSP treatment in Bmf knockdown cells compared to cells transfected non-target siRNA (**Figure 5.5 B**). And we also observed Bmf knock-down reduced MSP-induced HT29 cell growth inhibition from 50% to 30% (**Figure 5.5 C**).

MSC can also induce Bmf expression in HT29 cells. Knocking down Bmf significantly repressed MSC-induced caspase activation, PARP cleavage and cell growth inhibition, indicating Bmf induction could be very important for MSC's apoptotic effects (**Figure 5.5**).

5.5 Discussion

In previous studies, we have identified MSP as a deaminated metabolite of MSC, given that MSC is a good substrate of glutamine transaminase K (GTK) and GTK is widely distributed in tissues (368). In this study, for the first time, we provided the direct evidence that MSC can be transformed to MSP in the cells. It has been reported that *in vivo*, MSC can be absorbed and transported to tissues in intact form(373); therefore we assume that MSP could possibly be an active metabolite of MSC *in vivo*. In HPLC-MS-MS analysis of lysates from MSC-treated colon cancer cells, the concentration of generated MSP is about one-fortieth of that of MSC, which is in line with our observation that that 2-10μM MSP induced significant cell growth inhibition and apoptosis while 200μM of MSC was needed to induce similar effects in the same conditions.

P21 induction is consistently involved in the action of almost all the HDAC inhibitors in various cancer cells. Increased expression of p21 protein could arrest cells at G1 or G2/M phase and subsequently inhibit cancer cell growth. Archer et al. have reported that p21 induction is critical for HDACi-mediated growth inhibition in colon cancer cells demonstrated by the attenuated growth inhibitory effect of butyrate on the p21 deficient HCT116 cells (12). But cell growth arrest mediated by p21 induction is not the only mechanism for HDACi's inhibitory effects on cancer cell growth. MSP can induce both cell cycle arrest and apoptosis in colon cancer cells. Although in p21 deficient HCT116 cells, MSP-induced G2/M arrest was attenuated (data not shown), MSP still caused similar apoptotic and growth inhibitory effects in the presence or absence of p21. We assume that MSP-induced cell cycle arrest only

marginally contributes to its growth inhibitory effects and MSP-mediated apoptosis (independent of p21 induction) may play a greater role in MSP's anticancer efficacy.

MSP induced caspase-mediated apoptosis in colon cancer cells. Activation of caspase-9 but not -8 implicates that MSP may induce apoptosis via the mitochondrial apoptotic pathway. Many studies have shown that the initiating events in HDACi-induced apoptosis involve altered expression of Bcl-2 family members (371). In this paper, we report that MSP also increases the expression of some pro-apoptotic Bcl-2 genes and decreases the expression of anti-apoptotic gene Bcl-xL. Among these genes, Bmf was most dramatically induced, and its induction followed the same pattern as the induction of p21, indicating MSP could regulate Bmf expression on the transcriptional level probably accompanied by histone acetylation alteration in the promoter region. Zhang et al. have reported that HDAC inhibitors FK228 and CBHA enhanced Bmf promoter activity, and preferentially increased acetylation of H3 and H4 at the promoter region of the Bmf gene within one hour of treatment (372). Knocking down Bmf expression profoundly inhibited proapoptotic action of MSP in colon cancer cells, suggesting Bmf induction could be a crucial event in MSP-mediated apoptosis. But it is likely that increased Apaf-1, Bak (in HT29 cells only), Bim and decreased Bcl-xL also play a role in MSP-induced apoptosis in colon cancer cells, which may account for the growth inhibition induced by MSP and MSC in Bmf knockdown cells.

Bmf induction and its critical role in apoptosis mediation were also demonstrated in MSC-treated colon cancer cells, implying MSP could be an important executor for MSC's chemopreventive effects. This is consistent with our observation that MSC's anticancer effects were significantly repressed when the transaminse activities in the cells were inhibited by AOAA. But for the moment we cannot rule out the possibility that another presumptive metabolite methylselenol may also contribute to MSC-induced apoptosis. MSC is assumed to generate methylselenol via a β-elimination reaction catalyzed by cysteien-S-conjugate beta-lyase. Beta-lyase and transaminases share the same cofactor pyridoxal phosphate (PLP). AOAA function by interfering with PLP, and therefore inhibit activities of beta-lyase and transaminases at the same time. AOAA pretreatment could block generation of both MSP and methylselenol in the cells. Further studies are needed to probe molecular

mechanisms underlying MSC and MSP's anticancer effects in order to clarify the role of MSP in MSC's chemopreventive efficacy.

Figure 5.1 Generation of MSP from MSC in colon cancer cells. HCT116 and HT29 cells were treated with MSC for 6 hours. The media and cell lysates were examined by HPLC-MS-MS as described in Materials and methods. MSC (Rt 9.56min) and MSP (4.98min) were detected.

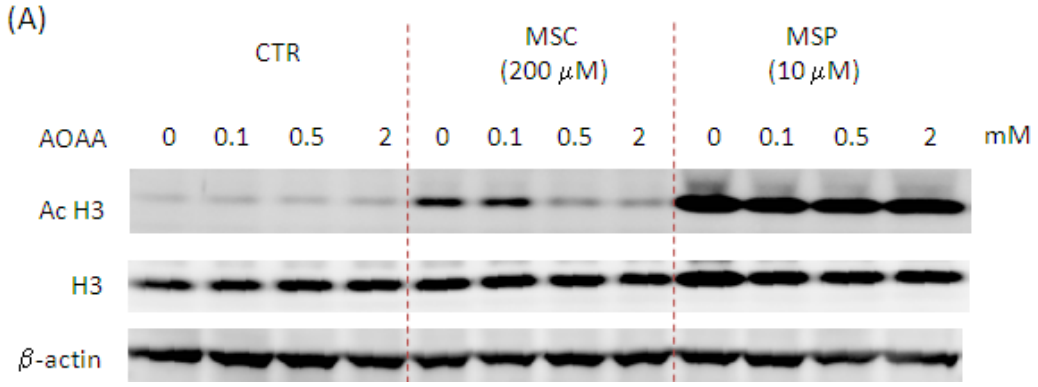
(A)
CTR
MSC
(200 μM)
MSP
(10 μM)
AOAA
0
0.1
0.5
2
0
0.1
0.5
2
0
0.1
0.5
2
mM
Ac H3
H3
β-actin

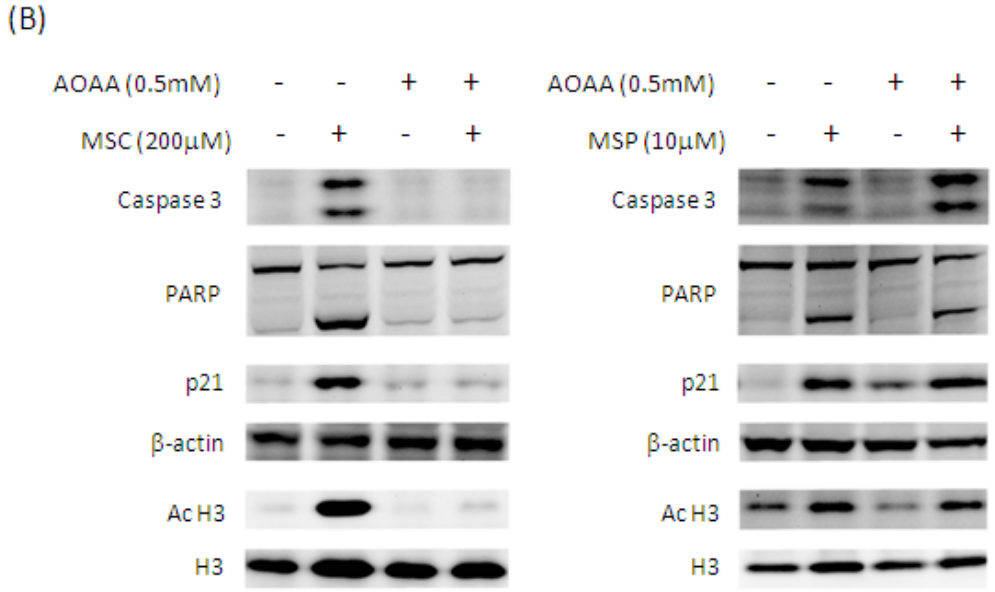
(B)
AOAA (0.5mM)
MSC (200μM)
Caspase 3
PARP
p21
β-actin
Ac H3
H3
AOAA (0.5mM)
MSP (10μM)
Caspase 3
PARP
p21
β-actin
Ac H3
H3

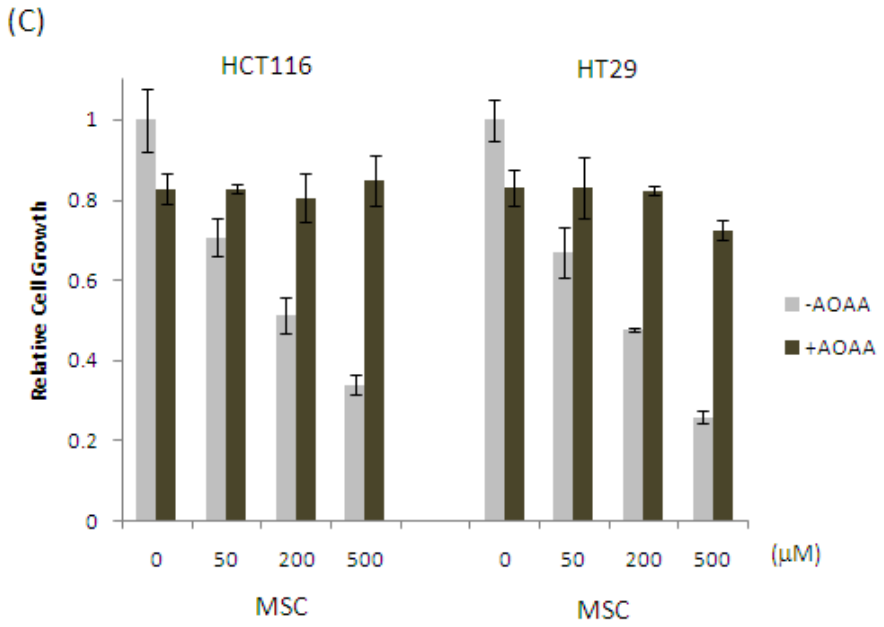

Figure 5.2 Pretreatment of transaminase inhibitor AOAA blocked MSC's chemopreventive effects. (A) HCT116 cells were pretreated with 0.1, 0.5 and 2mM AOAA for 1 hour, followed by 6 hour of MSC or MSP treatment. The levels of acetylated histone H3 and total histone H3 were examined by immunoblotting. (B) HCT116 cells were pretreated with 0.5mM AOAA for 1 hour, followed by 24 hour treatment of MSP or 36 hour treatment of MSC. The levels of p21, PARP cleavage, activated caspase-3, acetylated histone H3 and total histone H3 were examined by immunoblotting. (C) HCT116 and HT29 cells were treated with 0, 50, 200 and 500μM MSC for 48 hours in the presence/absence of 0.5mM AOAA. The relative numbers of viable cells was measured using MTT assay.

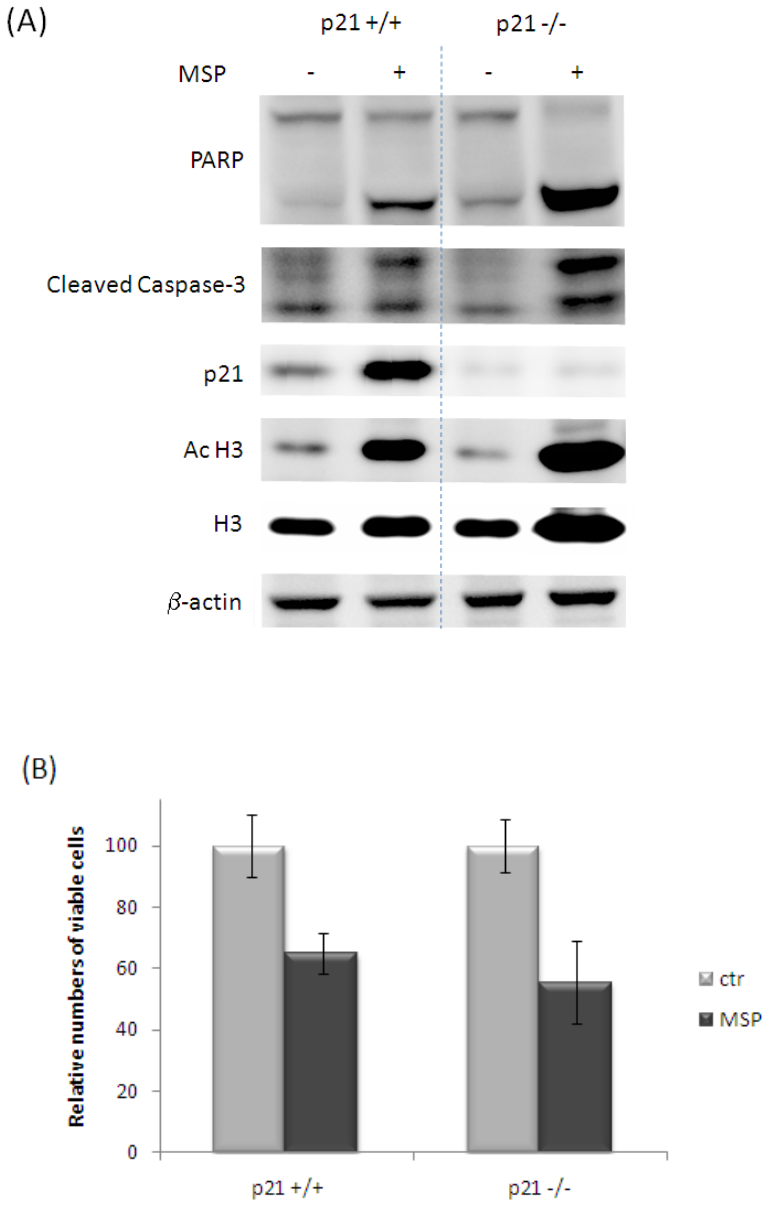

Figure 5.3 p21 induction is dispensible for MSP's anticancer effects. HCT116 p21 wild-type and HCT116 p21 knock-out cells were treated with 10μM MSP. (A) After 24 hours, the levels of PARP cleavage, activated caspase-3, p21, acetylated histone H3, total histone H3 were examined by immunoblotting. β-actin was also blotted as loading control. (B) After 48 hour of treatment, the relative numbers of viable cells were measured using MTT assay.

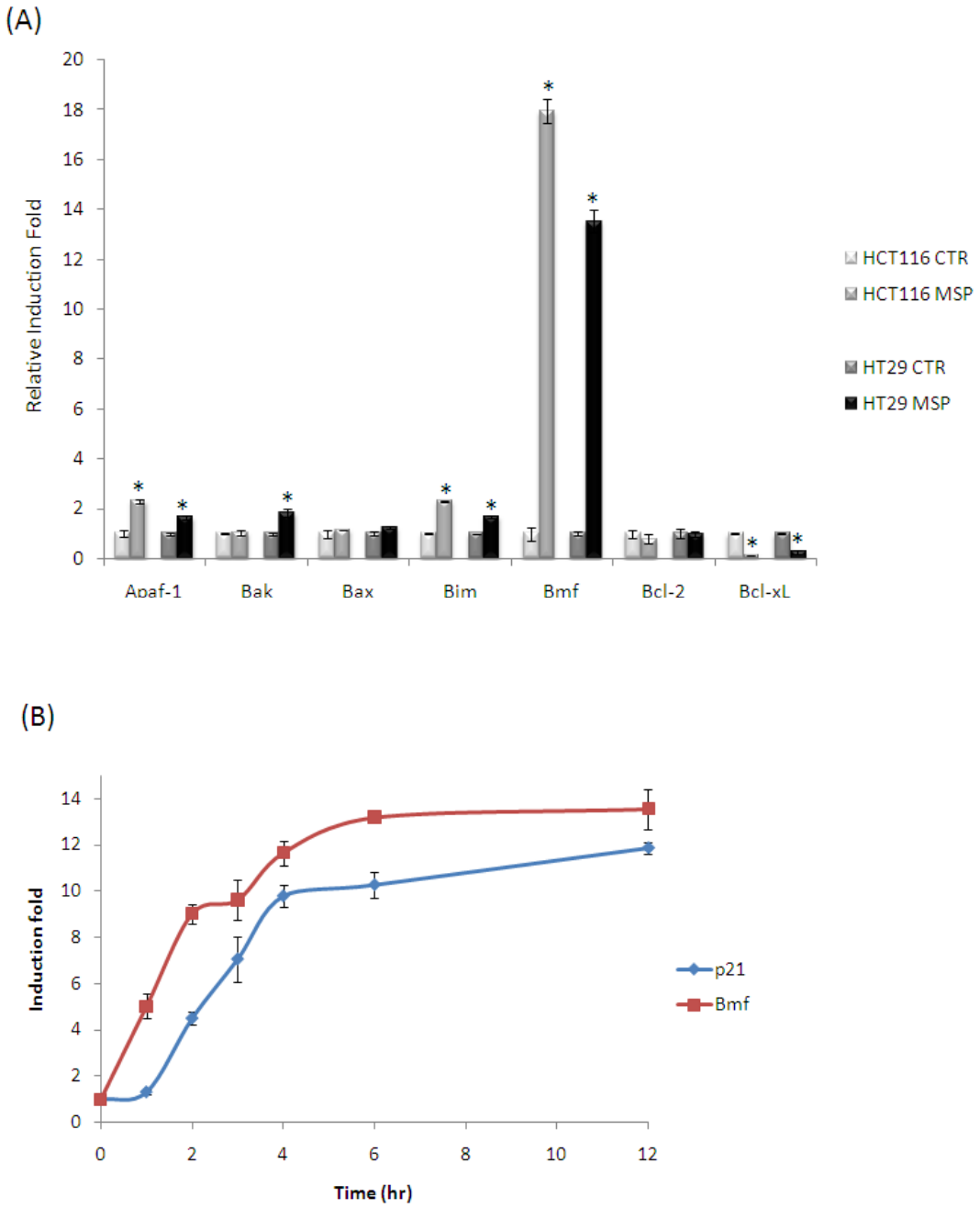

Figure 5.4 MSP decreased the expression levels of anti-apoptotic genes and increased the expression levels of pro-apoptotic genes. (A) HCT116 cells and HT29 cells were treated with 10μM MSP for 12 hours, the mRNA levels of indicated genes were examined by real-time PCR and rescaled relative to control cells. (B) 1, 2, 3, 4, 6 and 12 hour after 10μM MSP treatment in HT29 cells, Bmf and p21 mRNA levels were measured by Q-PCR and rescaled relative to control cells.

(A)

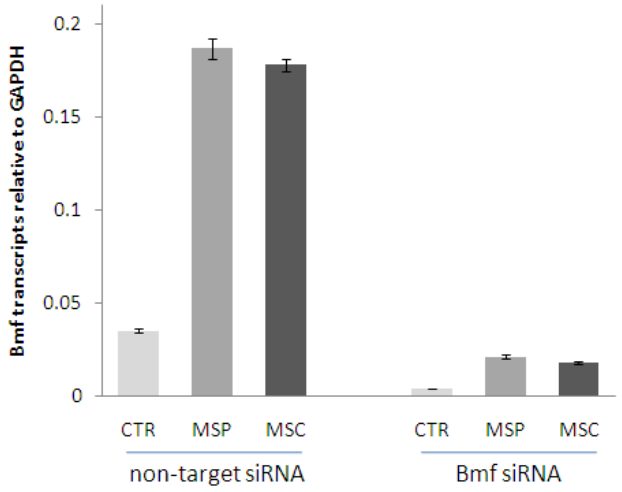
Bmf transcripts relative to GAPDH
0.2
0.15
0.1
0.05
0
CTR
MSP
MSC
CTR
MSP
MSC
non-target siRNA
Bmf siRNA

(B)

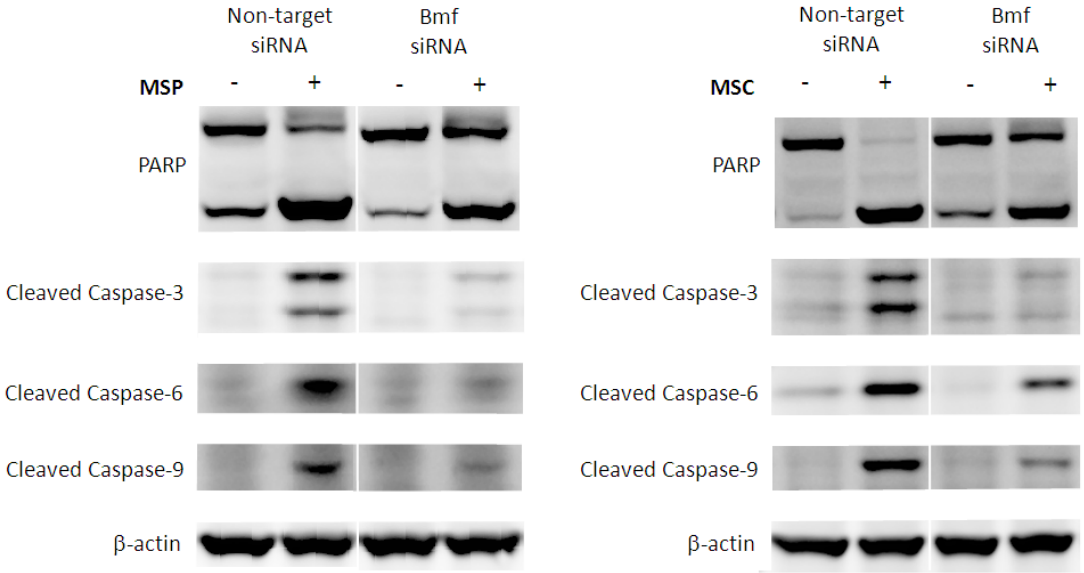
Non-target siRNA
Bmf siRNA
MSP
-
+
-
+
PARP
Cleaved Caspase-3
Cleaved Caspase-6
Cleaved Caspase-9
β-actin
Non-target siRNA
Bmf siRNA
MSC
-
+
-
+
PARP
Cleaved Caspase-3
Cleaved Caspase-6
Cleaved Caspase-9
β-actin

(C)

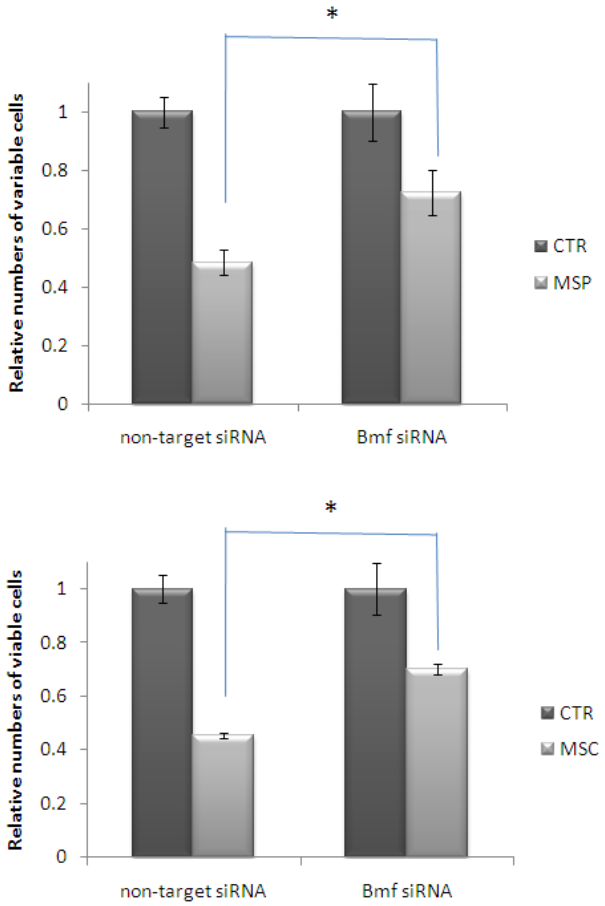

Figure 5.5 Bmf mRNA knockdown decreases MSP- and MSC-induced apoptosis. HT29 cells were transfected with Bmf siRNA for 72 hours, and cells transfected with non-target siRNA were used as controls. Then the cells were treated with 5μM MSP or 50μM MSC. (A) 12 hour after MSP or MSC treatment, Bmf mRNA levels were measured by real-time PCR and rescaled relative to GAPDH; (B) 24 hour after MSP treatment or 36 hour after MSC treatment, the protein levels of PARP, cleaved caspase-3, -6, and -9 were examined by immunoblotting, and β-actin was also blotted as loading control; (C) 48 hour after MSP or MSC treatment, cell growth was measured by MTT assay.

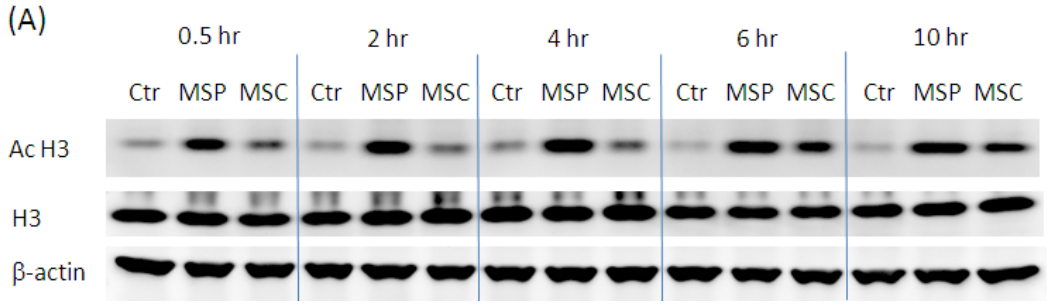
(A)
0.5 hr
2 hr
4 hr
6 hr
10 hr
Ctr MSP MSC Ctr MSP MSC Ctr MSP MSC Ctr MSP MSC Ctr MSP MSC
Ac H3
H3
β-actin

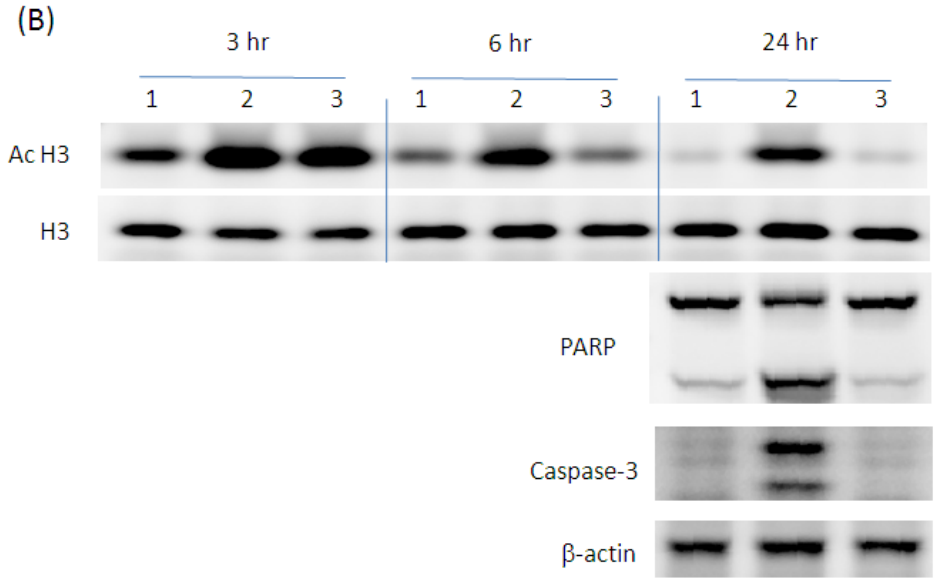
(B)
3 hr
6 hr
24 hr
1 2 3 1 2 3 1 2 3
Ac H3
H3
PARP
Caspase-3
β-actin

Figure 5S.1 MSP induced rapid, reversible and selective histone modifications in colon cancer cells. (A) HT29 colon cancer cells were incubated in 10μM MSP or 200μM MSC for 0.5h, 2h, 4h, 6h, and 10h, and the levels of acetylated histone H3 and total histone H3 were examined by immunoblotting. (B) HT29 colon cancer cells were subject to the following treatments (1) continuous incubation in control media (2) continuous incubation in 10μM MSP (3) incubation in 10μM MSP for 3 hours and then change to control media, and cells were harvested after 3h, 6h and 24h. The levels of acetylated histone H3, histone H3, PARP and activated caspase-3 were examined by immunoblotting. (C) HCT116 and HT29 cells were treated with 10μM MSP for 3 hours, and the levels of several types of modified histones were examined by immunoblotting. Total histone H3 and H4 were also blotted as loading control.

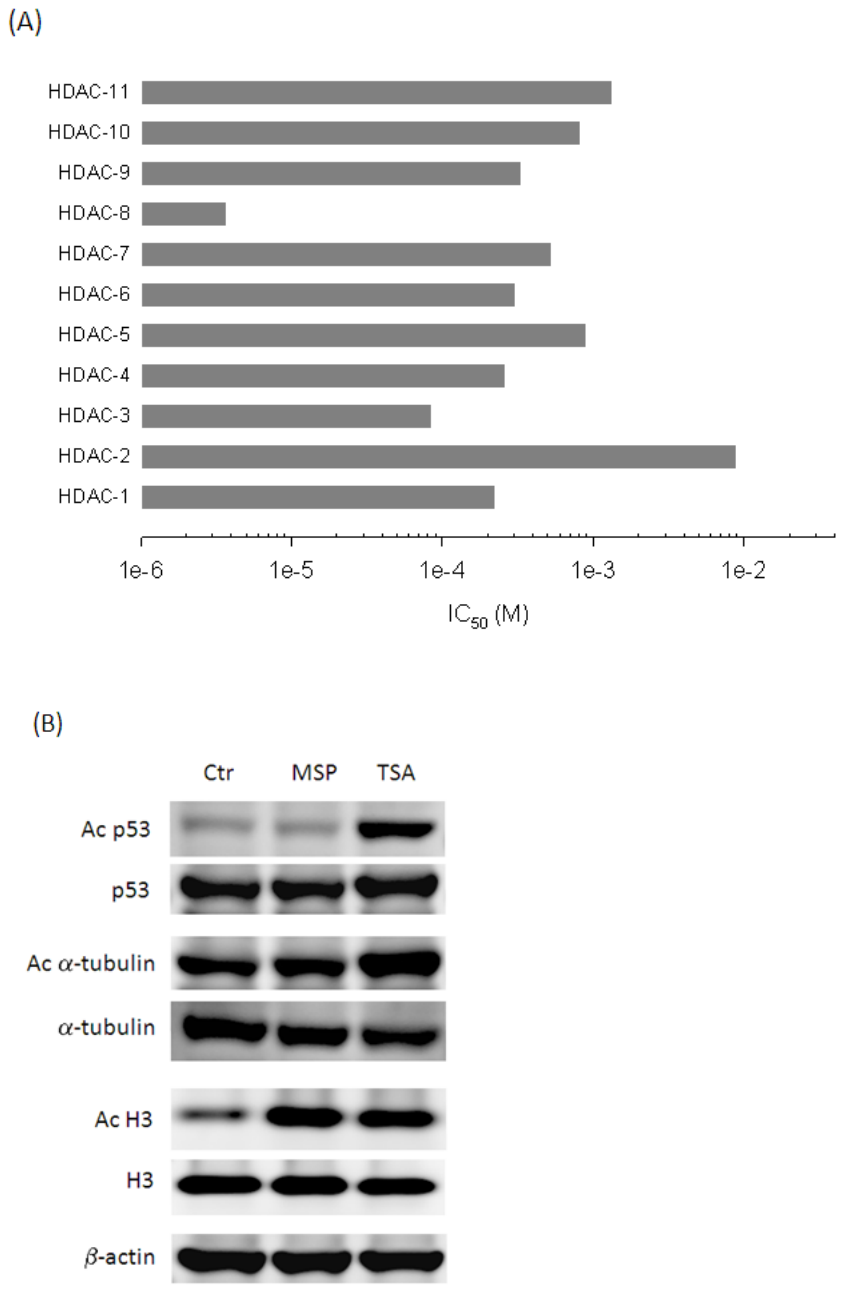

Figure 5S.2 MSP is a possible HDAC8-selective inhibitor. (A) *In vitro* HDAC panel profiling assay against MSP. IC_{50} values were derived from 10-dose mode in duplicate with 3-fold serial dilution starting at 5mM. (B) HT29 cells were treated with 10μM MSP or 0.2μM TSA for 6 hours, and the levels of acetylated p53, acetylated α-tubulin and acetylated histone H3 in the cells were examined by immunoblotting. Total p53, α-tubulin and histone H3 were also blotted as controls. Acetylated p53 and α-tubulin are the substrates of HDAC1/SIRT1 and HDAC6/SIRT2 respectively.

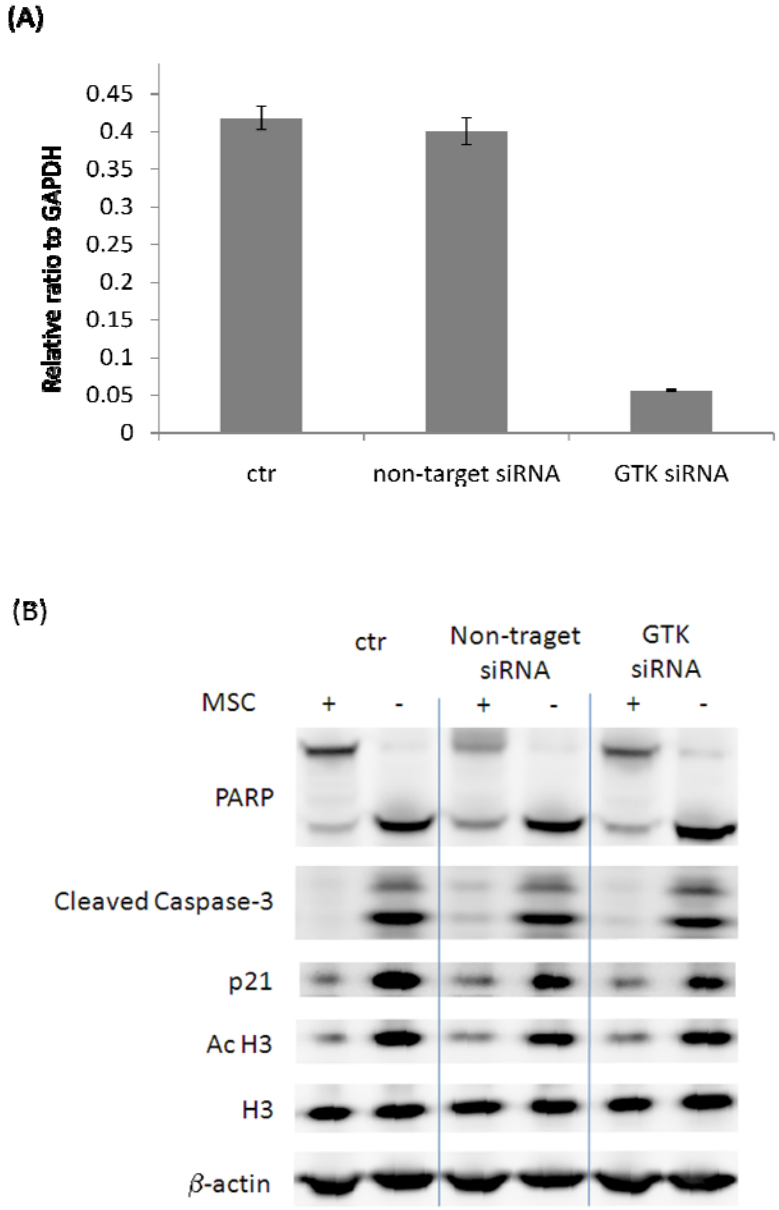

Figure 5S.3 GTK mRNA knockdown did not affect MSC's cellular effects. (A) GTK mRNA levels were examined in the HT29 cells transfected with non-target siRNA or GTK siRNA by Q-PCR, and rescaled relative to corresponding GAPDH. (B) HT29 cells were transfacted with GTK siRNA for 72 hours and then treated with 200μM MSC for another 48 hours. The levels of PARP cleavage, cleaved caspase-3, p21, acetylated histone H3 and total histone H3 were examined by immunoblotting.

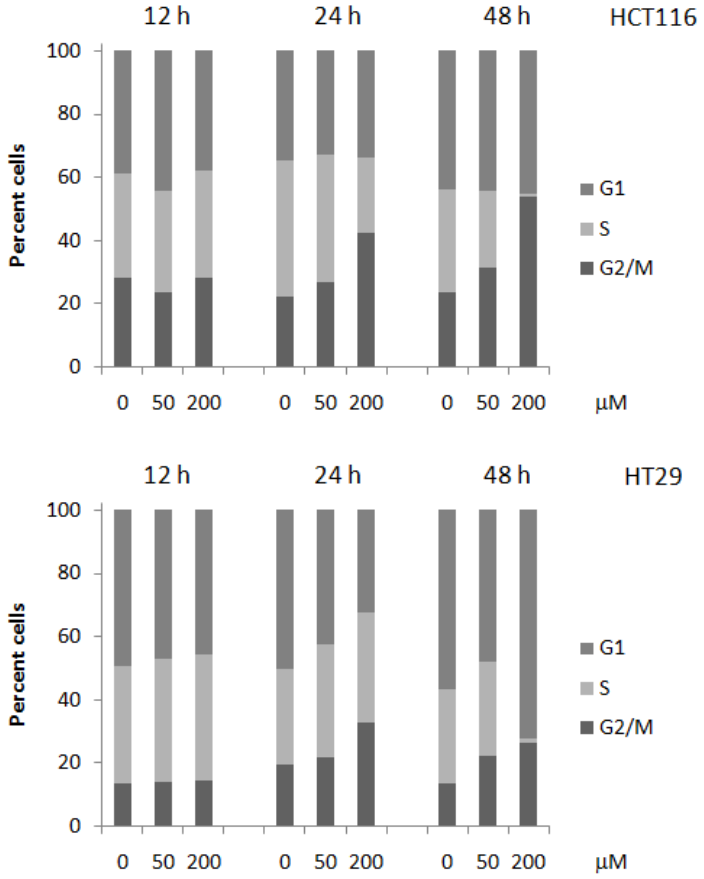

Figure 5S.4 MSC induced cell cycle arrest in colon cancer cells. HCT116 (upper) and HT29 (lower) cells were treated with 0, 50, and 200µM MSC for 12, 24, and 48 hours. The percentage of cells occupying G1, S, and G2/M phases of the cell cycle was determined by flow cytometry.

Chapter 6 Discussion and Conclusions

HDAC inhibitors are promising anticancer agents, although the mechanisms remains to be clarified. Investigation on the dietary HDAC inhibitors derived from natural organosulfur and organoselenium compounds added to our understanding in (1) HDAC inhibition by sulfur and pyruvic acid groups, (2) molecular events leading to HDAC inhibitors' anticancer effects, (3) molecular mechanisms underlying the chemopreventive effects of natural organosulfur and organoselenium compounds.

6.1 HDAC inhibition by AM, MSP, and KMSB

Most HDAC inhibitors discovered so far function by reversibly blocking access to the active site of HDAC. It is also the case for the three dietary HDAC inhibitors in this study: kinetics analysis indicated AM, MSP and KMSB inhibited HDAC activity in a competitive way. X-ray crystallographic analysis of HDAC-inhibitor has revealed a distinct mode of protein-ligand interactions (including hydrophobic interactions and Zn-chelating) whereby all the known four classes of HDAC inhibitors mediate enzyme inhibition. Specifically, TSA chelates Zn atom in the active pocket via hydroxamic acid group; depsipeptide undergoes metabolic activation through the reduction of the intramolecular disulfide bond, and one of the newly generating sulfhydryl groups chelates zinc atom; short-chain fatty acids like butyrate mediate HDAC inhibition primary through nonspecific hydrophobic interactions with surface residues inside the active pocket (**Figure 1.1**) (7). This protein-ligand interaction mode also applies to the three dietary HDAC inhibitors discussed here. As indicated by molecular simulation, AM mediates HDAC inhibition in a way similar to depsipeptide, i.e. via its sulfhydryl group chelating Zn atom. MSP and KMSB have similar structures to butyrate, and non-specific hydrophobic interactions within the active pocket of the enzyme may partly account for their inhibitory capabilities; at the same time, molecular docking results revealed α-keto acid group of MSP and KMSB could make a good chelating motif with α-carbonyl group and one of the carboxylate oxygen atoms coordinating Zn atom. Pyruvate, having the same functional group as MSP/KMSB, was recently reported to potentially inhibit HDAC activity(374). Generally speaking, the strength of interactions to Zn determines HDACi's inhibitory potency. Hydroxamic acid is the most potent Zn-chelating group and hence TSA is effective at

nanomolar concentrations, while butyrate is not binding to Zn and only works at millimolar concentrations. Other HDAC inhibitors fall between. The three dietary HDAC inhibitors AM, MSP and KMSB are supposed to have moderate Zn-chelating groups, and their effective concentrations are also within micromolar range. We have noticed that some deaminated products of natural amino acids have the similar structures as MSP and KMSB, with the potential Zn-chelating pyruvic acid group. However, when we replaced the selenium atom with a carbon atom, the resultant 2-oxohexanoic acid and 2-oxovaleric acid failed to show any inhibitory effects on HDAC activity, indicating somehow selenium is important for MSP and KMSB's HDAC inhibitory function (**Figure 4S.1**). To further evaluate the "critical" role of selenium, future studies should examine the effects of S-analogues of MSP and KMSB on HDAC activity in future studies.

Due to the high conservation of the active site among HDAC enzymes, most HDAC inhibitors with Zn-chelating group are pan-HDAC inhibitors which inhibit many of the Class I, II and IV isoforms. Although clinical trials have shown that pan-HDAC inhibitors are tolerated fairly well (normal cells appear to be more resistant to the apoptotic effects of HDAC inhibition), there is still evidence about the toxicity of pan-HDAC inhibitors by inhibiting several HDAC isoforms and hence disrupting multiple normal physiological functions(375). There is growing interest in pursuing isoform-specific HDAC inhibitors. We had *Reaction Biology Corporation (RBC)* perform an HDAC panel screening against MSP, showing that MSP had an IC_{50} of 3.5 μM for HDAC8 vs 85μM for HDAC3 and more than 200 μM for all other HDACs (**Figure 5S.2 A**). In our lab, we also found that IC_{50} for HDAC8 was about 20 μM vs more than 500 μM for HDAC1 and HDACs in Hela nuclear extracts. The difference in the IC_{50} values may lie in the different HDAC assay procedures used. Substrate type and assay conditions may affect the apparent IC_{50} values. Further studies are needed to evaluate and determine the optimal assay conditions that can simulate intracellular environment best. However, both the results indicated that MSP had 20-500 fold selectivity for HDAC8 over other HDACs. We also observed that in the colon cancer cells, MSP did not change the acetylation level of α-tubulin or p53, which are the substrates of HDAC1/SIRT1 and HDAC6/SIRT2 respectively, while the pan-HDAC inhibitor TSA significantly increased the acetylation levels of both proteins, implying selective inhibition of HDAC isoforms by MSP (**Figure 5S.2 B**). Only a few HDAC8

selective inhibitors have been developed so far, but they have shown promising chemopreventive effects against the childhood cancer neuroblastoma where HDAC8 expression is correlated selectively with advanced disease and metastasis(376). It has been reported that compared to other HDACs, HDAC8 has a unique side pocket in its catalytic domain, and HDAC8-selective inhibitors are assumed also able to fit into this sub-pocket of HDAC8(375). Further crystallographic or molecular simulation studies are needed to clarify the mechanism of HDAC8-selective inhibition by MSP, and it is also very interesting to examine MSP's anticancer effects in neuroblastoma.

6.2 Anticancer activities and mechanisms of AM, MSP and KMSB

In colon cancer cells, all the three dietary HDAC inhibitors decreased cellular HDAC activities, and induced quick and dramatic global histone H3/H4 acetylation. Increased acetylation occurred on all the lysine residues we have examined including H3K9, H3K14, H3K18, H4K12, H4K5/8/12/16 (**Figure 5S.1**). As a result of direct inhibition of HDAC activity, histone hyperacetylation happened immediately, within half an hour after AM, MSP or KMSB treatment. We found that MSP also increased H3K4 methylation and decreased H3K9 trimethylation (data not shown), but only after 6 hours of treatment when the expression of genes like p21 and Bmf was already induced. The modification on histone methylation by MSP probably does not mediate these immediate genes' expression, but may affect gene expression at later time. Like histone acetylation, H3K4 methylation and loss of H3K9 trimethylation are also associated with transcriptional activation. Further studies are needed to see whether histone methylation alteration following histone hyperacetylation is a common effect for these HDAC inhibitors. It may be an interesting question to look into how histone hyperacetylation further influences histone methylation to synergize the activation of gene expression.

Induction of cell cycle inhibitor p21, often a key event for HDAC inhibitors' action, was also observed in AM/MSP/KMSB-treated colon cancer cells. P21 was selectively up-regulated on the mRNA level in a Sp1/Sp3-dependent manner but irrespective of p53 status, which is consistent with previous reports on other HDAC inhibitors.

Like other known HDAC inhibitors, all the three dietary HDAC inhibitors in this study showed promising anticancer potential. All of them significantly repressed colon cancer cell growth, accompanied by cell cycle arrest and/or apoptosis. Cell cycle arrest at G2/M or G0/G1 was induced by all the three HDACis, and probably mediated by p21 induction. In p21 deficient HCT116 cells, MSP-induced cell cycle arrest was repressed (data not shown). MSP and KMSB could also induce apoptosis in the colon cancer cells, and the activation of caspase-9 indicated apoptosis is probably mediated via mitochondrial apoptotic pathway as what has been reported for other HDAC inhibitors in colon cancer cells. Bmf could be an important mediator for MSP-induced apoptosis since knockdown of Bmf significantly repressed MSP-induced caspase activation and growth inhibition. Bmf turned out to be one of the immediate genes up-regulated by MSP and KMSB (data not shown); MSP/KMSB induced apoptosis via direct regulation of gene expression, independent of cell cycle arrest.

6.3 Role of HDAC inhibition in dietary chemopreventive agents

Chemopreventive effects of garlic organosulfur compounds and natural organosulfur compounds have been demonstrated in many *in vitro* and *in vivo* studies. Characterization of dietary HDAC inhibitors derived from these compounds in this study could shed new light on the molecular mechanisms underlying their anticancer potential.

Diallyl disulfide, S-allylmercaptocysteine and ajoene have been reported to induce histone acetylation in cancer cell lines(164, 291). All of these compounds could be transformed to AM in the cells. We also found AM, organosulfur compounds and garlic extract can induce histone acetylation in mouse liver or intestine (**Figure 3S.4**), indicating AM could be an active metabolite of organosulfur compound *in vivo*.

Studies have shown that the chemopreventive effects of selenium depend on its specific chemical form. Organic forms of selenium ARE preferable than inorganic forms because of greater toxicity of inorganic selenium *in vivo*. Se-accumulating plants and Se-enriched yeast are two major sources of natural organoselenium compounds, among which methylselenocysteine and selenomethionine are the most abundant. It has been assumed that both MSC and SM are converted to active metabolite methylselenol by β/γ elimination to exert their chemopreventive effects. But some studies have implied that MSC could be a

more potent anticancer agent than SM. SM has shown negative effects on carcinogen-induced tumorigenesis in lung, colon and mammary gland in animal models(363, 377-379). One explanation for the negative outcome of recent SELECT trial is that pure SM was used as intervention agent whereas previous human trials had used selenium-enriched baker's yeast. Although SM represents the major form of selenium in high-selenium yeast, that product has been shown to include other chemical forms of selenium including MSC(380). In our lab, we also found that MSC significantly reduced tumor multiplicity in DMH-induced colon carcinogenesis while SM did not show any effect (**Figure 4S.3**). *In vitro*, MSC induced PARP cleavage and caspase-3 activation in HT29 colon cancer cells and CCRF-CEM leukemia cells but SM cannot (**Figure 4S.2**). It has been assumed that unlike SM having diverted metabolic pathways, MSC can be more efficiently transformed to the presumptive antitumorigenic metabolite methylselenol and hence exhibits greater chemopreventive potency. In our study, we propose that another metabolic pathway may also contribute to the different effects of these two organoselenium compounds, i.e. transamination pathway that generates alpha-keto acid metabolites. In the presence of glutamine transaminase K (GTK), MSC can be transformed to its deaminated metabolite, MSP, but the corresponding deaminated product of SM was undetectable. Although the alpha-keto acid metabolites from both compounds can act as HDAC inhibitors and inhibit cellular HDAC activities, histone hyperacetylation was only observed in MSC-treated cells. This could partly account for the differential effects of MSC and SM in the cells.

Several lines of evidence in this study indicate MSP may play an important role in MSC's anticancer effects. First, MSP can be generated from MSC in the cells, as we have shown by HPLC-MS-MS. The concentration of MSP in the cell is about one-fortieth that of MSC, and this is consistent with our observation that 2-10μM MSP induced significant caspase cleavage while 200μM of MSC was required to show similar effects in the same condition . Second, MSC induced histone acetylation in the cells 6 hour later than MSP that can increase histone acetylation immediately upon treatment (**Figure 5S.1 A**), probably because it takes time for MSC to generate and accumulate MSP in the cells. Consistent with this observation, caspase activation was first detected at 18 hour after MSP treatment but 24 hour after MSC treatment. Third, MSP and MSC caused similar cell cycle arrest and caspase(-3, -6, -7 ,-9)

activation patterns in colon cancer cells (**Figure 5S.4**). Both MSP and MSC induced Bmf expression, and Bmf knockdown repressed MSP- and MSC-mediated apoptosis. Fourth, pretreatment of transaminase inhibitor AOAA repressed MSC's chemopreventive effects.

Although MSP was first discovered as MSC's metabolite via GTK, GTK may not be the only enzyme that catalyzes this deamination reaction. In the GTK knockdown cells, MSC still induced histone hyperacetylation, indicating of generation of MSP in the cells (**Figure 5S.3**). There are probably some other enzymes for this conversion.

6.4 Conclusions

Natural organosulfur and organoselenium compounds can be transformed into HDACi metabolites, AM, KMSB and MSP, which could play an important role in their chemopreventive effects via modulating cell cycle and/or inducing apoptosis. This thesis work adds further support for the role of metabolism as a key factor in generating active forms of dietary constituent with the ability to influence HDAC activity and gene expression. The potential role of these metabolites *in vivo* warrants further investigation.

Bibliography

1. Strahl BD, Allis CD. 2000. *Nature* 403: 41-5
2. Gregory PD, Wagner K, Horz W. 2001. *Exp Cell Res* 265: 195-202
3. Marks PA, Miller T, Richon VM. 2003. *Curr Opin Pharmacol* 3: 344-51
4. Minucci S, Pelicci PG. 2006. *Nat Rev Cancer* 6: 38-51
5. Piekarz R, Bates S. 2004. *Curr Pharm Des* 10: 2289-98
6. de Ruijter AJ, van Gennip AH, Caron HN, Kemp S, van Kuilenburg AB. 2003. *Biochem J* 370: 737-49
7. Lin HY, Chen CS, Lin SP, Weng JR. 2006. *Med Res Rev* 26: 397-413
8. Wilson AJ, Byun DS, Popova N, Murray LB, L'Italien K, et al. 2006. *J Biol Chem* 281: 13548-58
9. Zhu P, Martin E, Mengwasser J, Schlag P, Janssen KP, Gottlicher M. 2004. *Cancer Cell* 5: 455-63
10. Nakagawa M, Oda Y, Eguchi T, Aishima S, Yao T, et al. 2007. *Oncol Rep* 18: 769-74
11. Spurling CC, Godman CA, Noonan EJ, Rasmussen TP, Rosenberg DW, Giardina C. 2008. *Mol Carcinog* 47: 137-47
12. Archer SY, Meng S, Shei A, Hodin RA. 1998. *Proc Natl Acad Sci U S A* 95: 6791-6
13. Heerdt BG, Houston MA, Augenlicht LH. 1994. *Cancer Res* 54: 3288-93
14. Mariadason JM, Corner GA, Augenlicht LH. 2000. *Cancer Res* 60: 4561-72
15. Hu E, Dul E, Sung CM, Chen Z, Kirkpatrick R, et al. 2003. *J Pharmacol Exp Ther* 307: 720-8
16. Ropero S, Fraga MF, Ballestar E, Hamelin R, Yamamoto H, et al. 2006. *Nat Genet* 38: 566-9
17. Wong CS, Sengupta S, Tjandra JJ, Gibson PR. 2005. *Dis Colon Rectum* 48: 549-59
18. Heerdt BG, Houston MA, Augenlicht LH. 1997. *Cell Growth Differ* 8: 523-32
19. Schwartz B, Avivi-Green C, Polak-Charcon S. 1998. *Mol Cell Biochem* 188: 21-30
20. Kobayashi H, Tan EM, Fleming SE. 2003. *Nutr Cancer* 46: 202-11
21. Xu WS, Perez G, Ngo L, Gui CY, Marks PA. 2005. *Cancer Res* 65: 7832-9
22. Siavoshian S, Blottiere HM, Cherbut C, Galmiche JP. 1997. *Biochem Biophys Res Commun* 232: 169-72
23. Nakano K, Mizuno T, Sowa Y, Orita T, Yoshino T, et al. 1997. *J Biol Chem* 272: 22199-206
24. Heerdt BG, Houston MA, Anthony GM, Augenlicht LH. 1998. *Cancer Res* 58: 2869-75
25. Hitomi T, Matsuzaki Y, Yokota T, Takaoka Y, Sakai T. 2003. *FEBS Lett* 554: 347-50
26. Chen Z, Clark S, Birkeland M, Sung CM, Lago A, et al. 2002. *Cancer Lett* 188: 127-40
27. Heruth DP, Zirnstein GW, Bradley JF, Rothberg PG. 1993. *J Biol Chem* 268: 20466-72
28. Wilson AJ, Velcich A, Arango D, Kurland AR, Shenoy SM, et al. 2002. *Cancer Res* 62: 6006-10
29. Archer SY, Johnson J, Kim HJ, Ma Q, Mou H, et al. 2005. *Am J Physiol Gastrointest Liver Physiol* 289: G696-703
30. Coradini D, Pellizzaro C, Marimpietri D, Abolafio G, Daidone MG. 2000. *Cell Prolif* 33: 139-46

31. Ruemmele FM, Dionne S, Qureshi I, Sarma DS, Levy E, Seidman EG. 1999. *Cell Death Differ* 6: 729-35
32. Ruemmele FM, Schwartz S, Seidman EG, Dionne S, Levy E, Lentze MJ. 2003. *Gut* 52: 94-100
33. Hague A, Diaz GD, Hicks DJ, Krajewski S, Reed JC, Paraskeva C. 1997. *Int J Cancer* 72: 898-905
34. Kim YH, Park JW, Lee JY, Kwon TK. 2004. *Carcinogenesis* 25: 1813-20
35. Hernandez A, Thomas R, Smith F, Sandberg J, Kim S, et al. 2001. *Surgery* 130: 265-72
36. Bonnotte B, Favre N, Reveneau S, Micheau O, Droin N, et al. 1998. *Cell Death Differ* 5: 480-7
37. Giardina C, Boulares H, Inan MS. 1999. *Biochim Biophys Acta* 1448: 425-38
38. Klampfer L, Huang J, Sasazuki T, Shirasawa S, Augenlicht L. 2004. *J Biol Chem* 279: 36680-8
39. Mariadason JM, Rickard KL, Barkla DH, Augenlicht LH, Gibson PR. 2000. *J Cell Physiol* 183: 347-54
40. Mariadason JM, Barkla DH, Gibson PR. 1997. *Am J Physiol* 272: G705-12
41. Musch MW, Bookstein C, Xie Y, Sellin JH, Chang EB. 2001. *Am J Physiol Gastrointest Liver Physiol* 280: G687-93
42. Schroder C, Eckert K, Maurer HR. 1998. *Int J Oncol* 13: 1335-40
43. Hodin RA, Shei A, Meng S. 1997. *J Gastrointest Surg* 1: 433-8; discussion 8
44. Iciek M, Kwiecien I, Wlodek L. 2009. *Environ Mol Mutagen* 50: 247-65
45. Shukla Y, Kalra N. 2007. *Cancer Lett* 247: 167-81
46. Amagase H. 2006. *J Nutr* 136: 716S-25S
47. Lanzotti V. 2006. *J Chromatogr A* 1112: 3-22
48. Lawson LD, Wang ZJ, Hughes BG. 1991. *Planta Med* 57: 363-70
49. Amagase H, Petesch BL, Matsuura H, Kasuga S, Itakura Y. 2001. *J Nutr* 131: 955S-62S
50. Germain E, Auger J, Ginies C, Siess MH, Teyssier C. 2002. *Xenobiotica* 32: 1127-38
51. Lachmann G, Lorenz D, Radeck W, Steiper M. 1994. *Arzneimittelforschung* 44: 734-43
52. Lawson LD, Wang ZJ. 2005. *J Agric Food Chem* 53: 1974-83
53. Koch H.P. Lld. 1996. *Garlic: the science and therapeutic application of allium sativum L. and related species*: Williams & Wilkins. 213-20 pp.
54. Rosen RT, Hiserodt RD, Fukuda EK, Ruiz RJ, Zhou Z, et al. 2000. *Biofactors* 13: 241-9
55. Tamaki T, Sonoki S. 1999. *J Nutr Sci Vitaminol (Tokyo)* 45: 213-22
56. de Rooij BM, Boogaard PJ, Rijksen DA, Commandeur JN, Vermeulen NP. 1996. *Arch Toxicol* 70: 635-9
57. Jandke J, Spiteller G. 1987. *J Chromatogr* 421: 1-8
58. Kodera Y, Suzuki A, Imada O, Kasuga S, Sumioka I, et al. 2002. *J Agric Food Chem* 50: 622-32
59. Steiner M, Li W. 2001. *J Nutr* 131: 980S-4S
60. Steinmetz KA, Kushi LH, Bostick RM, Folsom AR, Potter JD. 1994. *Am J Epidemiol* 139: 1-15
61. Key TJ, Silcocks PB, Davey GK, Appleby PN, Bishop DT. 1997. *Br J Cancer* 76: 678-87
62. Fleischauer AT, Poole C, Arab L. 2000. *Am J Clin Nutr* 72: 1047-52
63. Hsing AW, Chokkalingam AP, Gao YT, Madigan MP, Deng J, et al. 2002. *J Natl Cancer Inst* 94: 1648-51

64. Challier B, Perarnau JM, Viel JF. 1998. *Eur J Epidemiol* 14: 737-47
65. Sundaram SG, Milner JA. 1996. *J Nutr* 126: 1355-61
66. Singh SV, Mohan RR, Agarwal R, Benson PJ, Hu X, et al. 1996. *Biochem Biophys Res Commun* 225: 660-5
67. Xiao D, Lew KL, Kim YA, Zeng Y, Hahm ER, et al. 2006. *Clin Cancer Res* 12: 6836-43
68. Wargovich MJ. 2006. *J Nutr* 136: 832S-4S
69. Davenport DM, Wargovich MJ. 2005. *Food Chem Toxicol* 43: 1753-62
70. Guyonnet D, Belloir C, Suschetet M, Siess MH, Le Bon AM. 2000. *Mutat Res* 466: 17-26
71. Guyonnet D, Belloir C, Suschetet M, Siess MH, Le Bon AM. 2001. *Mutat Res* 495: 135-45
72. Sheen LY, Chen HW, Kung YL, Liu CT, Lii CK. 1999. *Nutr Cancer* 35: 160-6
73. Fukao T, Hosono T, Misawa S, Seki T, Ariga T. 2004. *Food Chem Toxicol* 42: 743-9
74. Chen C, Pung D, Leong V, Hebbar V, Shen G, et al. 2004. *Free Radic Biol Med* 37: 1578-90
75. Perchellet JP, Perchellet EM, Abney NL, Zirnstein JA, Belman S. 1986. *Cancer Biochem Biophys* 8: 299-312
76. Gudi VA, Singh SV. 1991. *Biochem Pharmacol* 42: 1261-5
77. Imai J, Ide N, Nagae S, Moriguchi T, Matsuura H, Itakura Y. 1994. *Planta Med* 60: 417-20
78. Knowles LM, Milner JA. 1998. *Nutr Cancer* 30: 169-74
79. Wu CC, Chung JG, Tsai SJ, Yang JH, Sheen LY. 2004. *Food Chem Toxicol* 42: 1937-47
80. Gunadharini DN, Arunkumar A, Krishnamoorthy G, Muthuvel R, Vijayababu MR, et al. 2006. *Cell Biochem Funct* 24: 407-12
81. Arunkumar A, Vijayababu MR, Srinivasan N, Aruldhas MM, Arunakaran J. 2006. *Mol Cell Biochem* 288: 107-13
82. Xiao D, Herman-Antosiewicz A, Antosiewicz J, Xiao H, Brisson M, et al. 2005. *Oncogene* 24: 6256-68
83. Xiao D, Pinto JT, Gundersen GG, Weinstein IB. 2005. *Mol Cancer Ther* 4: 1388-98
84. Herman-Antosiewicz A, Singh SV. 2004. *Mutat Res* 555: 121-31
85. Wu X, Kassie F, Mersch-Sundermann V. 2005. *Mutat Res* 589: 81-102
86. Balasenthil S, Rao KS, Nagini S. 2002. *Cell Biochem Funct* 20: 263-8
87. Balasenthil S, Rao KS, Nagini S. 2002. *Oral Oncol* 38: 431-6
88. Nakagawa H, Tsuta K, Kiuchi K, Senzaki H, Tanaka K, et al. 2001. *Carcinogenesis* 22: 891-7
89. Hong YS, Ham YA, Choi JH, Kim J. 2000. *Exp Mol Med* 32: 127-34
90. Kwon KB, Yoo SJ, Ryu DG, Yang JY, Rho HW, et al. 2002. *Biochem Pharmacol* 63: 41-7
91. Lu HF, Sue CC, Yu CS, Chen SC, Chen GW, Chung JG. 2004. *Food Chem Toxicol* 42: 1543-52
92. Filomeni G, Aquilano K, Rotilio G, Ciriolo MR. 2003. *Cancer Res* 63: 5940-9
93. Wen J, Zhang Y, Chen X, Shen L, Li GC, Xu M. 2004. *Biochem Pharmacol* 68: 323-31
94. Xiao D, Choi S, Johnson DE, Vogel VG, Johnson CS, et al. 2004. *Oncogene* 23: 5594-606
95. Sundaram SG, Milner JA. 1996. *Biochim Biophys Acta* 1315: 15-20
96. Park EK, Kwon KB, Park KI, Park BH, Jhee EC. 2002. *Exp Mol Med* 34: 250-7

97. Ip C, Hayes C, Budnick RM, Ganther HE. 1991. *Cancer Res* 51: 595-600
98. Neuhierl B, Thanbichler M, Lottspeich F, Bock A. 1999. *J Biol Chem* 274: 5407-14
99. Whanger PD. 2002. *J Am Coll Nutr* 21: 223-32
100. Zeng H, Combs GF, Jr. 2008. *J Nutr Biochem* 19: 1-7
101. Beilstein MA, Whanger PD. 1988. *J Inorg Biochem* 33: 31-46
102. Whanger PD. 2004. *Br J Nutr* 91: 11-28
103. Dong Y, Lisk D, Block E, Ip C. 2001. *Cancer Res* 61: 2923-8
104. Shamberger RJ, Frost DV. 1969. *Can Med Assoc J* 100: 682
105. Shamberger RJ, Rukovena E, Longfield AK, Tytko SA, Deodhar S, Willis CE. 1973. *J Natl Cancer Inst* 50: 863-70
106. van den Brandt PA, Goldbohm RA, van 't Veer P, Bode P, Dorant E, et al. 1993. *J Natl Cancer Inst* 85: 224-9
107. Yu MW, Horng IS, Hsu KH, Chiang YC, Liaw YF, Chen CJ. 1999. *Am J Epidemiol* 150: 367-74
108. Brooks JD, Metter EJ, Chan DW, Sokoll LJ, Landis P, et al. 2001. *J Urol* 166: 2034-8
109. Nomura AM, Lee J, Stemmermann GN, Combs GF, Jr. 2000. *Cancer Epidemiol Biomarkers Prev* 9: 883-7
110. Yoshizawa K, Willett WC, Morris SJ, Stampfer MJ, Spiegelman D, et al. 1998. *J Natl Cancer Inst* 90: 1219-24
111. Knekt P, Marniemi J, Teppo L, Heliovaara M, Aromaa A. 1998. *Am J Epidemiol* 148: 975-82
112. Bhattacharyya RS, Husbeck B, Feldman D, Knox SJ. 2008. *Int J Radiat Oncol Biol Phys* 72: 935-40
113. Yang Y, Huang F, Ren Y, Xing L, Wu Y, et al. 2009. *Oncol Res* 18: 1-8
114. Yan L, Yee JA, Li D, McGuire MH, Graef GL. 1999. *Anticancer Res* 19: 1337-42
115. Yan L, Yee JA, McGuire MH, Graef GL. 1997. *Nutr Cancer* 28: 165-9
116. Xu J, Yang F, An X, Hu Q. 2007. *J Agric Food Chem* 55: 5349-53
117. Spallholz JE, Boylan LM, Larsen HS. 1990. *Ann N Y Acad Sci* 587: 123-39
118. Gladyshev VN, Factor VM, Housseau F, Hatfield DL. 1998. *Biochem Biophys Res Commun* 251: 488-93
119. Behne D, Kyriakopoulos A, Kalcklosch M, Weiss-Nowak C, Pfeifer H, et al. 1997. *Biomed Environ Sci* 10: 340-5
120. Liu JZ, Gilbert K, Parker HM, Haschek WM, Milner JA. 1991. *Cancer Res* 51: 4613-7
121. Teel RW, Kain SR. 1984. *Mutat Res* 127: 9-14
122. Lu J, Jiang C. 2005. *Antioxid Redox Signal* 7: 1715-27
123. Lu J, Jiang C. 2001. *Nutr Cancer* 40: 64-73
124. Lu J. 2001. *Adv Exp Med Biol* 492: 131-45
125. Ganther HE. 1999. *Carcinogenesis* 20: 1657-66
126. Yoon SO, Kim MM, Chung AS. 2001. *J Biol Chem* 276: 20085-92
127. Zeng H, Briske-Anderson M, Idso JP, Hunt CD. 2006. *J Nutr* 136: 1528-32
128. Jiang C, Ganther H, Lu J. 2000. *Mol Carcinog* 29: 236-50
129. Nishikawa T, Yamada N, Hattori A, Fukuda H, Fujino T. 2002. *Biosci Biotechnol Biochem* 66: 2221-3
130. Singh A, Shukla Y. 1998. *Biomed Environ Sci* 11: 258-63
131. Singh A, Arora A, Shukla Y. 2004. *Eur J Cancer Prev* 13: 263-9

132. Wargovich MJ, Chen CD, Jimenez A, Steele VE, Velasco M, et al. 1996. *Cancer Epidemiol Biomarkers Prev* 5: 355-60
133. de Boer JG, Yang H, Holcroft J, Skov K. 2004. *Nutr Cancer* 50: 168-73
134. Hadjiolov D, Fernando RC, Schmeiser HH, Wiessler M, Hadjiolov N, Pirajnov G. 1993. *Carcinogenesis* 14: 407-10
135. Reddy BS, Rao CV, Rivenson A, Kelloff G. 1993. *Cancer Res* 53: 3493-8
136. Dwivedi C, Rohlfs S, Jarvis D, Engineer FN. 1992. *Pharm Res* 9: 1668-70
137. Schaffer EM, Liu JZ, Green J, Dangler CA, Milner JA. 1996. *Cancer Lett* 102: 199-204
138. Takahashi S, Hakoi K, Yada H, Hirose M, Ito N, Fukushima S. 1992. *Carcinogenesis* 13: 1513-8
139. Singh SV, Powolny AA, Stan SD, Xiao D, Arlotti JA, et al. 2008. *Cancer Res* 68: 9503-11
140. Howard EW, Ling MT, Chua CW, Cheung HW, Wang X, Wong YC. 2007. *Clin Cancer Res* 13: 1847-56
141. Wilpart M, Speder A, Roberfroid M. 1986. *Cancer Lett* 31: 319-24
142. Sundaresan S, Subramanian P. 2008. *Mol Cell Biochem* 310: 209-14
143. Mori H, Sugie S, Rahman W, Suzui N. 1999. *Cancer Lett* 143: 195-8
144. Hussain SP, Jannu LN, Rao AR. 1990. *Cancer Lett* 49: 175-80
145. Chihara T, Shimpo K, Kaneko T, Beppu H, Tomatsu A, Sonoda S. 2009. *Asian Pac J Cancer Prev* 10: 827-31
146. Das I, Saha T. 2009. *Nutrition* 25: 459-71
147. Dirsch VM, Gerbes AL, Vollmar AM. 1998. *Mol Pharmacol* 53: 402-7
148. Xu B, Monsarrat B, Gairin JE, Girbal-Neuhauser E. 2004. *Fundam Clin Pharmacol* 18: 171-80
149. Pinto JT, Rivlin RS. 2001. *J Nutr* 131: 1058S-60S
150. Wang YB, Qin J, Zheng XY, Bai Y, Yang K, Xie LP. 2009. *Phytomedicine*
151. Xiao D, Zeng Y, Hahm ER, Kim YA, Ramalingam S, Singh SV. 2009. *Environ Mol Mutagen* 50: 201-12
152. Xiao D, Singh SV. 2006. *Carcinogenesis* 27: 533-40
153. Li N, Guo R, Li W, Shao J, Li S, et al. 2006. *Carcinogenesis* 27: 1222-31
154. Chun HS, Kim HJ, Choi EH. 2001. *Biosci Biotechnol Biochem* 65: 2205-12
155. Hosono T, Fukao T, Ogihara J, Ito Y, Shiba H, et al. 2005. *J Biol Chem* 280: 41487-93
156. Nabekura T, Kamiyama S, Kitagawa S. 2005. *Biochem Biophys Res Commun* 327: 866-70
157. Elango EM, Asita H, Nidhi G, Seema P, Banerji A, Kuriakose MA. 2004. *J Appl Genet* 45: 469-71
158. Lin JG, Chen GW, Su CC, Hung CF, Yang CC, et al. 2002. *Am J Chin Med* 30: 315-25
159. Robert V, Mouille B, Mayeur C, Michaud M, Blachier F. 2001. *Carcinogenesis* 22: 1155-61
160. Tang ZG, Xu XP, Shen ZH. 2000. *Hunan Yi Ke Da Xue Xue Bao* 25: 27-9
161. Jo HJ, Song JD, Kim KM, Cho YH, Kim KH, Park YC. 2008. *Oncol Rep* 19: 275-80
162. Hui C, Jun W, Ya LN, Ming X. 2008. *Trop Biomed* 25: 37-45
163. Wu XJ, Kassie F, Mersch-Sundermann V. 2005. *Mutat Res* 579: 115-24
164. Druesne N, Pagniez A, Mayeur C, Thomas M, Cherbuy C, et al. 2004. *Carcinogenesis* 25: 1227-36

165. Sriram N, Kalayarasan S, Ashokkumar P, Sureshkumar A, Sudhandiran G. 2008. *Mol Cell Biochem* 311: 157-65
166. Arora A, Seth K, Shukla Y. 2004. *Carcinogenesis* 25: 941-9
167. Sigounas G, Hooker JL, Li W, Anagnostou A, Steiner M. 1997. *Nutr Cancer* 28: 153-9
168. Sigounas G, Hooker J, Anagnostou A, Steiner M. 1997. *Nutr Cancer* 27: 186-91
169. Gapter LA, Yuin OZ, Ng KY. 2008. *Biochem Biophys Res Commun* 367: 446-51
170. Seki T, Tsuji K, Hayato Y, Moritomo T, Ariga T. 2000. *Cancer Lett* 160: 29-35
171. Bjorkhem-Bergman L, Torndal UB, Eken S, Nystrom C, Capitanio A, et al. 2005. *Carcinogenesis* 26: 125-31
172. Thirunavukkarasu C, Singh JP, Selvendiran K, Sakthisekaran D. 2001. *Cell Biochem Funct* 19: 265-71
173. Fang W, Han A, Bi X, Xiong B, Yang W. 2009. *Int J Cancer*
174. Dorado RD, Porta EA, Aquino TM. 1985. *Hepatology* 5: 1201-8
175. Feng Y, Finley JW, Davis CD, Becker WK, Fretland AJ, Hein DW. 1999. *Toxicol Appl Pharmacol* 157: 36-42
176. Ip C, Zhu Z, Thompson HJ, Lisk D, Ganther HE. 1999. *Anticancer Res* 19: 2875-80
177. Jiang W, Jiang C, Pei H, Wang L, Zhang J, et al. 2009. *Mol Cancer Ther* 8: 682-91
178. Wang L, Bonorden MJ, Li GX, Lee HJ, Hu H, et al. 2009. *Cancer Prev Res (Phila Pa)* 2: 484-95
179. Mukherjee B, Ghosh S, Chatterjee M. 1996. *J Exp Ther Oncol* 1: 209-17
180. Ip C, White G. 1987. *Carcinogenesis* 8: 1763-6
181. Ip C, Lisk DJ. 1994. *Nutr Cancer* 21: 203-12
182. Finley JW, Davis CD. 2001. *Biofactors* 14: 191-6
183. Finley JW, Ip C, Lisk DJ, Davis CD, Hintze KJ, Whanger PD. 2001. *J Agric Food Chem* 49: 2679-83
184. Finley JW, Davis CD, Feng Y. 2000. *J Nutr* 130: 2384-9
185. Jiang C, Jiang W, Ip C, Ganther H, Lu J. 1999. *Mol Carcinog* 26: 213-25
186. Lu J, Pei H, Ip C, Lisk DJ, Ganther H, Thompson HJ. 1996. *Carcinogenesis* 17: 1903-7
187. Yamanoshita O, Ichihara S, Hama H, Ichihara G, Chiba M, et al. 2007. *Tohoku J Exp Med* 212: 191-8
188. Yoshida M, Okada T, Namikawa Y, Matsuzaki Y, Nishiyama T, Fukunaga K. 2007. *Biosci Biotechnol Biochem* 71: 2198-205
189. Liu JG, Zhao HJ, Liu YJ, Wang XL. 2009. *Res Vet Sci* 87: 438-44
190. Oh SH, Park KK, Kim SY, Lee KJ, Lee YH. 1995. *Carcinogenesis* 16: 2995-8
191. Lu J, Kaeck M, Jiang C, Wilson AC, Thompson HJ. 1994. *Biochem Pharmacol* 47: 1531-5
192. Watrach AM, Milner JA, Watrach MA, Poirier KA. 1984. *Cancer Lett* 25: 41-7
193. Stewart MS, Davis RL, Walsh LP, Pence BC. 1997. *Cancer Lett* 117: 35-40
194. Xiang N, Zhao R, Zhong W. 2009. *Cancer Chemother Pharmacol* 63: 351-62
195. Rudolf E, Rudolf K, Cervinka M. 2008. *Cell Biol Toxicol* 24: 123-41
196. Rooprai HK, Kyriazis I, Nuttall RK, Edwards DR, Zicha D, et al. 2007. *Int J Oncol* 30: 1263-71
197. Kralova V, Brigulova K, Cervinka M, Rudolf E. 2009. *Toxicol In Vitro* 23: 1497-503
198. Berggren M, Sittadjody S, Song Z, Samira JL, Burd R, Meuillet EJ. 2009. *Nutr Cancer* 61: 322-31

199. Huang F, Nie C, Yang Y, Yue W, Ren Y, et al. 2009. *Free Radic Biol Med* 46: 1186-96
200. Unni E, Koul D, Yung WK, Sinha R. 2005. *Breast Cancer Res* 7: R699-707
201. Unni E, Kittrell FS, Singh U, Sinha R. 2004. *Breast Cancer Res* 6: R586-92
202. Unni E, Singh U, Ganther HE, Sinha R. 2001. *Biofactors* 14: 169-77
203. Sinha R, Kiley SC, Lu JX, Thompson HJ, Moraes R, et al. 1999. *Cancer Lett* 146: 135-45
204. Wang J, Jiao NL, Zheng J. 2008. *Ai Zheng* 27: 119-25
205. Hurst R, Elliott RM, Goldson AJ, Fairweather-Tait SJ. 2008. *Cancer Lett* 269: 117-26
206. Yeo JK, Cha SD, Cho CH, Kim SP, Cho JW, et al. 2002. *Cancer Lett* 182: 83-92
207. Schroterova L, Kralova V, Voracova A, Haskova P, Rudolf E, Cervinka M. 2009. *Toxicol In Vitro* 23: 1406-11
208. Baines A, Taylor-Parker M, Goulet AC, Renaud C, Gerner EW, Nelson MA. 2002. *Cancer Biol Ther* 1: 370-4
209. Verma A, Atten MJ, Attar BM, Holian O. 2004. *Nutr Cancer* 49: 184-90
210. Goulet AC, Chigbrow M, Frisk P, Nelson MA. 2005. *Carcinogenesis* 26: 109-17
211. Redman C, Scott JA, Baines AT, Basye JL, Clark LC, et al. 1998. *Cancer Lett* 125: 103-10
212. Chigbrow M, Nelson M. 2001. *Anticancer Drugs* 12: 43-50
213. Jiang W, Zhu Z, Ganther HE, Ip C, Thompson HJ. 2001. *Cancer Lett* 162: 167-73
214. Zhu Z, Jiang W, Ganther HE, Ip C, Thompson HJ. 2000. *Biochem Pharmacol* 60: 1467-73
215. Abdulah R, Faried A, Kobayashi K, Yamazaki C, Suradji EW, et al. 2009. *BMC Cancer* 9: 414
216. Ip C, Lisk DJ, Stoewsand GS. 1992. *Nutr Cancer* 17: 279-86
217. El-Bayoumy K, Sinha R, Pinto JT, Rivlin RS. 2006. *J Nutr* 136: 864S-9S
218. Myzak MC, Dashwood RH. 2006. *Cancer Lett* 233: 208-18
219. Pinto JT, Krasnikov BF, Cooper AJ. 2006. *J Nutr* 136: 835S-41S
220. Higdon JV, Delage B, Williams DE, Dashwood RH. 2007. *Pharmacol Res* 55: 224-36
221. Clarke JD, Dashwood RH, Ho E. 2008. *Cancer Lett*
222. Powolny AA, Singh SV. 2008. *Cancer Lett*
223. Knasmuller S, de Martin R, Domjan G, Szakmary A. 1989. *Environ Mol Mutagen* 13: 357-65
224. Das T, Roychoudhury A, Sharma A, Talukder G. 1993. *Environ Mol Mutagen* 21: 383-8
225. Tiku AB, Abraham SK, Kale RK. 2008. *Environ Mol Mutagen* 49: 335-42
226. Fiorio R, Bronzetti G. 1995. *Environ Mol Mutagen* 25: 344-6
227. Fimognari C, Berti F, Cantelli-Forti G, Hrelia P. 2005. *Environ Mol Mutagen* 46: 260-7
228. Zhang Y, Talalay P, Cho CG, Posner GH. 1992. *Proc Natl Acad Sci U S A* 89: 2399-403
229. Fahey JW, Zhang Y, Talalay P. 1997. *Proc Natl Acad Sci U S A* 94: 10367-72
230. Fimognari C, Hrelia P. 2007. *Mutat Res* 635: 90-104
231. Juge N, Mithen RF, Traka M. 2007. *Cell Mol Life Sci* 64: 1105-27
232. Shapiro TA, Fahey JW, Dinkova-Kostova AT, Holtzclaw WD, Stephenson KK, et al. 2006. *Nutr Cancer* 55: 53-62
233. Milner JA. 2006. *J Nutr* 136: 827S-31S
234. Myzak MC, Dashwood RH. 2006. *Curr Drug Targets* 7: 443-52
235. Liu CT, Sheen LY, Lii CK. 2007. *Mol Nutr Food Res* 51: 1353-64
236. Pittler MH, Ernst E. 2007. *Mol Nutr Food Res* 51: 1382-5
237. Sener G, Sakarcan A, Yegen BC. 2007. *Mol Nutr Food Res* 51: 1345-52

238. Nagini S. 2008. *Anticancer Agents Med Chem* 8: 313-21
239. Millen AE, Subar AF, Graubard BI, Peters U, Hayes RB, et al. 2007. *Am J Clin Nutr* 86: 1754-64
240. Delage B, Dashwood RH. 2008. *Annu Rev Nutr* 28: 347-66
241. Kondo Y, Issa JP. 2004. *Cancer Metastasis Rev* 23: 29-39
242. Gronbaek K, Hother C, Jones PA. 2007. *APMIS* 115: 1039-59
243. Gal-Yam EN, Saito Y, Egger G, Jones PA. 2008. *Annu Rev Med* 59: 267-80
244. Fraga MF, Ballestar E, Villar-Garea A, Boix-Chornet M, Espada J, et al. 2005. *Nat Genet* 37: 391-400
245. Seligson DB, Horvath S, Shi T, Yu H, Tze S, et al. 2005. *Nature* 435: 1262-6
246. Ono S, Oue N, Kuniyasu H, Suzuki T, Ito R, et al. 2002. *J Exp Clin Cancer Res* 21: 377-82
247. Chen YX, Fang JY, Lu R, Qiu DK. 2007. *World J Gastroenterol* 13: 2209-13
248. Wade PA. 2001. *Hum Mol Genet* 10: 693-8
249. Dokmanovic M, Marks PA. 2005. *J Cell Biochem* 96: 293-304
250. McLaughlin F, La Thangue NB. 2004. *Biochem Pharmacol* 68: 1139-44
251. Mariadason JM. 2008. *Epigenetics* 3: 28-37
252. Marks P, Rifkind RA, Richon VM, Breslow R, Miller T, Kelly WK. 2001. *Nat Rev Cancer* 1: 194-202
253. Butler LM, Zhou X, Xu WS, Scher HI, Rifkind RA, et al. 2002. *Proc Natl Acad Sci U S A* 99: 11700-5
254. Glaser KB, Staver MJ, Waring JF, Stender J, Ulrich RG, Davidsen SK. 2003. *Mol Cancer Ther* 2: 151-63
255. Kumagai T, Wakimoto N, Yin D, Gery S, Kawamata N, et al. 2007. *Int J Cancer* 121: 656-65
256. Okamoto H, Fujioka Y, Takahashi A, Takahashi T, Taniguchi T, et al. 2006. *J Atheroscler Thromb* 13: 183-91
257. Rocchi P, Tonelli R, Camerin C, Purgato S, Fronza R, et al. 2005. *Oncol Rep* 13: 1139-44
258. Sowa Y, Orita T, Minamikawa S, Nakano K, Mizuno T, et al. 1997. *Biochem Biophys Res Commun* 241: 142-50
259. Donadelli M, Costanzo C, Faggioli L, Scupoli MT, Moore PS, et al. 2003. *Mol Carcinog* 38: 59-69
260. Komatsu N, Kawamata N, Takeuchi S, Yin D, Chien W, et al. 2006. *Oncol Rep* 15: 187-91
261. Marks PA. 2007. *Oncogene* 26: 1351-6
262. Fantin VR, Richon VM. 2007. *Clin Cancer Res* 13: 7237-42
263. Itoh Y, Suzuki T, Miyata N. 2008. *Curr Pharm Des* 14: 529-44
264. Jones P, Steinkuhler C. 2008. *Curr Pharm Des* 14: 545-61
265. Xu WS, Parmigiani RB, Marks PA. 2007. *Oncogene* 26: 5541-52
266. Riggs MG, Whittaker RG, Neumann JR, Ingram VM. 1977. *Nature* 268: 462-4
267. Cummings JH, Englyst HN. 1987. *Am J Clin Nutr* 45: 1243-55
268. Cummings JH, Pomare EW, Branch WJ, Naylor CP, Macfarlane GT. 1987. *Gut* 28: 1221-7
269. Sekhavat A, Sun JM, Davie JR. 2007. *Biochem Cell Biol* 85: 751-8

270. Gottlicher M. 2004. *Ann Hematol* 83 Suppl 1: S91-2
271. Jung M. 2001. *Curr Med Chem* 8: 1505-11
272. Chung YL, Lee MY, Wang AJ, Yao LF. 2003. *Mol Ther* 8: 707-17
273. Gardian G, Yang L, Cleren C, Calingasan NY, Klivenyi P, Beal MF. 2004. *Neuromolecular Med* 5: 235-41
274. Gardian G, Browne SE, Choi DK, Klivenyi P, Gregorio J, et al. 2005. *J Biol Chem* 280: 556-63
275. Hogarth P, Lovrecic L, Krainc D. 2007. *Mov Disord* 22: 1962-4
276. Ryu H, Smith K, Camelo SI, Carreras I, Lee J, et al. 2005. *J Neurochem* 93: 1087-98
277. Shen G, Xu C, Chen C, Hebbar V, Kong AN. 2006. *Cancer Chemother Pharmacol* 57: 317-27
278. Parnaud G, Li P, Cassar G, Rouimi P, Tulliez J, et al. 2004. *Nutr Cancer* 48: 198-206
279. Gamet-Payrastre L, Li P, Lumeau S, Cassar G, Dupont MA, et al. 2000. *Cancer Res* 60: 1426-33
280. Fimognari C, Nusse M, Cesari R, Iori R, Cantelli-Forti G, Hrelia P. 2002. *Carcinogenesis* 23: 581-6
281. Singh SV, Herman-Antosiewicz A, Singh AV, Lew KL, Srivastava SK, et al. 2004. *J Biol Chem* 279: 25813-22
282. Myzak MC, Karplus PA, Chung FL, Dashwood RH. 2004. *Cancer Res* 64: 5767-74
283. Myzak MC, Hardin K, Wang R, Dashwood RH, Ho E. 2006. *Carcinogenesis* 27: 811-9
284. Pledgie-Tracy A, Sobolewski MD, Davidson NE. 2007. *Mol Cancer Ther* 6: 1013-21
285. Myzak MC, Dashwood WM, Orner GA, Ho E, Dashwood RH. 2006. *Faseb J* 20: 506-8
286. Myzak MC, Tong P, Dashwood WM, Dashwood RH, Ho E. 2007. *Exp Biol Med (Maywood)* 232: 227-34
287. Warrell RP, Jr., He LZ, Richon V, Calleja E, Pandolfi PP. 1998. *J Natl Cancer Inst* 90: 1621-5
288. Dashwood RH, Ho E. 2007. *Semin Cancer Biol* 17: 363-9
289. Hu R, Khor TO, Shen G, Jeong WS, Hebbar V, et al. 2006. *Carcinogenesis* 27: 2038-46
290. Lea MA, Randolph VM, Lee JE, desBordes C. 2001. *Int J Cancer* 92: 784-9
291. Lea MA, Rasheed M, Randolph VM, Khan F, Shareef A, desBordes C. 2002. *Nutr Cancer* 43: 90-102
292. Sheen LY, Wu CC, Lii CK, Tsai SJ. 1999. *Food Chem Toxicol* 37: 1139-46
293. Nian H, Delage B, Pinto JT, Dashwood RH. 2008. *Carcinogenesis*
294. Druesne-Pecollo N, Chaumontet C, Pagniez A, Vaugelade P, Bruneau A, et al. 2007. *Biochem Biophys Res Commun* 354: 140-7
295. Bianchini F, Vainio H. 2001. *Environ Health Perspect* 109: 893-902
296. Dashwood RH, Myzak MC, Ho E. 2006. *Carcinogenesis* 27: 344-9
297. Delage B, Dashwood RH. 2008. *Annu Rev Nutr*
298. Mork CN, Faller DV, Spanjaard RA. 2005. *Curr Pharm Des* 11: 1091-104
299. Rosato RR, Grant S. 2003. *Cancer Biol Ther* 2: 30-7
300. Furumai R, Komatsu Y, Nishino N, Khochbin S, Yoshida M, Horinouchi S. 2001. *Proc Natl Acad Sci U S A* 98: 87-92
301. Hosono T, Hosono-Fukao T, Inada K, Tanaka R, Yamada H, et al. 2008. *Carcinogenesis*
302. Yang SR, Chida AS, Bauter MR, Shafiq N, Seweryniak K, et al. 2006. *Am J Physiol Lung Cell Mol Physiol* 291: L46-57

303. Finnin MS, Donigian JR, Cohen A, Richon VM, Rifkind RA, et al. 1999. *Nature* 401: 188-93
304. Hellebrekers DM, Melotte V, Vire E, Langenkamp E, Molema G, et al. 2007. *Cancer Res* 67: 4138-48
305. Taniguchi H, Yamamoto H, Hirata T, Miyamoto N, Oki M, et al. 2005. *Oncogene* 24: 7946-52
306. Mitic T, McKay JS. 2005. *Toxicol Pathol* 33: 792-9
307. Mitsiades CS, Mitsiades NS, McMullan CJ, Poulaki V, Shringarpure R, et al. 2004. *Proc Natl Acad Sci U S A* 101: 540-5
308. Chen C, Kong AN. 2005. *Trends Pharmacol Sci* 26: 318-26
309. Ross SA, Finley JW, Milner JA. 2006. *J Nutr* 136: 852S-4S
310. Belloir C, Singh V, Daurat C, Siess MH, Le Bon AM. 2006. *Food Chem Toxicol* 44: 827-34
311. Block E. 1985. *Sci Am* 252: 114-9
312. Ameen M, Musthapa MS, Abidi P, Ahmad I, Rahman Q. 2003. *J Biochem Mol Toxicol* 17: 366-71
313. Sambucetti LC, Fischer DD, Zabludoff S, Kwon PO, Chamberlin H, et al. 1999. *J Biol Chem* 274: 34940-7
314. Guida M, Colucci G. 2007. *Ann Oncol* 18 Suppl 6: vi149-52
315. Suzuki T, Nagano Y, Kouketsu A, Matsuura A, Maruyama S, et al. 2005. *J Med Chem* 48: 1019-32
316. Dixon M. 1953. *Biochem J* 55: 170-1
317. Vannini A, Volpari C, Filocamo G, Casavola EC, Brunetti M, et al. 2004. *Proc Natl Acad Sci U S A* 101: 15064-9
318. Fang JY, Lu YY. 2002. *World J Gastroenterol* 8: 400-5
319. Kim YK, Han JW, Woo YN, Chun JK, Yoo JY, et al. 2003. *Oncogene* 22: 6023-31
320. Davis CD, Ross SA. 2007. *Nutr Rev* 65: 88-94
321. Ondetti MA, Rubin B, Cushman DW. 1977. *Science* 196: 441-4
322. Whittaker M, Floyd CD, Brown P, Gearing AJ. 1999. *Chem Rev* 99: 2735-76
323. Suzuki T, Kouketsu A, Matsuura A, Kohara A, Ninomiya S, et al. 2004. *Bioorg Med Chem Lett* 14: 3313-7
324. Hu E, Chen Z, Fredrickson T, Zhu Y, Kirkpatrick R, et al. 2000. *J Biol Chem* 275: 15254-64
325. Niculescu AB, 3rd, Chen X, Smeets M, Hengst L, Prives C, Reed SI. 1998. *Mol Cell Biol* 18: 629-43
326. Iacomino G, Medici MC, Napoli D, Russo GL. 2006. *J Cell Biochem* 99: 1122-31
327. Antosiewicz J, Herman-Antosiewicz A, Marynowski SW, Singh SV. 2006. *Cancer Res* 66: 5379-86
328. Herman-Antosiewicz A, Singh SV. 2005. *J Biol Chem* 280: 28519-28
329. Kobayashi H, Tan EM, Fleming SE. 2004. *Int J Cancer* 109: 207-13
330. Huang L, Sowa Y, Sakai T, Pardee AB. 2000. *Oncogene* 19: 5712-9
331. Ryu H, Lee J, Olofsson BA, Mwidau A, Dedeoglu A, et al. 2003. *Proc Natl Acad Sci U S A* 100: 4281-6
332. Ammanamanchi S, Freeman JW, Brattain MG. 2003. *J Biol Chem* 278: 35775-80
333. Xiao H, Hasegawa T, Isobe K. 2000. *J Biol Chem* 275: 1371-6

334. Sowa Y, Orita T, Minamikawa-Hiranabe S, Mizuno T, Nomura H, Sakai T. 1999. *Cancer Res* 59: 4266-70
335. Xiao H, Hasegawa T, Isobe K. 1999. *J Cell Biochem* 73: 291-302
336. Suzuki T, Kimura A, Nagai R, Horikoshi M. 2000. *Genes Cells* 5: 29-41
337. Huang W, Zhao S, Ammanamanchi S, Brattain M, Venkatasubbarao K, Freeman JW. 2005. *J Biol Chem* 280: 10047-54
338. Zhao Y, Lu S, Wu L, Chai G, Wang H, et al. 2006. *Mol Cell Biol* 26: 2782-90
339. Roy S, Tenniswood M. 2007. *J Biol Chem* 282: 4765-71
340. Bossi G, Sacchi A. 2007. *Head Neck* 29: 272-84
341. Vikhanskaya F, Lee MK, Mazzoletti M, Broggini M, Sabapathy K. 2007. *Nucleic Acids Res* 35: 2093-104
342. Blagosklonny MV, Trostel S, Kayastha G, Demidenko ZN, Vassilev LT, et al. 2005. *Cancer Res* 65: 7386-92
343. Myzak MC, Ho E, Dashwood RH. 2006. *Mol Carcinog* 45: 443-6
344. Walton TJ, Li G, Seth R, McArdle SE, Bishop MC, Rees RC. 2008. *Prostate* 68: 210-22
345. Zhu WG, Otterson GA. 2003. *Curr Med Chem Anticancer Agents* 3: 187-99
346. Gammelgaard B, Gabel-Jensen C, Sturup S, Hansen HR. 2008. *Anal Bioanal Chem* 390: 1691-706
347. Ip C, Thompson HJ, Ganther HE. 2000. *Cancer Epidemiol Biomarkers Prev* 9: 49-54
348. Zhao R, Domann FE, Zhong W. 2006. *Mol Cancer Ther* 5: 3275-84
349. Cherukuri DP, Goulet AC, Inoue H, Nelson MA. 2005. *Cancer Biol Ther* 4: 175-80
350. Goel A, Fuerst F, Hotchkiss E, Boland CR. 2006. *Cancer Biol Ther* 5: 529-35
351. Ip C, Thompson HJ, Zhu Z, Ganther HE. 2000. *Cancer Res* 60: 2882-6
352. Cooper AJ, Pinto JT, Krasnikov BF, Niatsetskaya ZV, Han Q, et al. 2008. *Arch Biochem Biophys* 474: 72-81
353. Nian H, Delage B, Pinto JT, Dashwood RH. 2008. *Carcinogenesis* 29: 1816-24
354. Somoza JR, Skene RJ, Katz BA, Mol C, Ho JD, et al. 2004. *Structure* 12: 1325-34
355. Cardozo T, Totrov M, Abagyan R. 1995. *Proteins* 23: 403-14
356. Totrov M, Abagyan R. 1997. *Proteins* Suppl 1: 215-20
357. Datto MB, Yu Y, Wang XF. 1995. *J Biol Chem* 270: 28623-8
358. Nian H, Delage B, Ho E, Dashwood RH. 2009. *Environ Mol Mutagen*
359. Chiba T, Yokosuka O, Arai M, Tada M, Fukai K, et al. 2004. *J Hepatol* 41: 436-45
360. Tavares TS, Nanus D, Yang XJ, Gudas LJ. 2008. *Cancer Biol Ther* 7: 1607-18
361. Davis CD, Zeng H, Finley JW. 2002. *J Nutr* 132: 307-9
362. Davis CD, Feng Y, Hein DW, Finley JW. 1999. *J Nutr* 129: 63-9
363. Reddy BS, Hirose Y, Lubet RA, Steele VE, Kelloff GJ, Rao CV. 2000. *Int J Mol Med* 5: 327-30
364. Ip C, Birringer M, Block E, Kotrebai M, Tyson JF, et al. 2000. *J Agric Food Chem* 48: 2062-70
365. Spallholz JE, Shriver BJ, Reid TW. 2001. *Nutr Cancer* 40: 34-41
366. Gopalakrishna R, Gundimeda U. 2001. *Nutr Cancer* 40: 55-63
367. Cooper AJ. 2004. *Neurochem Int* 44: 557-77
368. Lee JI, Nian H, Cooper AJ, Sinha R, Dai J, et al. 2009. *Cancer Prev Res (Phila Pa)* 2: 683-93

369. Lippman SM, Klein EA, Goodman PJ, Lucia MS, Thompson IM, et al. 2009. *JAMA* 301: 39-51
370. Nian H, Bisson WH, Dashwood WM, Pinto JT, Dashwood RH. 2009. *Carcinogenesis* 30: 1416-23
371. Bolden JE, Peart MJ, Johnstone RW. 2006. *Nat Rev Drug Discov* 5: 769-84
372. Zhang Y, Adachi M, Kawamura R, Imai K. 2006. *Cell Death Differ* 13: 129-40
373. Suzuki KT, Tsuji Y, Ohta Y, Suzuki N. 2008. *Toxicol Appl Pharmacol* 227: 76-83
374. Thangaraju M, Carswell KN, Prasad PD, Ganapathy V. 2009. *Biochem J* 417: 379-89
375. Balasubramanian S, Verner E, Buggy JJ. 2009. *Cancer Lett* 280: 211-21
376. Oehme I, Deubzer HE, Lodrini M, Milde T, Witt O. 2009. *Expert Opin Investig Drugs* 18: 1605-17
377. Das A, Desai D, Pittman B, Amin S, El-Bayoumy K. 2003. *Nutr Cancer* 46: 179-85
378. Prokopczyk B, Amin S, Desai DH, Kurtzke C, Upadhyaya P, El-Bayoumy K. 1997. *Carcinogenesis* 18: 1855-7
379. Lane HW, Teer P, Dukes J, Johnson J, White MT. 1990. *Cancer Lett* 50: 39-44
380. Hatfield DL, Gladyshev VN. 2009. *Mol Interv* 9: 18-21